NASA CR-134537

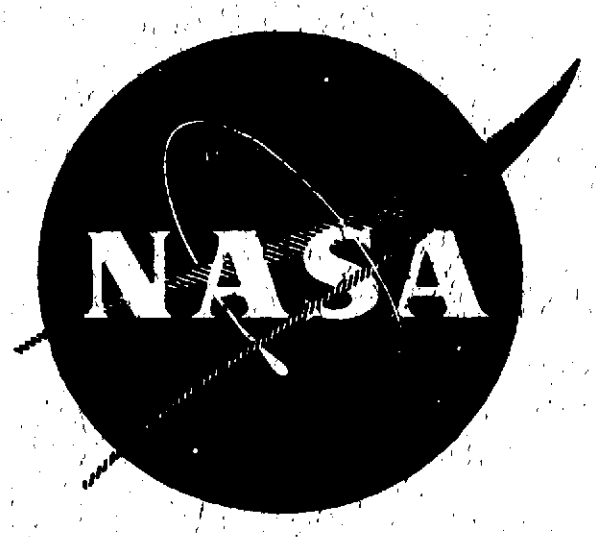

ENVIRONMENTAL PROTECTION TO 922 K (1200°F) FOR TITANIUM ALLOYS

by
M.T. GROVES
TRW INC.

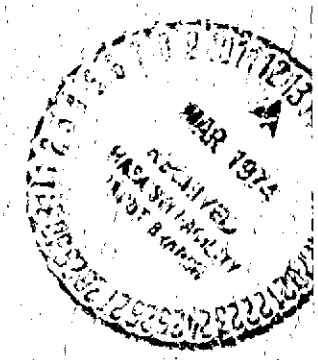

Prepared for
NATIONAL AERONAUTICS AND SPACE ADMINISTRATION

NOVEMBER 1973

NASA LEWIS RESEARCH CENTER
CONTRACT NAS 3-14339

1. Report No. NASA CR- 134537	2. Government Accession No.	3. Recipient's Catalog No.
4. Title and Subtitle ENVIRONMENTAL PROTECTION TO 922°K (1200°F) FOR TITANIUM ALLOYS		5. Report Date NOVEMBER 1973 6. Performing Organization Code
7. Author(s) M. T. GROVES		8. Performing Organization Report No. ER-7704
9. Performing Organization Name and Address TRW INC. MATERIALS TECHNOLOGY 23555 EUCLID AVENUE CLEVELAND, OHIO 44117		10. Work Unit No. 11. Contract or Grant No. NAS 3-14339
12. Sponsoring Agency Name and Address NATIONAL AERONAUTICS AND SPACE ADMINISTRATION WASHINGTON, D.C. 20546		13. Type of Report and Period Covered CONTRACTOR FINAL REPORT 14. Sponsoring Agency Code

15. Supplementary Notes
PROJECT MANAGER, FREDRIC H. HARF
RESEARCH ADVISOR, DR. HUGH R. GRAY, MATERIALS AND STRUCTURES DIVISION
NASA LEWIS RESEARCH CENTER
CLEVELAND, OHIO 44135

16. Abstract The purpose of this program was to evaluate potential coating systems for protection of titanium alloys from hot-salt stress-corrosion up to temperatures of 755°K (900°F) and from oxidation embrittlement up to temperatures of 922°K (1200°F). Diffusion type coatings containing Si, Al, Cr, Ni or Fe as single coating elements or in various combinations were evaluated for oxidation protection, hot-salt stress-corrosion (HSSC) resistance, effects on tensile properties, fatigue properties, erosion resistance and ballistic impact resistance on an α+β titanium alloy (Ti-6Al-2Sn-4Zr-2Mo). All of the coatings investigated demonstrated excellent oxidation protectiveness, but none of the coatings provided protection from hot-salt stress-corrosion. Experimental results indicated that both the aluminide and silicide types of coatings actually decreased the HSSC resistance of the substrate alloy. Oxidation exposed coatings (922°K (1200°F)) exhibited some degradation in tensile properties compared to unexposed Ti-6-2-4-2. When compared to uncoated Ti-6-2-4-2 comparably exposed at 922°K (1200°F), about half of the coated specimens had strengths comparable to the uncoated substrate and tensile elongation values that exceeded those of the uncoated substrate. Fatigue properties were degraded by the presence of the coatings. Ballistic impact damage degraded the mechanical properties of the coated specimens. Only two of the coatings protected the substrate against erosion resistance at a 20° impingement angle, while none of the coatings were protective at an impingement angle of 90°. Tests with a β titanium alloy (Ti-13V-11Cr-3Al) indicated oxidation protectiveness comparable to the α+β alloy, but the thermal cycles employed in coating deposition severely degraded the mechanical properties of the β alloy. It was concluded that the types of coatings which have typically been used for oxidation protection of refractory metals and nickel base superalloys are not suitable for titanium alloys because they increase the susceptibility to hot-salt stress-corrosion, and that entirely new coating concepts must be developed for titanium alloy protection in advanced turbine engines.

17. Key Words (Suggested by Author(s))
TITANIUM ALLOYS
COATINGS
ALUMINIDES
SILICIDES
OXIDATION TESTS
HOT SALT STRESS CORROSION
EROSION RESISTANCE
BALLISTIC IMPACT TESTS

18. Distribution Statement

19. Security Classif. (of this report)	20. Security Classif. (of this page)	21. No. of Pages	22. Price*
UNCLASSIFIED	UNCLASSIFIED	~~111~~ 114	~~$3.75~~ $8.75 Domestic $6.75 Foreign

* For sale by the National Technical Information Service, Springfield, Virginia 22151

FOREWORD

The work described herein was performed by TRW Inc. under sponsorship of the National Aeronautics and Space Administration Contract NAS3-14339. The program was administered for TRW Inc. by Dr. J. V. Peck and Dr. K. D. Sheffler. Principal Investigators were J. F. Nejedlik and M. T. Groves. The NASA Research Advisor was Dr. H. R. Gray.

TABLE OF CONTENTS

TABLE OF CONTENTS (continued)

LIST OF FIGURES

LIST OF FIGURES (continued)

LIST OF TABLES

LIST OF TABLES (continued)

1.0 SUMMARY

This work was undertaken to evaluate potential coating systems for protection of titanium alloys from hot-salt stress-corrosion to temperatures of 755°K (900°F) and from oxidation embrittlement to temperatures of 922°K (1200°F). Ten experimental coating systems were evaluated: Al, Si, Al-Si, Al-Mg, Si-Cr-Al, Ni-Cr-Al, Ni-Fe-Al-Si, Cr+(Al-Mg), Cr+(Al-Si), (Cr-Fe)+(Al-Mg). Evaluation consisted of oxidation protectiveness, effect on substrate tensile properties, hot-salt stress-corrosion resistance (HSSC) and erosion resistance on Ti-6Al-2Sn-4Zr-2Mo (Ti-6-2-4-2) $\alpha + \beta$ alloy sheet. The five most promising coatings were further evaluated for fatigue properties and ballistic impact resistance on the Ti-6-2-4-2 sheet and for effect on substrate tensile properties and HSSC resistance on Ti-13V-11Cr-3Al (Ti-13-11-3) β alloy sheet.

Electron microprobe analyses of coated Ti-6-2-4-2 specimens indicated that all ten of the coatings protected the substrate from oxidation under 1000 hour/922°K (1200°F) exposure conditions. Tensile tests were performed on coated Ti-6-2-4-2 specimens that had been oxidation exposed for 100 and 1000 hours at 922°K (1200°F). Compared to unexposed, uncoated material, the coatings degraded the tensile properties, particularly tensile elongation. When compared to comparably exposed uncoated Ti-6-2-4-2, however, about half of the coatings had strengths equivalent to uncoated material and tensile elongation values exceeding the uncoated material. The best tensile properties were obtained from the Si and Al-Mg coatings.

Hot-salt stress-corrosion tests performed with self-stressed bend specimens exposed at 755°K (900°F) did not provide a definitive ranking of the coatings. All ten coatings on self-stressed specimens cracked during specimen fabrication thus indicating low coating ductility. In addition, it was noted that the presence of these cracks in the coatings appeared to intensity subsequent HSSC cracking.

All ten coatings were evaluated for erosion resistance on Ti-6-2-4-2. At an impingement angle of 20° only the Cr+(Al-Mg) and Al-Mg coatings protected the substrate. At an impingement angle of 90° none of the coatings protected the substrate.

The five coatings selected for further evaluation of fatigue and impact properties and on Ti-13-11-3 included the Al, Si, Al-Mg, Ni-Cr-Al and Ni-Fe-Al-Si coatings. All of these coatings reduced the endurance limit of uncoated Ti-6-2-4-2 sheet. The ratio of coated endurance limit to uncoated endurance limit varied from 0.57 to 0.74 with the Ni-Cr-Al coating displaying the highest fatigue resistance. Ballistic impact testing consisted of evaluating the coatings for resistance to impact damage, tensile properties after oxidation exposure of damaged coatings and hot-salt stress-corrosion resistance after damage. Impact resistance was lower for the coated alloys than for the uncoated material. Tensile properties and HSSC resistance of the coated alloys were degraded by impact damage. On Ti-13-11-3 sheet, the coatings drastically reduced tensile properties. Self-stressed hot-salt stress-corrosion specimens were too brittle to provide definitive test results. The poor performance of the coatings on Ti-13-11-3 was attributed to the thermal treatments associated with coating application, which resulted in excessive grain growth.

Further work was directed towards investigating the poor HSSC resistance of the coatings under creep-exposure conditions, 100 hours exposure at 755°K (900°F). Test results indicated all five of the coatings selected for further evaluation (Al, Si, Al-Mg, Ni-Cr-Al and Ni-Fe-Al-Si) appeared to increase sensitivity to HSSC on the Ti-6-2-4-2 sheet material. Additional testing performed on Ti-6-2-4-2 bar stock disclosed that all of the coatings drastically reduced resistance to HSSC. An embrittlement threshold stress of 103.4 MN/m^2 (15.0 ksi) was determined for the bar stock. The Al, Al-Mg, Ni-Cr-Al and Ni-Fe-Al-Si coatings exhibited evidence of embrittlement under stresses as low as 17.2 MN/m^2 (2.5 ksi) while the Si coating had a threshold embrittlement stress of 34.5 MN/m^2 (5.0 ksi).

The present study has shown that the most serious problem associated with the diffusion coatings tested on the program is their poor resistance to hot-salt stress-corrosion at 755°K (900°F). While good oxidation protection and minimal reduction in tensile properties could be obtained with some of the coatings, the fact that the coatings intensified hot-salt stress-corrosion would preclude their use in turbine engine environments. The problem may lie with the inherently poor ductility of the diffusion coatings or a combination of poor coating ductility and unfavorable electrochemical reactions. Based on the hot-salt stress-corrosion results, it was concluded that the aluminide and silicide types of coatings which typically have been used for oxidation protection of nickel base superalloys and refractory metals are not suitable for use on titanium, and entire new coating concepts must be developed for titanium alloy protection in advanced turbine engines.

2.0 INTRODUCTION

Titanium alloys are used extensively for turbine engine compressor components at temperatures up to about 700-750°K (800-900°F) because of excellent strength-to-weight ratio, fracture toughness and structural stability. These unique properties have been utilized in the manufacture of turbine engine compressor and fan blades, inlet cases, disks and other components[1]. Titanium alloys with a greater strength capability are being developed for use in advanced engines at temperatures to 922°K (1200°F). The use of titanium alloys in some applications may be restricted by erosion and hot-salt stress-corrosion cracking. In addition, as the use temperature of advanced titanium alloys exceeds about 755°K (900°F), another potential problem limiting their long term use may be oxygen contamination.

If the full potential of titanium alloys is to be exploited, coating systems must be developed to protect against the damaging influence of the higher temperature turbine engine environment. The purpose of this program was to evaluate potential coating systems for protection of titanium alloys from oxidation, hot-salt stress-corrosion and erosion at temperatures to 922°K (1200°F). In addition, tensile, fatigue and ballistic impact properties were to be evaluated for possible degradation by the coatings.

Coatings previously investigated for the protection of titanium from oxidation have included aluminides, silicides and various other intermetallic compounds. An aluminide coating was developed for short term protection at 1255°K (1800°F), but there was some evidence that the diffused aluminide could offer long term protection in the 811-922°K (1000-1200°F) temperature range[2]. Silicide coatings were protective at 1033°K (1400°F), but substrate properties were adversely affected by the high deposition temperatures[3]. The silicide coatings were generally applied at 1478°K (2200°F). Protection from oxygen contamination under 1000 hour /922°K (1200°F) exposure conditions has been obtained from diffusion coatings of aluminum, silicon, nickel, zinc, chromium and nickel aluminide[4]. The aluminide and silicide coatings were considered more protective than the remainder of the diffused coatings because they exhibited low weight gains and an absence of scale formation. Other titanium intermetallic compounds that have shown good oxidation resistance at temperatures up to 1033°K (1400°F) are TiC, TiN, TiB and TiNi[5,6,7].

Coatings deposited on titanium alloys that have exhibited resistance to hot-salt stress-corrosion cracking include nickel plate, diffused aluminum, plasma sprayed aluminum, diffused zinc, diffused chromium and diffused silicon. Stress corrosion testing of electroplated nickel and diffused aluminum indicated that these coatings offered protection for at least 10,000 hours of exposure at 589°K (600°F)[8]. Plasma sprayed aluminum was considered to be protective in 728°K (850°F) stress corrosion tests[9]. Diffused aluminum and chromium coatings provided protection against hot-salt stress-corrosion for at least 1000 hours at 672°F (750°F)[4]. Diffused silicon and zinc coatings exhibited some cracking after 1000 hours of exposure at 672°K (750°F); however, failure was attributed to insufficient coating thickness or incomplete coating coverage[4].

Hard chromium plate has provided better dust erosion protection than aluminides, beryllides, borides and nickel oxides[10]. A titanium carbide coating

applied by chemical vapor deposition displayed excellent erosion resistance but significantly reduced fatigue strength[11]. Erosion tests on diffusion coatings indicated that nickel and chromium were protective at impingement angles of 20° and 90° while aluminum and silicon were protective only at the 20° impingement angle[4].

In this program, aluminides and silicides were evaluated as potential protective coating systems for titanium alloys. Deposition of aluminide coatings on superalloys and silicide coatings on refractory metals by diffusion techniques are well developed processes. Previous work indicated that diffusion coatings containing aluminum or silicon could provide oxidation and stress corrosion protection for titanium alloys. In addition, previous work indicated that diffusion coatings containing chromium and nickel provided erosion protection at both high and low impingement angles. Therefore, coatings selected for evaluation included both unmodified and modified variations of aluminides and silicides.

3.0 EXPERIMENTAL PROGRAM

The experimental program was divided into two major tasks: Task I - Screening Studies and Task II - Hot-Salt Stress-Corrosion Resistance. Specific subtasks in Task I were as follows:

a) Screen ten experimental coating compositions for oxidation and hot-salt stress-corrosion protectiveness on Ti-6-2-4-2 sheet.

b) Evaluate the ten experimental coatings for erosion resistance on Ti-6-2-4-2 sheet.

c) Select the five most promising coatings for evaluation of fatigue and ballistic impact properties on Ti-6-2-4-2 sheet.

d) Evaluate the five selected coatings for oxidation and hot-salt stress-corrosion protectiveness on Ti-13-11-3 sheet.

e) Select coatings for further investigation in Task 2.0.

The original objective of Task II involved optimization of the coatings selected in Task I. However, work in Task I disclosed that hot-salt stress-corrosion was a greater problem than originally anticipated. As a result of this finding, the Task II effort was redirected toward a more detailed evaluation of hot-salt stress-corrosion resistance under the following conditions:

a) Uncoated Ti-6-2-4-2 sheet from two separate heats.

b) Coated Ti-6-2-4-2 sheet.

c) Uncoated Ti-6-2-4-2 bar stock.

d) Coated Ti-6-2-4-2 bar stock.

3.1 Materials and Test Specimen Configurations

3.1.1 Substrate Materials

Chemical compositions and mill forms of the substrate materials used in this investigation are listed in Table I. The primary program material was the 1.27 mm (0.050 inch) sheet supplied by Timet (Heat No. V-3467). All of the Task I and the majority of the Task II effort on Ti-6-2-4-2 was performed with this material. Additional work on Ti-6-2-4-2 in Task 2.0 was performed using 1.57 mm (0.062 inch) sheet supplied by RMI (Heat No. 302824) and 1.91 cm (0.75 inch) diameter bar (Heat No. 293180) obtained from NASA. Heat treatments and vendor certified mechanical properties (where available) of the substrate materials are listed in Table II.

3.1.2 Test Specimen Configuration and Preparation

Tensile tests on sheet material were performed using the specimen configuration shown in Figure 1a. Creep tests were performed using the modified

TABLE I

CHEMICAL COMPOSITION OF TITANIUM ALLOY SUBSTRATE MATERIALS (WEIGHT PERCENT)

Alloy[a]	Vendor	Heat No.	Form	Source of Analysis	Al	Sn	Zr	Mo	V	Cr	Fe	N	C	O	H
6-2-4-2	Timet	V-3467	1.27 mm (0.050") sheet	Vendor[b]	6.3	2.02	4.38	2.03			0.22	0.02	0.044	0.06	0.009
	"	"	" " "	TRW[c]	6.5	2.17	4.45	1.99			.12	.002	.016	.03	.0074
6-2-4-2	RMI	302824	1.57 mm (0.062") sheet	Vendor[b]	6.3	2.1	3.8	2.1			.07	.007	.02	.129	.0036
6-2-4-2	RMI	293180	1.91 cm (0.75") bar	NASA[d]	6.3	2.0	3.8	2.0			.07	.009	.01	.098	.0070
13-11-3	Timet	G-4231	1.27 mm (0.050") sheet	Vendor[b]	3.25				13.8	11.2	.31	.03	.028	.15	.020

NOTES: (a) 6-2-4-2: Ti-6Al-2Sn-4Zr-2Mo
13-11-3: Ti-13V-11Cr-3Al

(b) Vendor - Certified Chemical Analysis

(c) TRW - Analysis No. 68551

(d) Literature - NASA TN D-6498 (Reference No. 12)

TABLE II

TITANIUM ALLOY HEAT TREATMENTS AND VENDOR CERTIFIED MECHANICAL PROPERTIES

Alloy[a]	Heat No.	Heat Treatment Cycles Studied		Tensile Strength		0.2% Yield Strength		% R.A.	% El.
		Designation	Treatment	(MN/m^2)	(ksi)	(MN/m^2)	(ksi)		
6-2-4-2	V-3467	Mill Anneal	As Received; 1200°K(1700°F), 1/2 hr, A.C.	944	137	881.9	128.0	-	19
↓	↓	Duplex Anneal	1228°K(1750°F), 1/2 hr, furnace cool plus 1061°K(1450°F), 1/4 hr, furnace cool	-	-	-	-	-	-
		Simulated Coating Cycle	1228°K(1750°F), 15 hrs, furnace cool	-	-	-	-	-	-
6-2-4-2	302824	Duplex Anneal	1172°K(1650°F), 1/2 hr, A.C. 1061°K(1450°F), 1/4 hr, A.C.	-	-	-	-	-	-
6-2-4-2	293180[b]	Mill Anneal	As Received; 1172°K(1650°F), 1 hr, A.C.	1120	162	-	-	33	18
13-11-3	G-4231	Mill Anneal	As Received; 1089°K(1500°F), 1/2 hr, A.C.	919.8	133.5	915.0	132.8	-	20
"	"	Duplex Anneal	1033°K(1400°F), 1/2 hr, A.C. 755°K(900°F), 48 hrs, A.C.	-	-	-	-	-	-

NOTES: (a) Ti-6-2-4-2 - Ti-6Al-2Sn-4Zr-2Mo
Ti-13-11-3 - Ti-13V-11Cr-3Al

(b) Data from NASA TND-6498 (Reference 12)

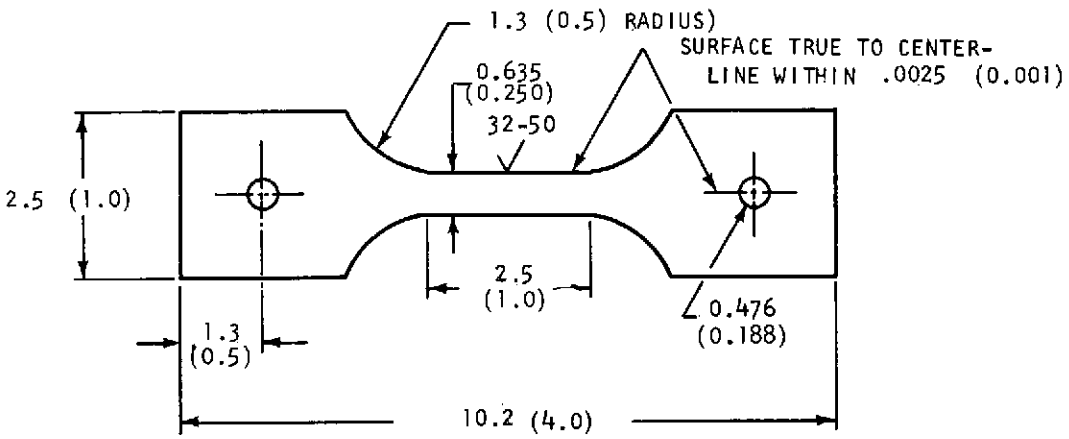

(a) Tensile and HSSC Specimens (Sheet)

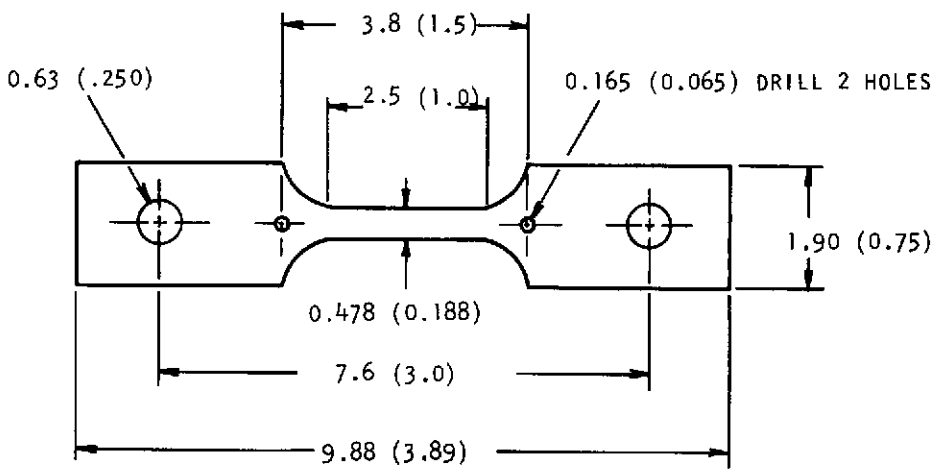

(b) Creep Specimen

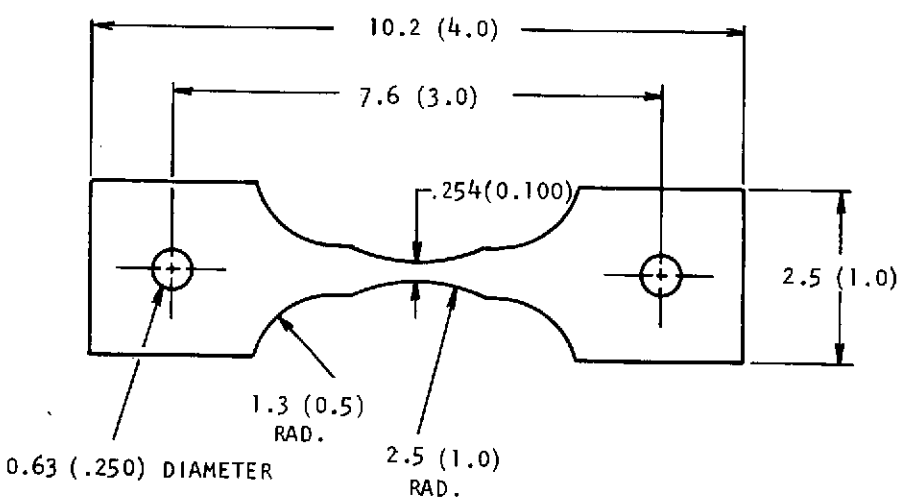

(c) Fatigue Specimen

Figure 1. Mechanical Test Specimens (All Dimensions are in cm (in.))

specimen shown in Figure 1b. Holes bored in the shoulder of the creep specimens permitted mounting of an extensometer. Mechanical fatigue tests were performed using the specimen shown in Figure 1c.

Hot-salt stress-corrosion testing was conducted using the flat tensile specimen shown in Figure 1a (sheet material), the tubular specimen shown in Figure 2a (bar stock) and the self-stressed bend specimen shown in Figure 2b (sheet material). Self-stressed bend specimens were fabricated in the following sequence:

a) Preform specimen details.

b) Coat specimen details.

c) Check detail geometry after coating.

d) Remove coating at detail end faying surfaces.

e) Double spot weld ends.

f) Trim excess material from ends (if necessary).

All test specimens were stress relieved by chemical milling in a solution of 3 volume percent hydrofluoric acid, 30 volume percent nitric acid and 67 volume percent water prior to coating and testing. A minimum of 0.0025 cm (0.001 inch) of metal was removed from all surfaces. In addition, the reduced sections of the fatigue specimens were polished with 600 grit emery paper. The polishing direction was such that all residual scratches were parallel to the specimen axis.

Metallographic specimens were prepared from the substrates and coatings using standard techniques. All specimens were etched in a solution 2 volume percent hydrofluoric acid, 2 volume percent nitric acid and 96 volume percent water.

3.2 Task I - Screening Tests

3.2.1 Coating Deposition Parameter Study

The purpose of the coating parameter study was to determine deposition parameters for obtaining two coating thickness levels for ten experimental coatings on Ti-6-2-4-2. Deposition temperatures had been established in previous work[13] so that the present parameter study was restricted to determining coating thickness as a function of deposition time. Table III lists coating source compositions, deposition processes and deposition temperatures for the 10 experimental coatings. The coatings were deposited using either pack cementation or slurry processes. Some of the coatings were applied in two separate deposition steps (duplex coatings) as indicated in the table. Table IV lists the vendors and particle sizes of the coating source materials. Silicon, chromium, magnesium and nickel were used in the form of elemental powders, while the remainder of the materials were purchased as alloy powders.

The deposition specimens were 1.27 x 1.91 x 3.81 cm (0.050 x 0.75 x 1.5 inch) coupons which were tumbled to round edges, chemically milled, and cleaned

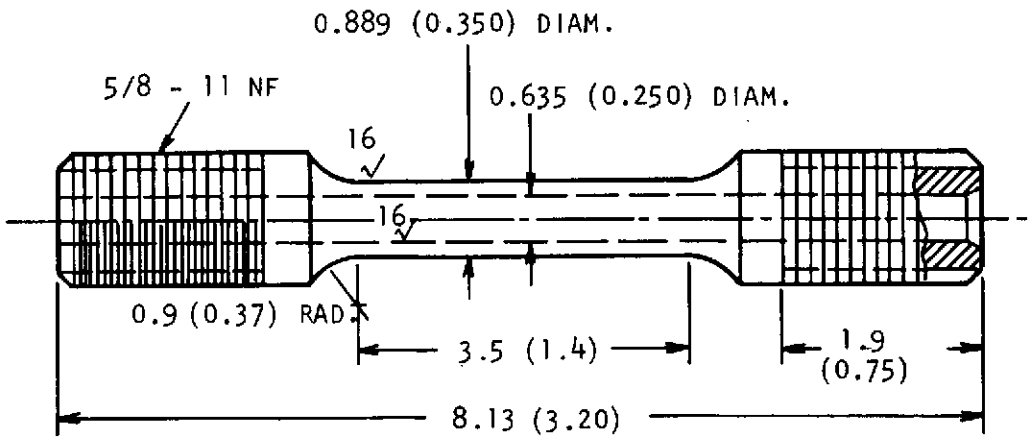

(a) Tubular Specimen (Bar Stock)

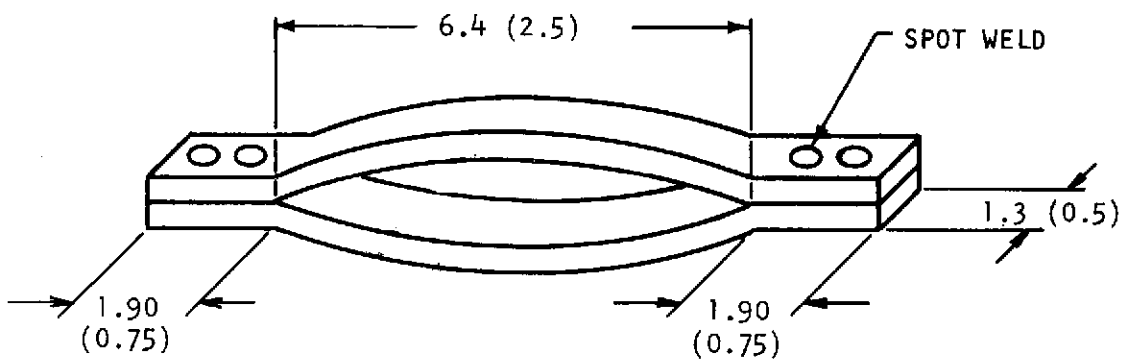

(b) Self-Stressed Specimen (Sheet)

Figure 2. Hot-Salt Stress-Corrosion Test Specimens (All Dimensions are in cm (in.))

TABLE III

EXPERIMENTAL COATING SYSTEMS

Coating No.	System Designation	Source Composition (weight percent) and Deposition Method	Deposition Temperature °K	Deposition Temperature °F
1	Al	56Cr-44Al Alloy, Pack Cementation	1200	1700
2	Si	Si Metal, Slurry	1228	1750
3	Duplex Cr / Al-Mg	Cr Metal, Slurry 90(56Cr-44Al Alloy) + 10 Mg, Pack Cementation	1228 1200	1750 1700
4	Al-Si	87Al-13Si, Slurry	922	1200
5	Al-Mg	90(56Cr-44Al Alloy) + 10 Mg, Pack Cementation	1200	1700
6	Duplex Cr-Fe / Al-Mg	(75Cr-25Fe Alloy), Slurry 90(56Cr-44Al Alloy) + 10 Mg, Pack Cementation	1228 1200	1750 1700
7	Si-Cr-Al	71Si + 25Cr + 4 (87Al-13Si Alloy), Slurry	1228	1750
8	Ni-Cr-Al-Si	50Ni + 20Cr + 30 (87Al-13Si Alloy), Slurry	1200	1700
9	Duplex Cr / Al-Si	Cr Metal, Slurry, (87Al-13Si Alloy), Slurry	1228 922	1750 1200
10	Ni-Fe-Al-Si	40Ni + 40(50Fe-50Al Alloy) + 20 (87Al-13Si Alloy), Slurry	1228	1750

TABLE IV

SOURCE MATERIALS USED TO DEPOSIT COATINGS

Composition	Particle Size[(a)] (μm)	Vendor
Si	4.0	Cerac Inc.
Cr	1.3	Cerac Inc.
Mg	177 - 210	Fisher Scientific Co.
Ni	44	Charles Hardy Inc.
56 w/o Cr - 44 w/o Al Alloy	44-297	TRW Metals Division
87 w/o Al - 13 w/o Si Alloy	44	Valley Metallurgical Processing Co.
75 w/o Cr - 25 w/o Fe Alloy	44-297	Shieldalloy
50 w/o Fe - 50 w/o Al Alloy	0.55	Cerac Inc.

NOTE: (a) Average particle sizes, except where range is indicated.

with acetone prior to coating. Slurry coatings were applied by dipping in suspensions consisting of 100 grams of powder in 300 ml of cellulose nitrate to obtain a bisque weight of approximately 50 mg/cm^2. The green bisques were air dried and fired in a 10^{-2} torr vacuum furnace (Figure 3). The slurry coated specimens were supported by bubbled alumina contained within Inconel retorts during firing. Pack cementation coatings were deposited from packs containing source material plus 1/2 weight percent $CrCl_3$ activator. The packs were contained in Inconel retorts and heated in a 10^{-2} torr vacuum.

Coating thickness levels were designated as A and B. Deposition times were adjusted so that the B levels were approximately twice the A levels. Coating thickness data is summarized in Figure 4. A complete tabulation of the coating data can be found in Appendix A, Table A-1. Representative microstructures of the coatings on Ti-6-2-4-2 are compared with uncoated material in Figures 5 through 8. Except for coating No. 4, the coated substrates exhibited growth of the β phase during coating deposition at 1200 or 1228°K (1700 or 1750°F). Coating No. 4 was deposited at 922°K (1200°F) and the substrate appears to be comparable to uncoated material. Observations on individual coatings are summarized below.

Coating No. 1, an aluminide containing small amounts of chromium, produced an α case in the substrate adjacent to the coating (Figure 5c). Coating No. 5, Figure 5d, deposited from a Mg modified Cr/Al pack, is similar in appearance to coating No. 1. Coating thicknesses of up to 38 μm (0.0015 inch)were obtained from both pack compositions at the maximum deposition time of 8 hours.

As-deposited microstructure of coating No. 2, a Si slurry, and coating No. 7, a Si-Cr-Al slurry, are shown in Figure 6. Both coatings consist of a single phase outer layer with a band of a precipitated phase adjacent to the unaffected substrate. While elemental chromium was an integral part of the slurry used for coating No. 7, its deposition was either minor or its beta stabilizing effect was offset by α stabilizing aluminum. Metallographic coating thicknesses of up to 19 μm (0.00075 inch) were obtained for both coatings at the maximum deposition time of 12 hours.

As-deposited microstructures of the duplex coatings are shown in Figure 7. Chromium pre-coats were deposited for coatings No. 3 and 9 (Figures 7a and 7b) using a chromium slurry. An Fe/Cr slurry was used to deposit the pre-coat for coating No. 6 (Figure 7c). The pre-coated specimens were subsequently aluminized by either the pack or slurry processes. These coatings consist of an outer aluminide layer with a chromium rich layer adjacent to the unaffected substrate. All three coatings probably contain appreciable amounts of β phase in the layer adjacent to the unaffected substrate due to the presence of the β stabilizing elements Fe and Cr. Maximum coating thicknesses obtained for the pre-coats were 76 μm (0.003 inch) for Cr and 45 μm (0.00175 inch) for Fe/Cr. Maximum total coating thicknesses obtained were 102 μm (0.004 inch), 64 μm (0.0025 inch) and 83 μm (0.00325 inch) for coatings No. 3, 6 and 9, respectively.

Microstructures of as-deposited slurry coatings No. 4, 8 and 10 are presented in Figure 8. Coating No. 4, Al-Si, consists of a distinct layer with no apparent α stabilized zone beneath the coating (Figure 8a). Maximum coating thickness for coating No. 4 was 25 μm (0.001 inch). Coating No. 8, Ni-Cr-Al-Si, consists of a single phase outer coating with no apparent stabilized zone

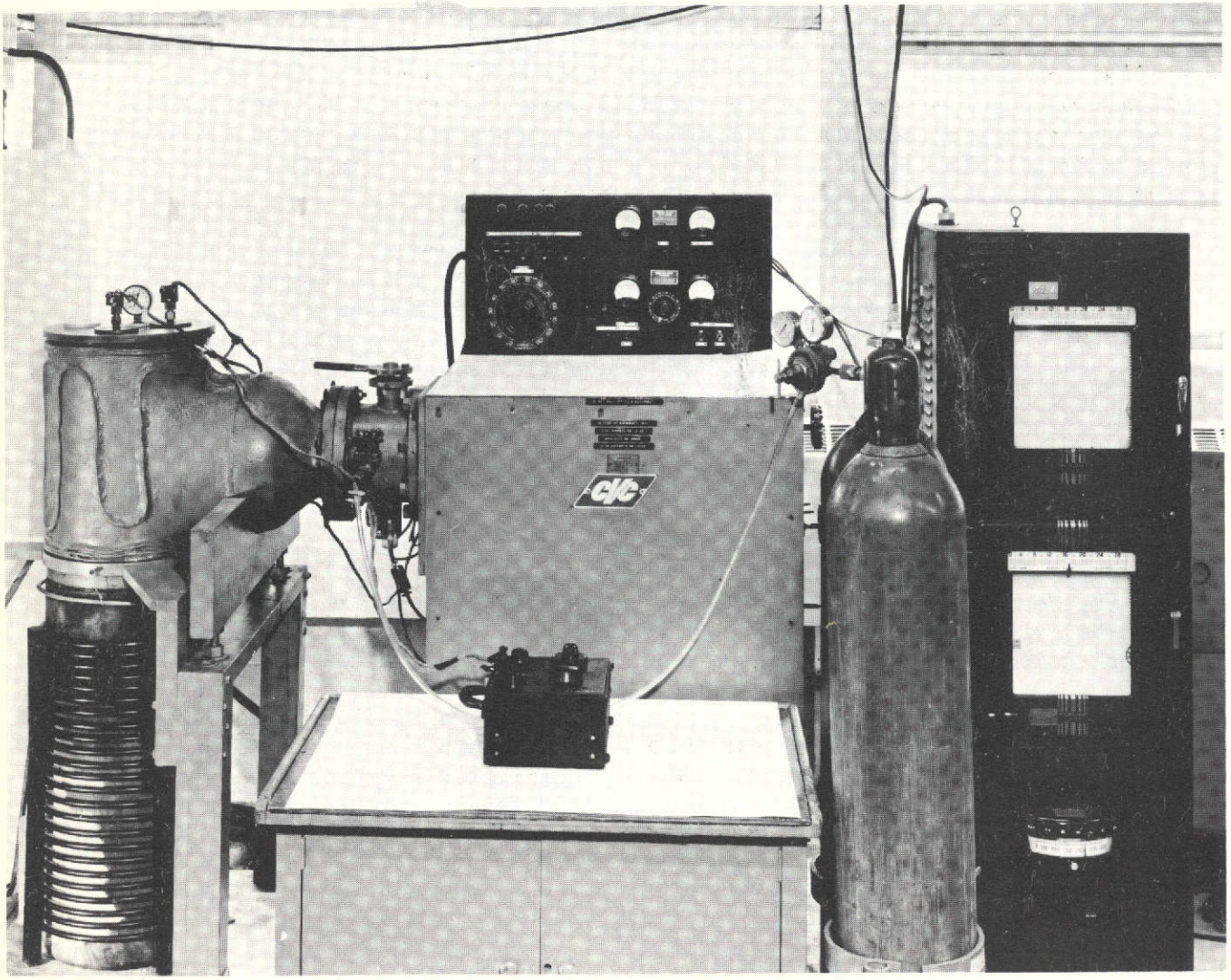

Figure 3. Vacuum Coating Furnace

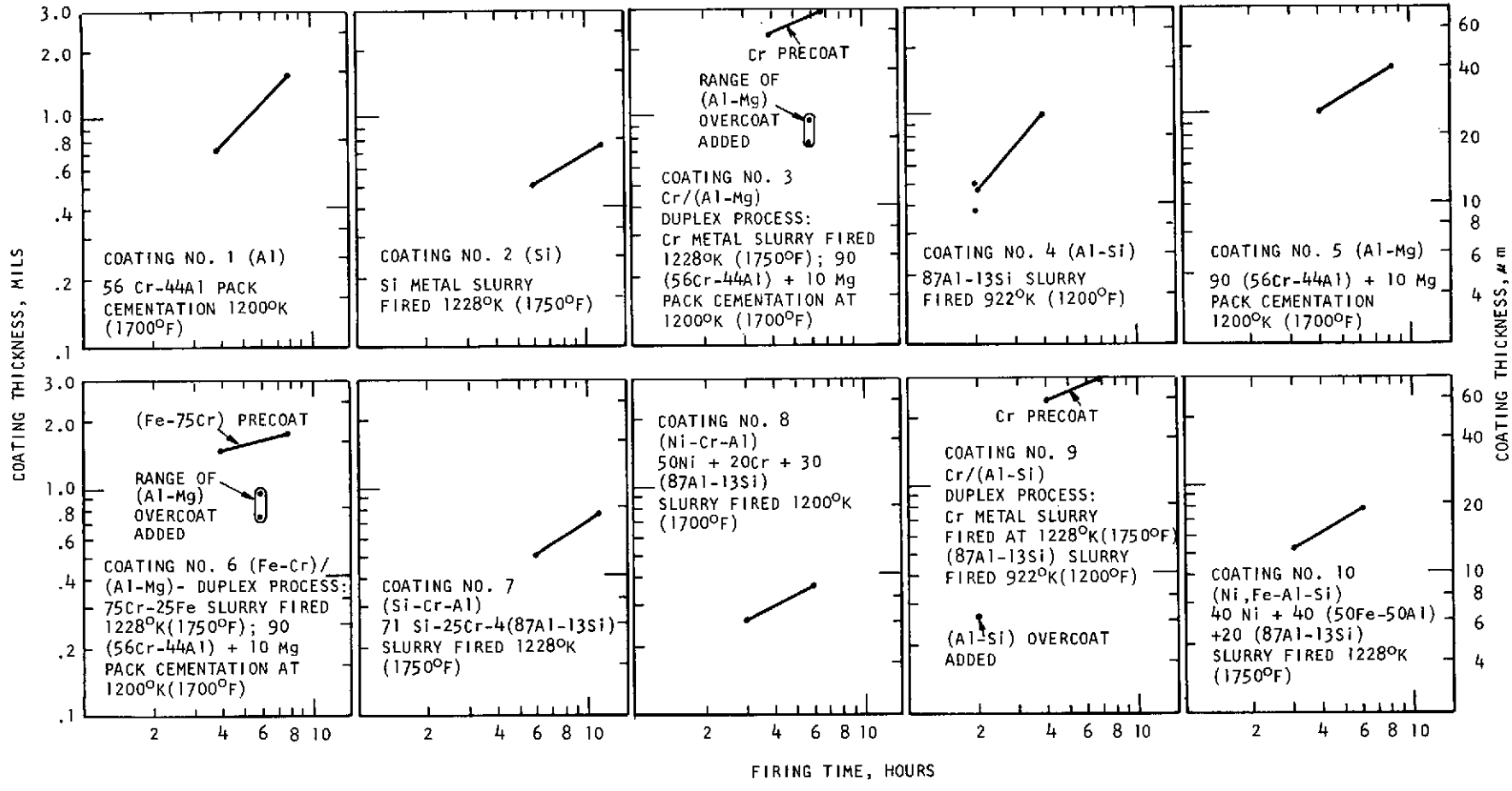

Figure 4. Influence of Deposition Time on Metallographic Coating Thickness

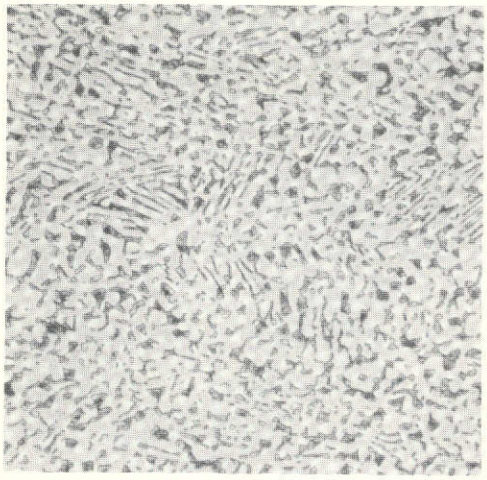

(a) Ti-6-2-4-2,
Transverse

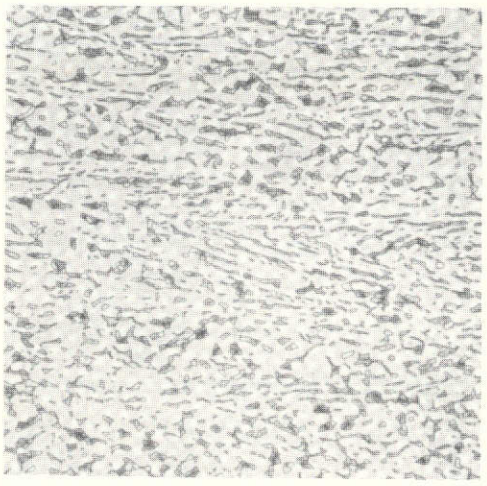

(b) Ti-6-2-4-2,
Longitudinal

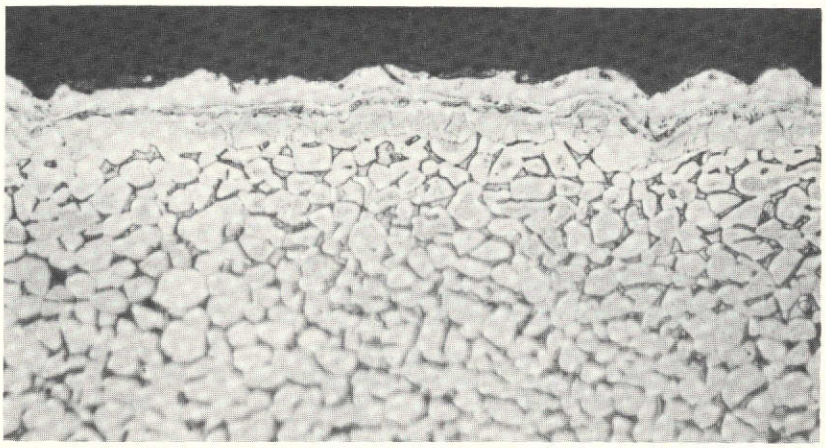

(c) Coating No. 1 - Al

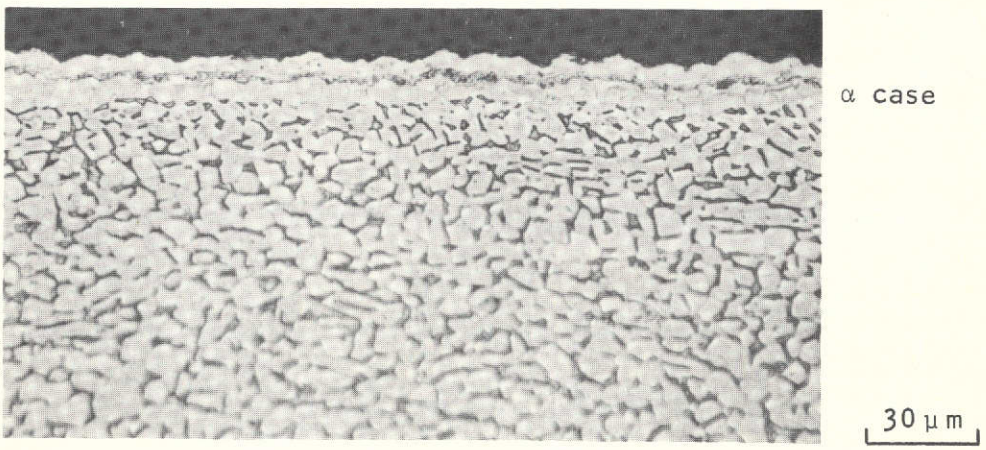

(d) Coating No. 5 - Al-Mg

Figure 5. Microstructure of Uncoated Ti-6-2-4-2 Transverse and Longitudinal to the Major Rolling Direction, (a) and (b) and Coatings No. 1 and No. 5, (c) and (d)

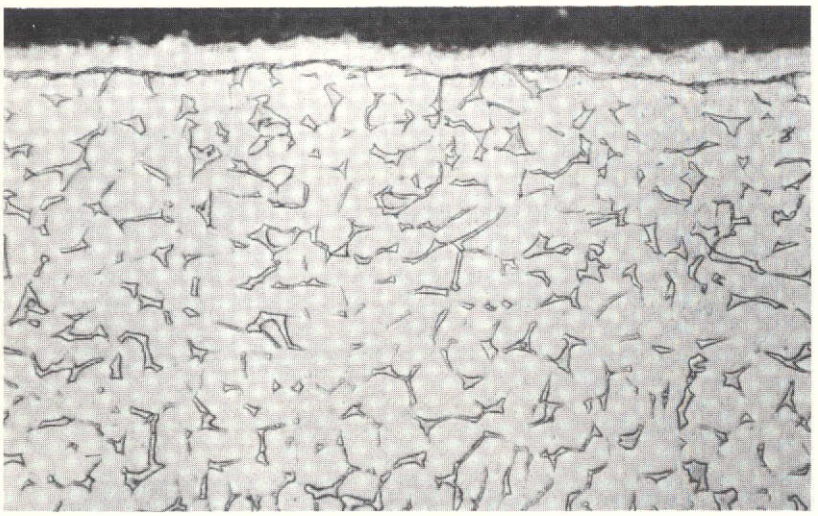

(a) Coating No. 2 - Si

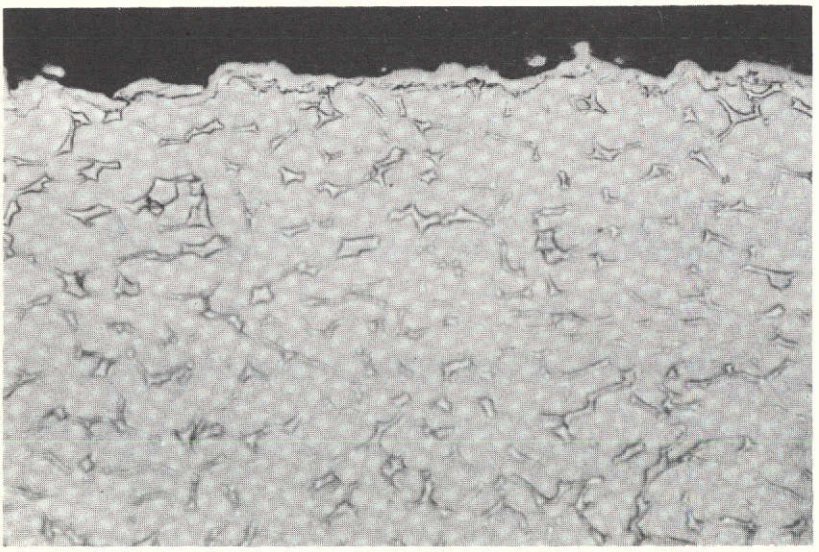

(b) Coating No. 7 - Si-Cr-Al

Figure 6. As Deposited Microstructures of Coatings 2 and 7 on Ti-6-2-4-2

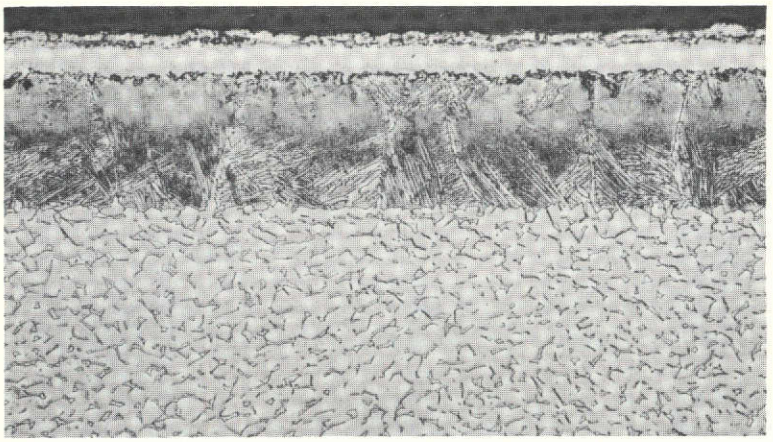

(a) Coating No. 3 - Cr + (Al-Mg)

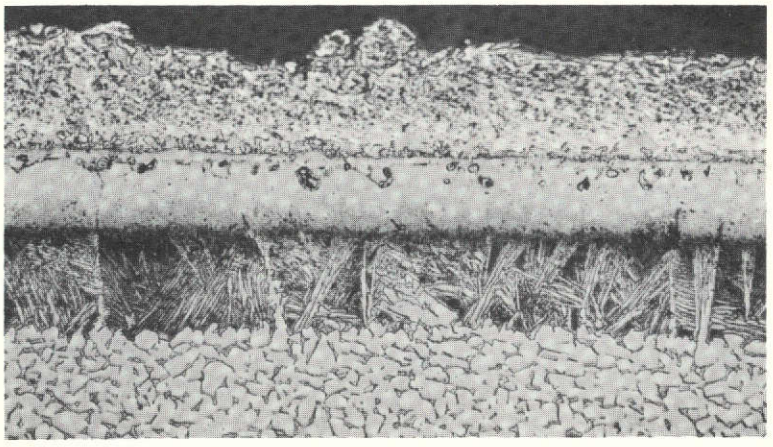

(b) Coating No. 9 - Cr + (Al-Si)

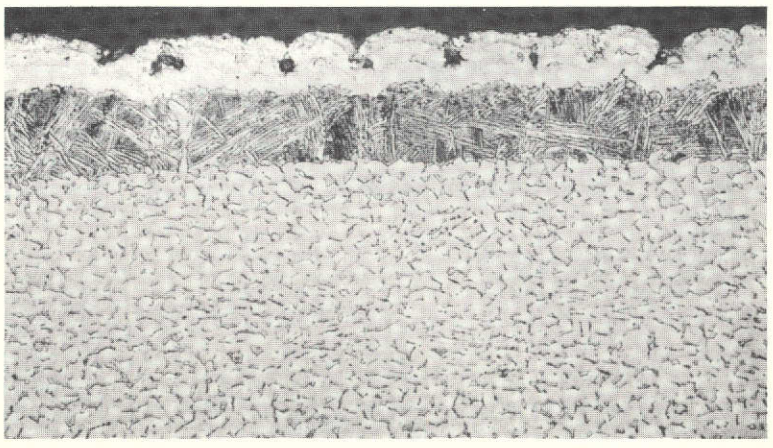

(c) Coating No. 6 - (Cr-Fe) + (Al-Mg)

Figure 7. Microstructures of Duplex Coatings No. 3, 9 and 6

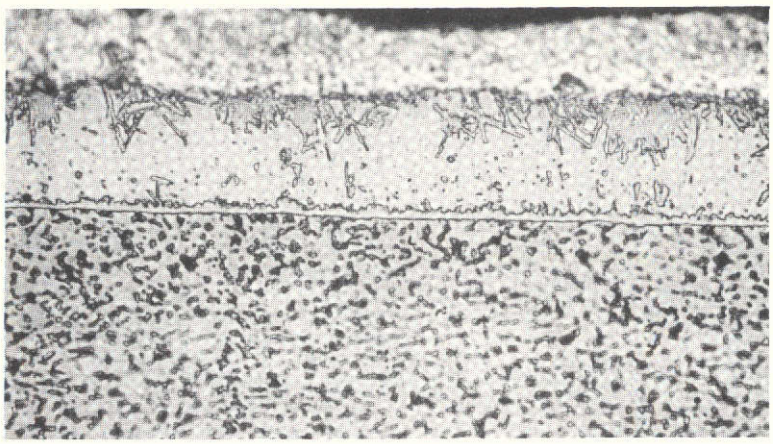

(a) Coating No. 4 - Al-Si

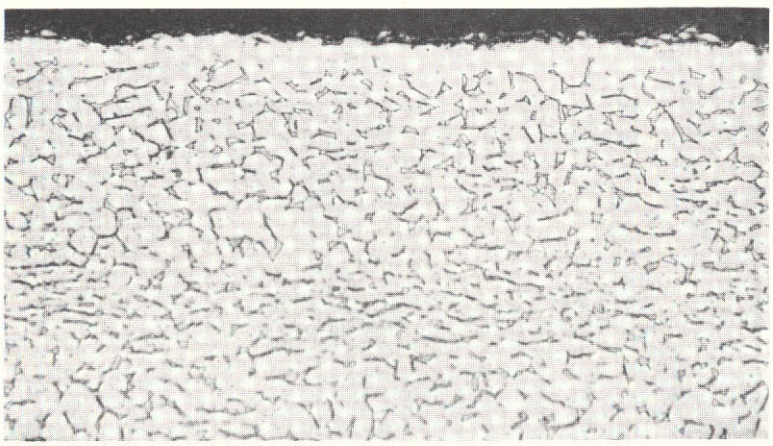

(b) Coating No. 8 - Ni-Cr-Al-Si

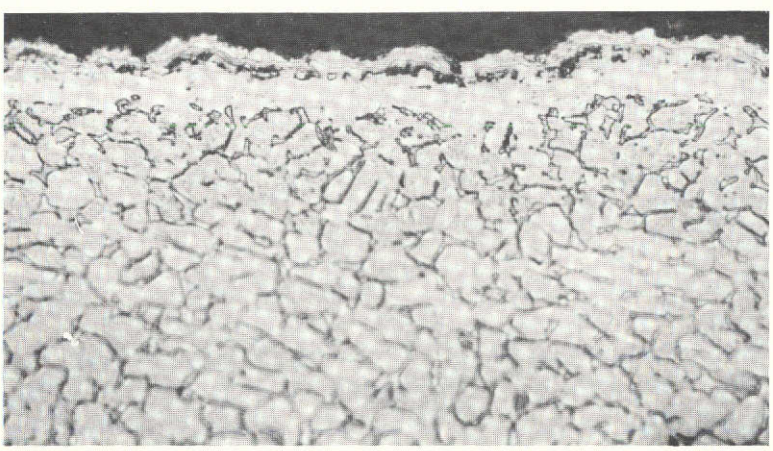

(c) Coating No. 10 - Ni-Fe-Al-Si

Figure 8. Microstructure of Slurry Deposited Coatings No. 4, 8 and 10 on Ti-6-2-4-2

adjacent to the substrate. Maximum coating thickness for coating No. 8 was 9 μm (0.00035 inch). Coating No. 10, Ni-Fe-Al-Si, contained a distinct zone of secondary phase at the coating mid-thickness. Maximum coating thickness for coating No. 10 was 19 μm (0.00075 inch).

3.2.2 Coating of Ti-6-2-4-2 Evaluation Specimens

Evaluation specimens of Ti-6-2-4-2 were coated using deposition parameters selected from the work described in Section 3.2.1. Coatings were deposited at the A and B thickness levels on mill annealed Ti-6-2-4-2 tensile and fatigue specimens, self-stressed corrosion blanks and coupons. Ti-13V-11Cr-3Al coupons were included in each run to determine deposition parameters for this alloy. To improve uniformity, slurry coatings were sprayed rather than dipped; otherwise, deposition procedures were identical to those used for the parameter studies. Complete coating parameter data, weight gains and coating thickness data can be found in Appendix A, Tables A-2 and A-3. Coating thickness data is summarized in Table V. On Ti-6-2-4-2 the B (heavier) coating thickness was usually less than twice the A coating thickness. For coating No. 2, the same thickness was obtained at both 4 and 15 hour deposition times. Coating thicknesses obtained on the Ti-13-11-3 alloy were comparable to those obtained on Ti-6-2-4-2.

3.2.3 Oxidation Exposure Tests

3.2.3.1 Weight Gains of Exposed Tensile Specimens

Coated and uncoated tensile specimens were oxidation exposed in static air unstressed for 1000 hours at 922°K (1200°F). Weight gains of the specimens were determined by cycling to room temperature at 100 hour intervals. Cumulative weight gains for all coatings and the uncoated specimens are plotted in Figure 9 and the total weight after 1000 hours of exposure is summarized in Table VI. Nearly all coatings provided significant protection from oxidation as reflected by the lower weight gains exhibited by the coated specimens. Particularly outstanding were coatings 1, 3, 5 and 6. These coatings had weight gains in the range 0.025 to 0.088 mg/cm^2 compared to 1.110 mg/cm^2 for uncoated material. The large drop in weight gain shown by coating 4 after 200 hours of exposure was primarily due to removal of the bisque. Although difficult to remove after coating, the bisque was easily removed after 200 hours of exposure.

3.2.3.2 Electron Microprobe Analysis of Oxidation Exposed Specimens

Coated and uncoated specimens of Ti-6-2-4-2 exposed for 1000 hours at 922°K (1200°F) were semi-quantitatively analyzed for oxygen content using a Phillips electron probe microanalyzer. The analysis consisted of continuous 100 second scans of areas immediately below the coatings (or surface of uncoated specimens) and at the substrate mid-thickness as shown in Figure 10. The scan area beneath the coatings was the α layer in those instances where an α layer was present in the microstructure. Results of the analysis are presented in Table VII. The uncoated specimen exhibited a significantly higher concentration of oxygen near the surface compared to the mid-thickness. Coated specimens had oxygen contents near the surface either lower or approximately equivalent (coatings 2A and 9A) to the oxygen contents at the specimen mid-thickness. The data indicate that all of the coatings protected the substrate from oxidation at 922°K (1200°F).

TABLE V

COATING DEPOSITION DATA FOR Ti-6-2-4-2 EVALUATION SPECIMENS AND Ti-13-11-3 COUPONS

Coating No.	Coating Source	Ti-6-2-4-2				Ti-13-11-3			
		A Thickness		B Thickness		A Thickness		B Thickness	
		µm	in.x.001	µm	in.x.001	µm	in.x.001	µm	in. x.001
1	Cr/Al Pack	9.7	0.38	19.1	0.75	11.2	0.44	19.1	0.75
2	Si Slurry	6.4	0.25	6.4	0.25	4.8	0.19	6.4	0.25
3	Cr Slurry Cr/Al+Mg Pack	25.4 45.7	1.0 1.8	12.7-25.4 50.8	0.5-1.0 2.0	12.7 15.2	0.50 0.60	16.0 15.2	0.63 0.60
4	Al/Si Slurry	6.4	0.25	20.8	0.82	3.8	0.15	6.4	0.25
5	Cr/Al+Mg Pack	12.7	0.5	19.1	0.75	12.7	0.50	19.1	0.75
6	Fe/Cr Slurry Cr/Al+Mg Pack	9.7 9.7	0.38 0.38	12.7 12.7	0.50 0.50	12.7 15.2	0.50 0.60	16.0 15.2	0.63 0.60
7	Si+Cr+Al/Si Slurry	5.1	0.20	12.7	0.50	3.3	0.13	12.7	0.50
8	Ni+Cr+Al/Si Slurry	12.7	0.50	19.1	0.75	6.4	0.25	12.7	0.50
9	Cr Slurry Al/Si Slurry	12.7 31.8	0.50 1.25	19.1 33.0	0.75 1.30	15.2 31.8	0.60 1.25	15.2 31.8	0.60 1.25
10	Ni+Fe/Al+Al/Si Slurry	6.4	0.25	19.1	0.75	6.4	0.25	15.2	0.60

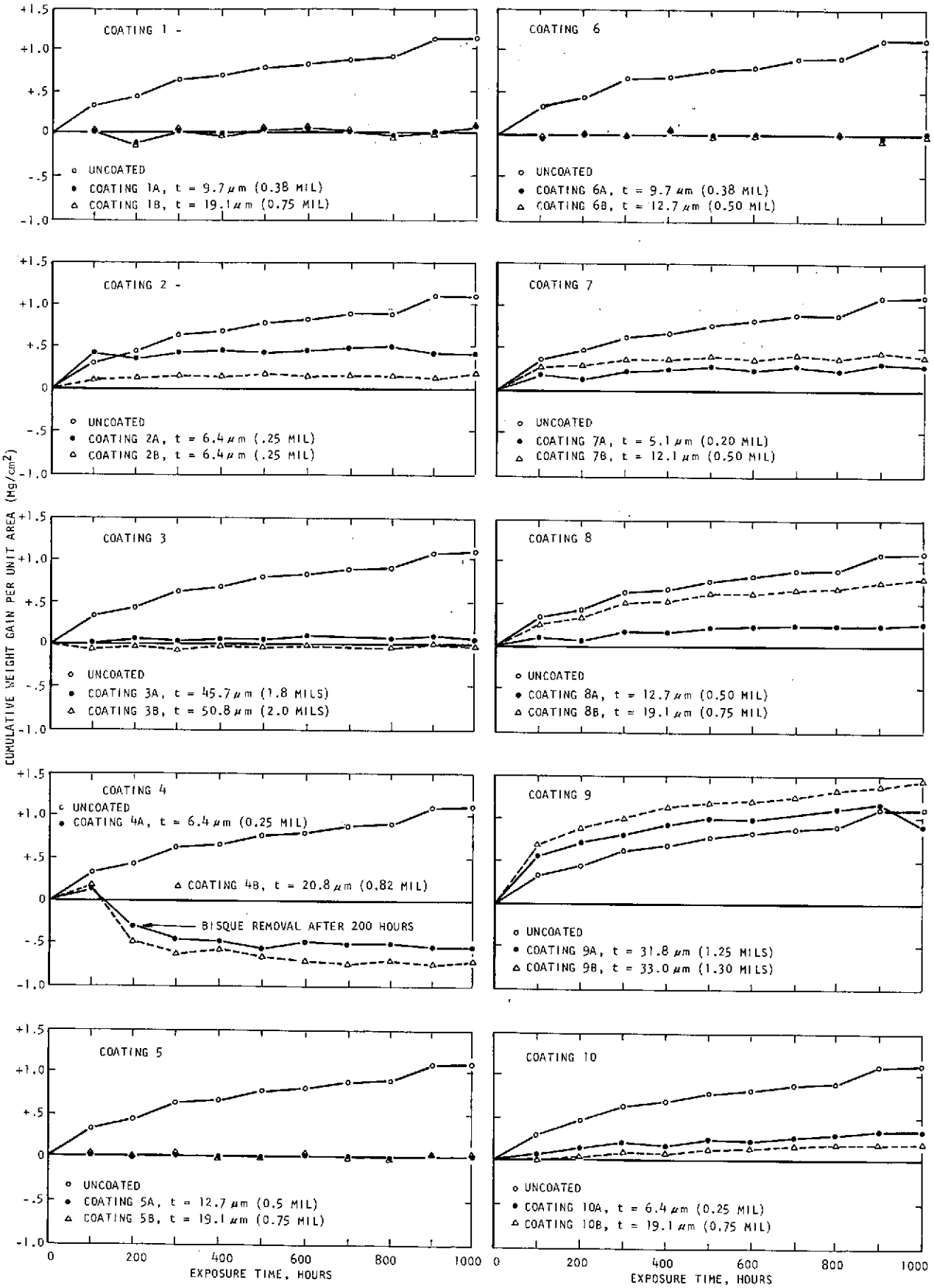

Figure 9. Cumulative Weight Gains of Uncoated, Mill-Annealed Ti-6-2-4-2 and Coated Ti-6-2-4-2 Exposed at 922°K (1200°F).

TABLE VI

TOTAL WEIGHT GAINS FOR COATED AND UNCOATED
Ti-6-2-4-2 AFTER 1000 HR/922°K (1200°F) OXIDATION EXPOSURE

Coating No.	Rank[a]	Average Wt. Gain, A Level mg/cm^2	Average Wt. Gain, B Level mg/cm^2
Uncoated	-	1.110	-
6	1	0.05	0.025
3	2	0.075	0.012
5	3	0.075	0.075
1	4	0.075	0.088
10	5	0.275	0.250
2	6	0.463	0.200
7	7	0.325	0.438
8	8	0.278	0.820
9	9	0.903	1.463
4	-	-0.53	-0.70

NOTE: (a) Coating No. 4 was omitted from the ranking because the true weight gain could not be established.

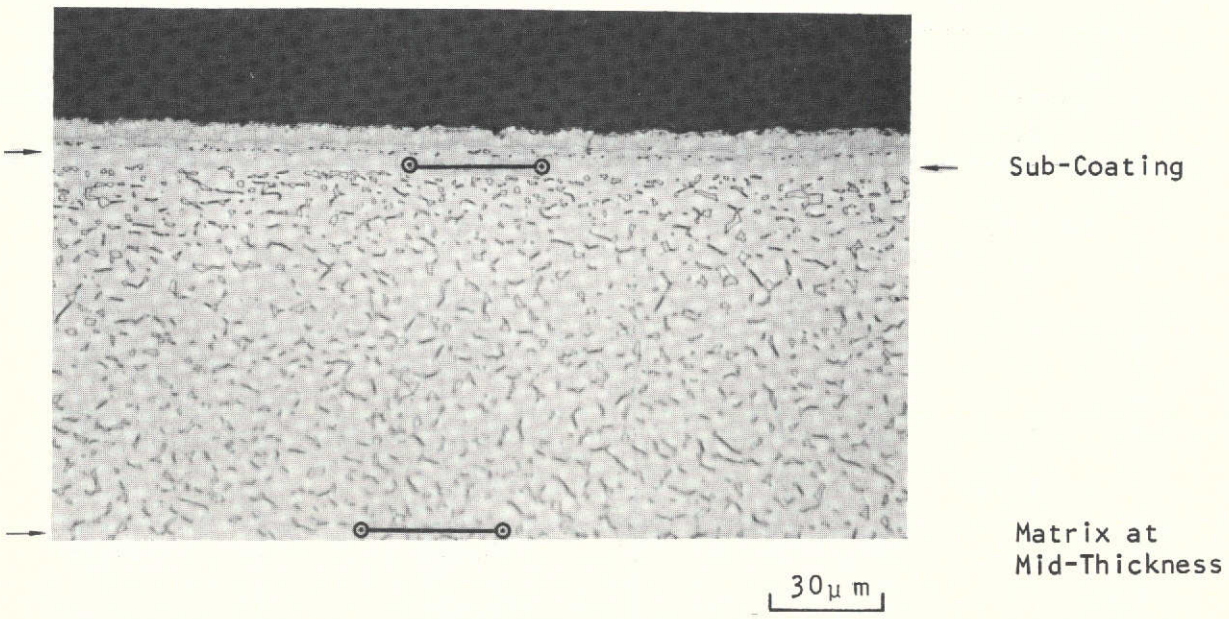

Figure 10. Location of EMP Oxygen Analyses

TABLE VII

MICROPROBE ANALYSIS OF EXPOSED[a] COATED AND UNCOATED Ti-6-2-4-2

Specimen	Oxygen (Counts per 1000 seconds) Surface[b]	Matrix[c]	Ratio Surface/Matrix
Uncoated	1448	1092	1.33
1A	892	1035	0.86
2A	1005	1000	1.05
3A	797	920	0.86
4A	925	977	0.95
5A	952	1035	0.92
6A	662	712	0.93
7A	617	672	0.92
8A	562	675	0.83
9A	1092	1076	1.01
10A	1032	1097	0.94

NOTES: (a) 1000 hours at 922°K (1200°F) in air.

(b) Approximately 12.7 μm beneath the surface of uncoated specimen and 12.7 μm beneath the coating/substrate interface.

(c) Variation in matrix counts due to slight variation in beam current which was maintained constant for each specimen but varied from specimen to specimen.

3.2.3.3 Metallography of Exposed Coatings

Coated Ti-6-2-4-2 specimens at the A thickness level were evaluated metallographically in the as-deposited condition and after 1000 hr/922°K (1200°F) static oxidation exposure together with comparably exposed uncoated Ti-6-2-4-2. Microstructures of uncoated mill annealed Ti-6-2-4-2 in the unexposed and exposed conditions are shown in Figure 11. An appreciable oxide film formed on the surface of the exposed specimen, but there was apparently insufficient oxygen penetration in the substrate to produce a stabilized α layer beneath the oxide. Microstructures of as-deposited and exposed coated specimens are compared in Figures 12 through 16. Exposure did not result in observable structural changes in coatings 1, 2, 3, 4, 5, 7, 8 and 10. Structural changes were observed in coatings 6 and 9. Exposure of coating 6 (Figures 14c and 14d) resulted in a band of fine precipitates delineating the boundary between the aluminide layer and the Fe/Cr layer. Exposure of coating 9 (Figures 16a and 16b) produced an apparent inward diffusion of chromium as evidenced by broadening of the chromized layer. Gross oxide penetration in the aluminide layer is also evident in the exposed microstructure of coating 9.

3.2.3.4 Tensile Tests

Tensile specimens of Ti-6-2-4-2 coated with each of the 10 coating systems at two thicknesses per coating were oxidized in static air at 922°K (1200°F) for times of 100 and 1000 hours. Uncoated mill annealed Ti-6-2-4-2 and uncoated Ti-6-2-4-2 that had been heat treated in argon for 15 hours at 1228°K (1750°F) were exposed together with the coated specimens. The 15 hr/1228°K (1750°F) heat treatment simulated the most severe coating thermal cycle. Following exposure the specimens were tensile tested at room temperature on an Instron test machine using a constant cross-head speed of 0.125 mm/min (0.005 in/min). Tensile properties were also determined for uncoated, unexposed specimens in the mill annealed and 15 hr/1228°K (1750°F) heat treated conditions.

All of the tensile data is listed in Appendix B (Table B-1). Average tensile properties of the uncoated specimens are summarized in Table VIII. Unexposed, mill annealed material had an UTS of 945.3 MN/m^2 (137.2 ksi), a 0.2% Y.S. of 842.6 MN/m^2 (122.3 ksi) and an elongation of 14.2%. The simulated coating thermal cycle lowered the U.T.S. and 0.2% Y.S. to 922.6 MN/m^2 (133.9 ksi) and 824.0 MN/m^2 (119.6 ksi), respectively, and reduced the elongation to 9.6%. Upon exposure the tensile properties of both heat treated conditions followed a similar pattern. Exposure for 100 hours increased the yield strength and decreased elongation. After 1000 hours of exposure, strength and elongation were degraded with respect to both the unexposed and 100 hour exposed conditions. The property most severely degraded by the exposure was tensile elongation. After 1000 hours of exposure, both heat treated conditions had a residual elongation of only 4.7%.

To obtain a quantitative rating of coating performance, duplicate data were obtained from coated specimens. Comparisons were made between the unexposed coated specimens and the uncoated specimens on the basis of U.T.S., 0.2% Y.S. and % elongation. Tensile properties of the uncoated Ti-6-2-4-2 specimens in the following conditions were used as base lines:

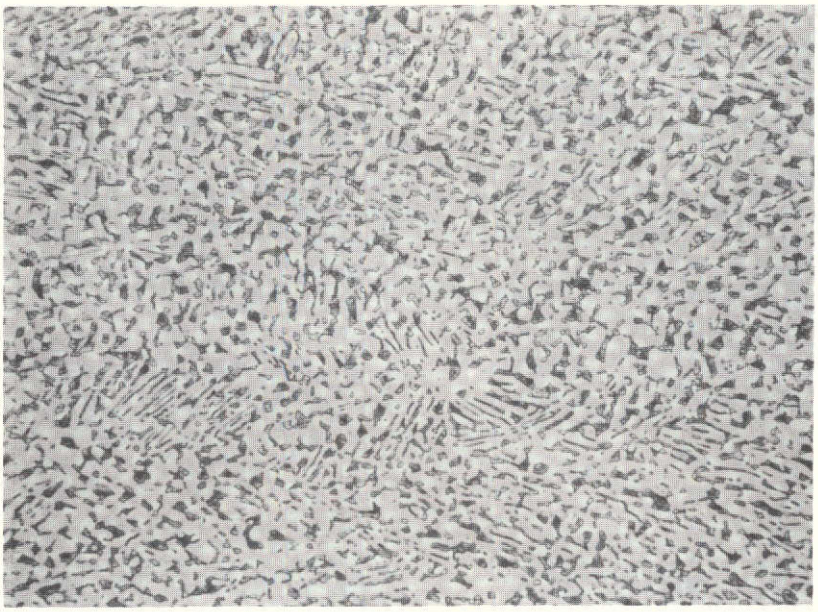

(a)

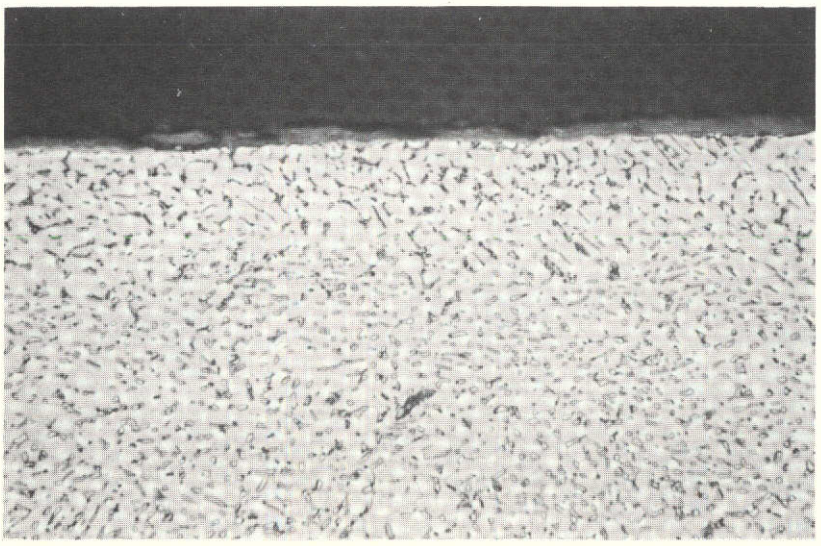

(b)

Figure 11. Microstructures of Uncoated Mill Annealed Ti-6-2-4-2 in the Unexposed Condition (a) and After 1000 Hr/922°K (1200°F) Exposure (b). Both Sections are Perpendicular to the Major Rolling Direction of the Sheet

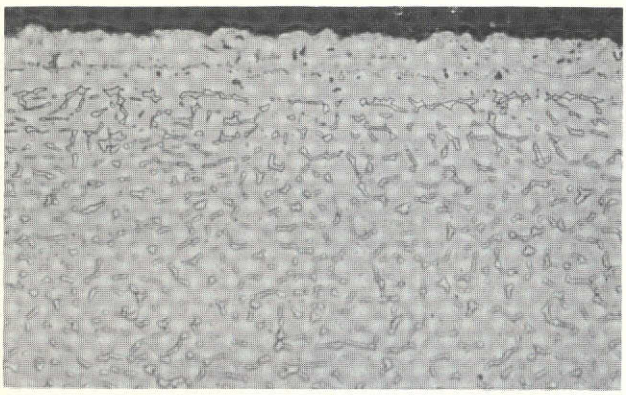

(a) Coating No. 1 - Al, As Deposited

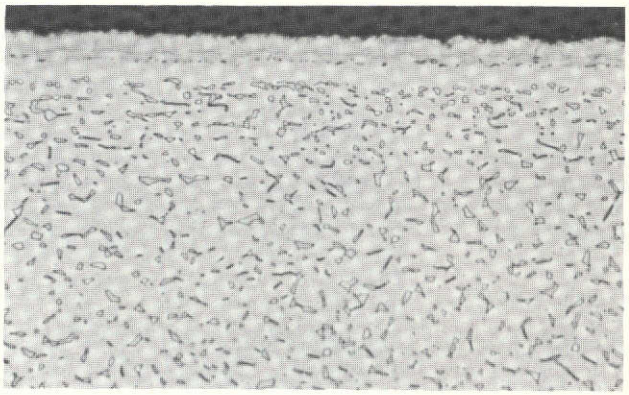

(b) Coating No. 1 - Al, Exposed

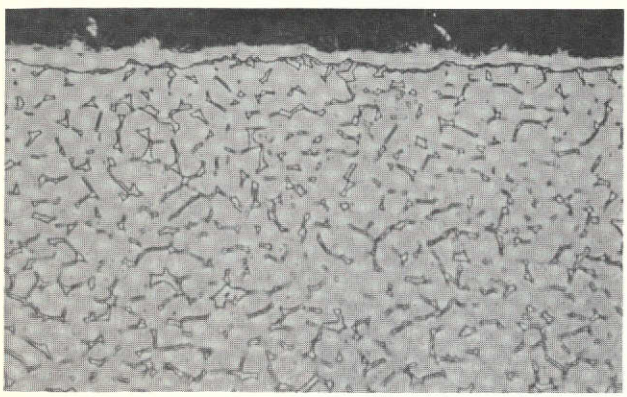

(c) Coating No. 2 - Si, As Deposited

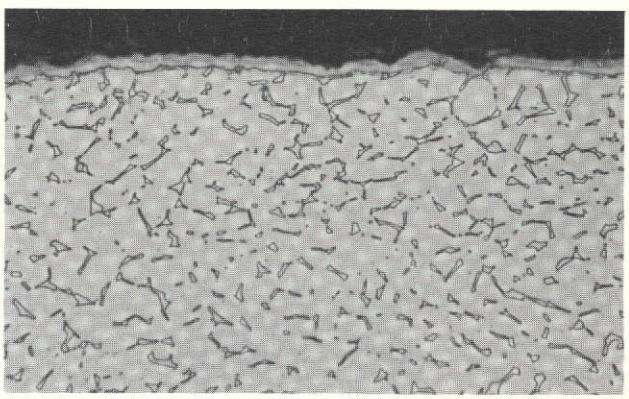

(d) Coating No. 2 - Si Exposed

30 μm

Figure 12. Microstructures of Coatings Nos. 1 and 2 on Ti-6-2-4-2 in the As-Deposited Condition and After 1000 hr/922°K (1200°F) Oxidation Exposure

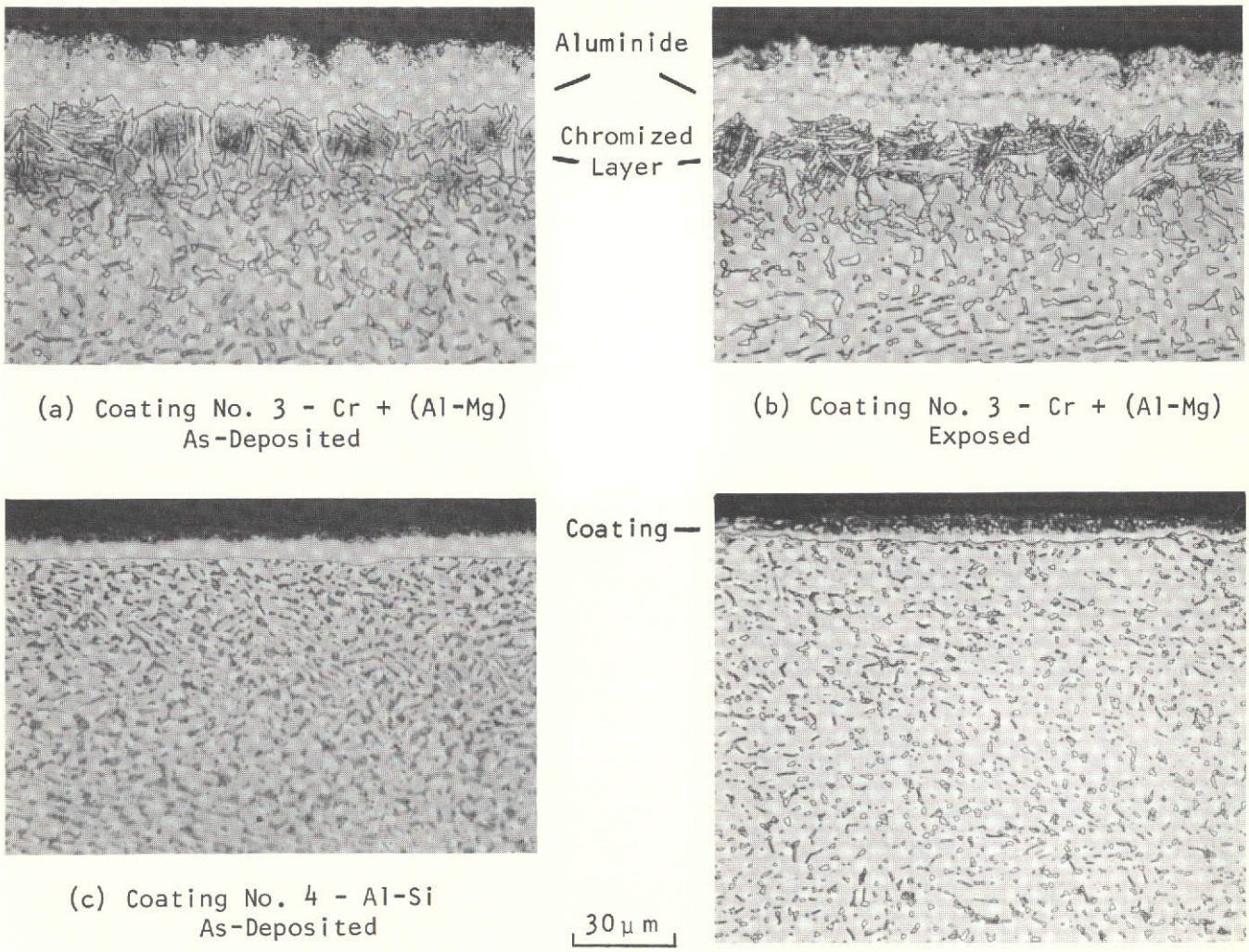

(a) Coating No. 3 - Cr + (Al-Mg) As-Deposited

(b) Coating No. 3 - Cr + (Al-Mg) Exposed

(c) Coating No. 4 - Al-Si As-Deposited

(d) Coating No. 4 - Al-Si Exposed

Figure 13. Microstructures of Coating Nos. 3 and 4 on Ti-6-2-4-2 in the As-Deposited Condition and After 1000 hr/922°K (1200°F) Oxidation Exposure

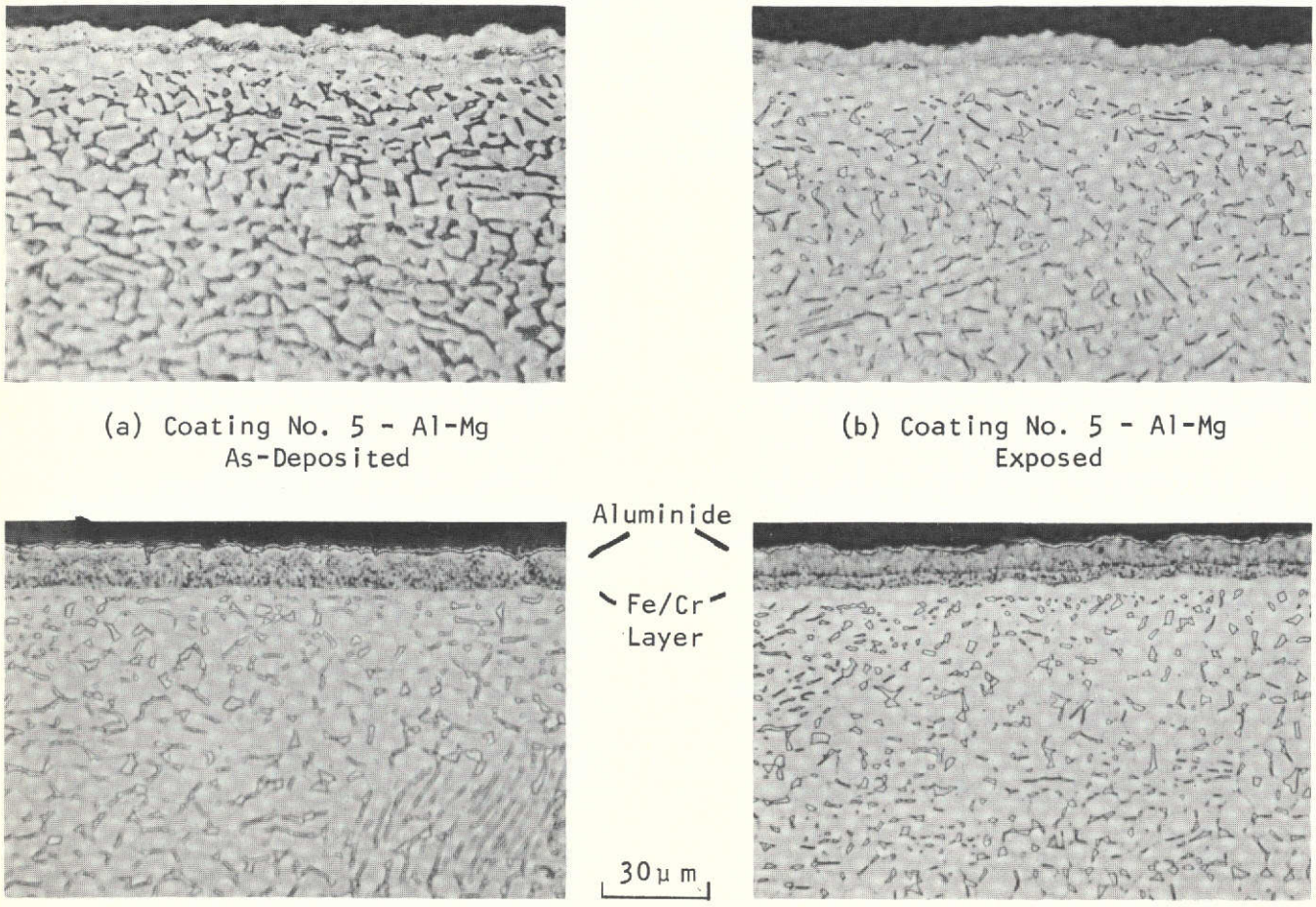

(a) Coating No. 5 - Al-Mg
As-Deposited

(b) Coating No. 5 - Al-Mg
Exposed

(c) Coating No. 6 - (Cr-Fe) + (Al-Mg)
As-Deposited

(d) Coating No. 6 - (Cr-Fe) + (Al-Mg)
Exposed

Figure 14. Microstructures of Coating Nos. 5 and 6 on Ti-6-2-4-2 in the As-Deposited Condition and After 1000 hr/922°K (1200°F) Oxidation Exposure

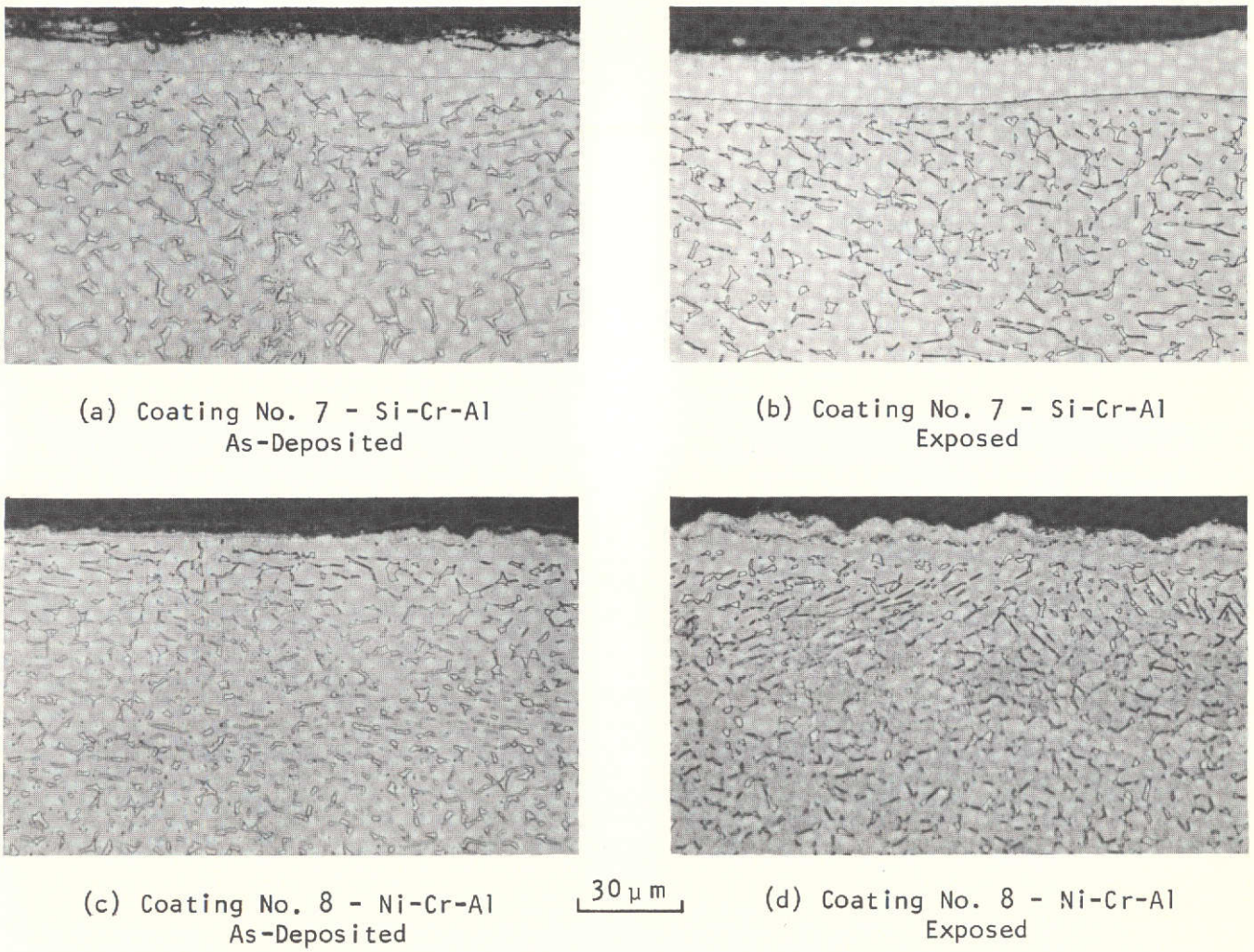

(a) Coating No. 7 - Si-Cr-Al As-Deposited

(b) Coating No. 7 - Si-Cr-Al Exposed

(c) Coating No. 8 - Ni-Cr-Al As-Deposited

(d) Coating No. 8 - Ni-Cr-Al Exposed

Figure 15. Microstructure of Coating Nos. 7 and 8 on Ti-6-2-4-2 in the As-Deposited Condition and After 1000 Hr/922°K (1200°F) Oxidation Exposure

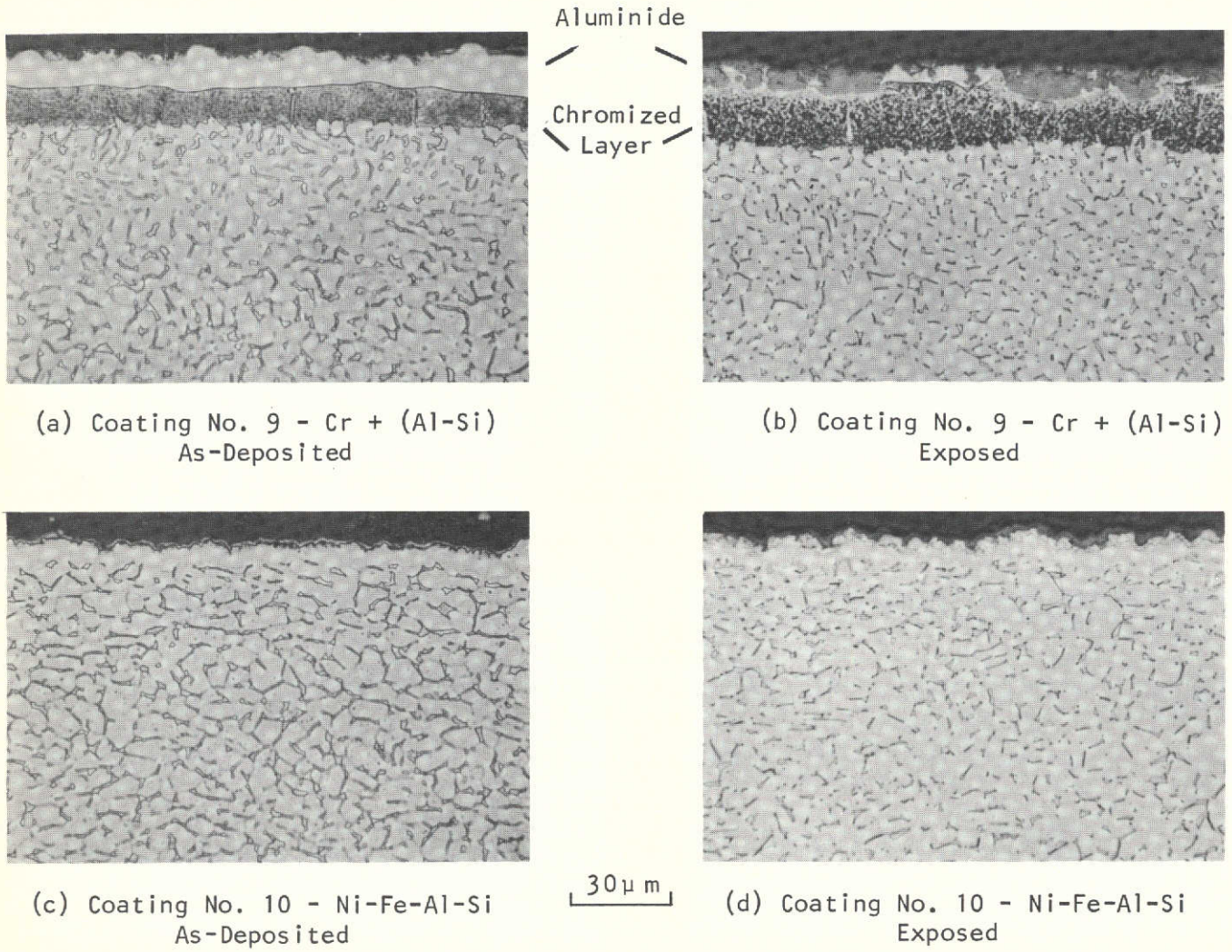

(a) Coating No. 9 - Cr + (Al-Si) As-Deposited

(b) Coating No. 9 - Cr + (Al-Si) Exposed

(c) Coating No. 10 - Ni-Fe-Al-Si As-Deposited

(d) Coating No. 10 - Ni-Fe-Al-Si Exposed

Figure 16. Microstructure of Coating Nos. 9 and 10 on Ti-6-2-4-2 in the As-Deposited Condition and After 1000 Hr/922°K (1200°F) Oxidation Exposure

TABLE VIII

TENSILE PROPERTIES OF UNCOATED, UNEXPOSED Ti-6-2-4-2
AND 922°K (1200°F) OXIDATION EXPOSED, UNCOATED Ti-6-2-4-2

Heat Treatment	Exposure Time (Hrs)	U.T.S.		0.2% Y.S.		% Elong.
		MN/m^2	ksi	MN/m^2	ksi	
Mill Annealed	None	945.3	137.2	842.6	122.3	14.2
↓	100	952.2	138.2	882.6	128.1	11.7
↓	1000	877.8	127.4	839.9	121.9	4.7
15 Hr/1228°K (1750°F)	None	922.6	133.9	824.0	119.6	9.6
↓	100	913.6	132.6	851.6	123.6	7.5
↓	1000	817.8	118.7	792.4	115.0	4.7

a) Unexposed, mill annealed.

b) Unexposed, heat treated 15 hr/1228°K (1750°F).

c) Exposed, mill annealed.

d) Exposed, heat treated 15 hr/1228°K (1750°F).

Comparisons of the coated specimens with the uncoated specimens, using the baselines described above, are made in the bar graphs presented in Figures 17 through 20. The property values for the coatings are expressed in terms of the percentage of the respective baselines.

Figure 17 compares the tensile properties of 100 and 1000 hours exposed coated specimens with uncoated, unexposed mill annealed Ti-6-2-4-2. Tensile elongation of the coated, exposed specimens was the property degraded the most with respect to uncoated, unexposed mill annealed Ti-6-2-4-2. Coatings 2A, 2B, 4A, 4B, 5A and 5B had elongations in the range of 90-97% of the baseline after 100 hours of exposure. Both thicknesses of coatings 3, 6 and 9 had the poorest elongation values. After 100 hours of exposure, the tensile elongation of these specimens was in the range of 3 to 17% of the elongation of the baseline. Except for coatings 3B, 6A, 9A and 9B, exposure for 1000 hours further decreased the tensile elongation. Decreases in tensile elongation with respect to the baseline ranged from 2% to 44%. Improvements in tensile elongation shown by coatings 3B, 6A, 9A and 9B after 1000 hours of exposure amounted to 5-8% of the baseline. There was no systematic variation of tensile elongation with coating thickness.

The data in Figure 17 show that the strengths of the exposed coated specimens were degraded to a lesser extent than elongation when compared to uncoated, unexposed mill annealed material. After 100 hours of exposure, coatings 1A, 2A, 2B and 7A had an ultimate tensile strength equivalent (98% or better) to uncoated, unexposed material. Coatings achieving 90% or more of the U.T.S. of this baseline included 1B, 5A, 5B, 7B, 8A, 8B, 9A, 10A and 10B. With few exceptions, longer exposure (1000 hours) decreased the U.T.S. by about 1-4% in respect to the baseline. Coatings for which the U.T.S. increased after the longer exposure included 3A, 3B, 6A, 6B, 4A and 10B. The increase in U.T.S. with respect to the baseline for these coatings was about 1 to 4%. Increased coating thickness generally decreased the U.T.S. by about 1 to 4% with respect to the baseline. Yield strengths equivalent to uncoated, unexposed material were obtained from coatings 1A, 2A, 2B, 5A, 7A, 8A, 8B, 9A, 9B and 10A in the 100 hour exposed condition. The remainder of the coatings had yield strengths that were at least 94% of the yield strength of the baseline. The effect of longer exposure and increased coating thickness on yield strength was similar to the effect of the variables on U.T.S. With a few exceptions, exposure for 1000 hours and increased coating thickness generally decreased the yield strength of the coated specimens by a small amount (1 to 5%).

A comparison of the tensile properties of exposed coatings and uncoated, unexposed, 15 hr/1228°K (1750°F) argon heat treated material is shown in Figure 18. The percentage of achievement of each coating for each of the properties is increased over the mill annealed baseline, reflecting the lower strength and ductility of the uncoated material heat treated to simulate the most severe coating thermal cycle.

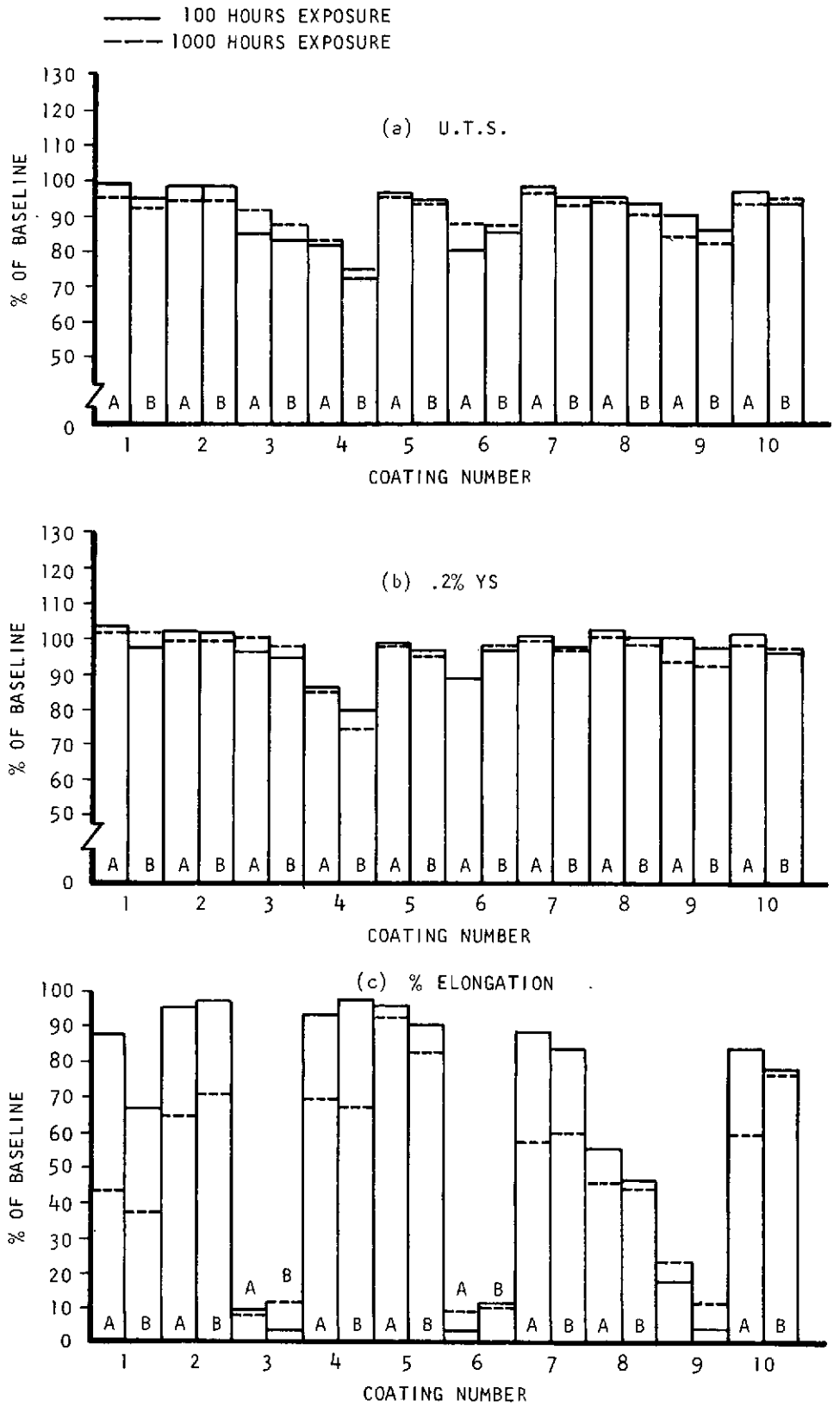

Figure 17. Tensile Properties of Coated Ti-6-2-4-2 After Exposure at 922°K(1200°F) Compared to Uncoated, Unexposed Mill Annealed Ti-6-2-4-2

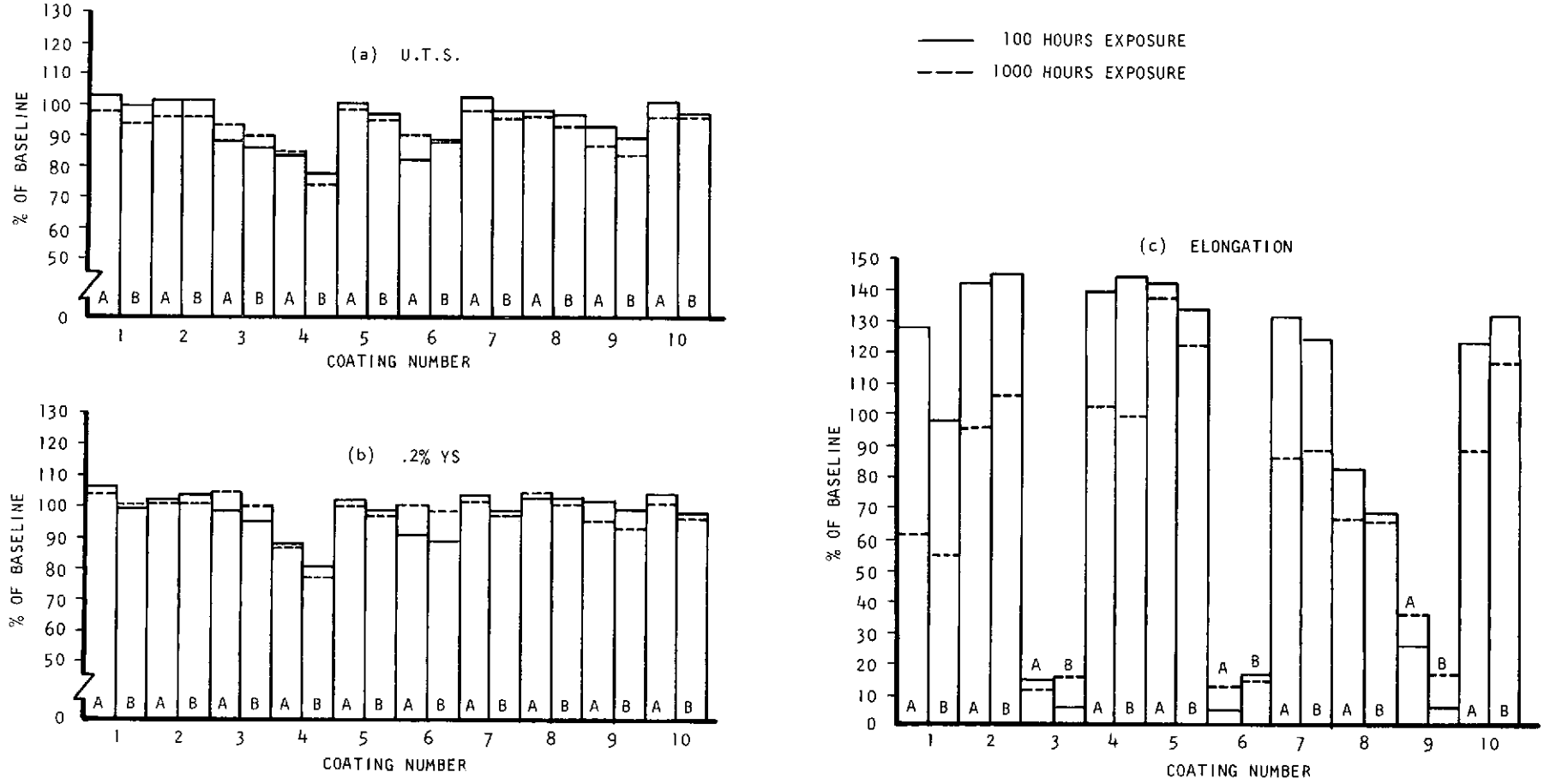

Figure 18. Tensile Properties of Coated Ti-6-2-4-2 After Exposure at 922°K(1200°F) Uncoated, Unexposed, Heat Treated Ti-6-2-4-2

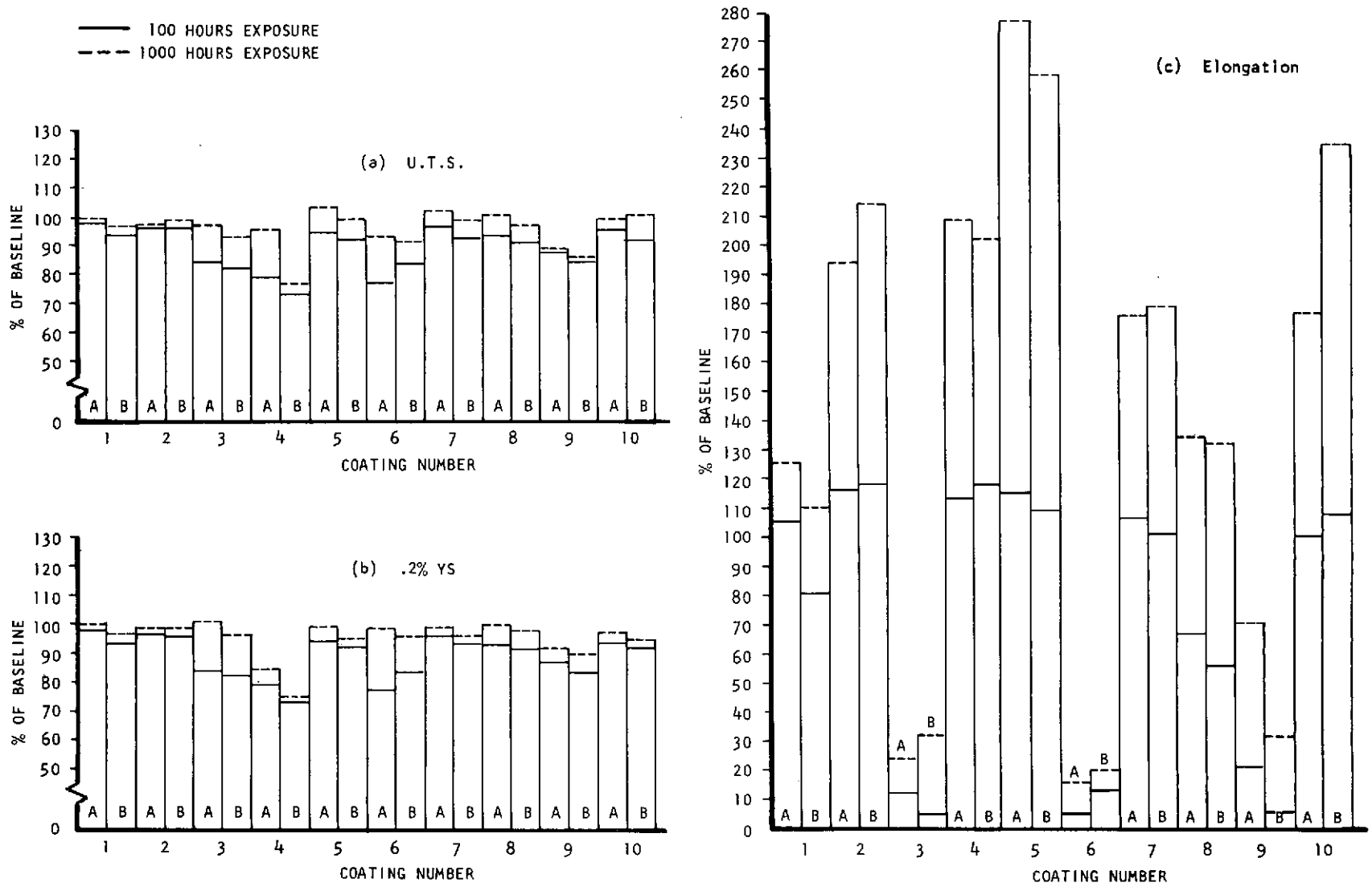

Figure 19. Tensile Properties of Coated Ti-6-2-4-2 After Exposure at 922°K(1200°F) Compared to Uncoated, Exposed, Mill Annealed Ti-6-2-4-2

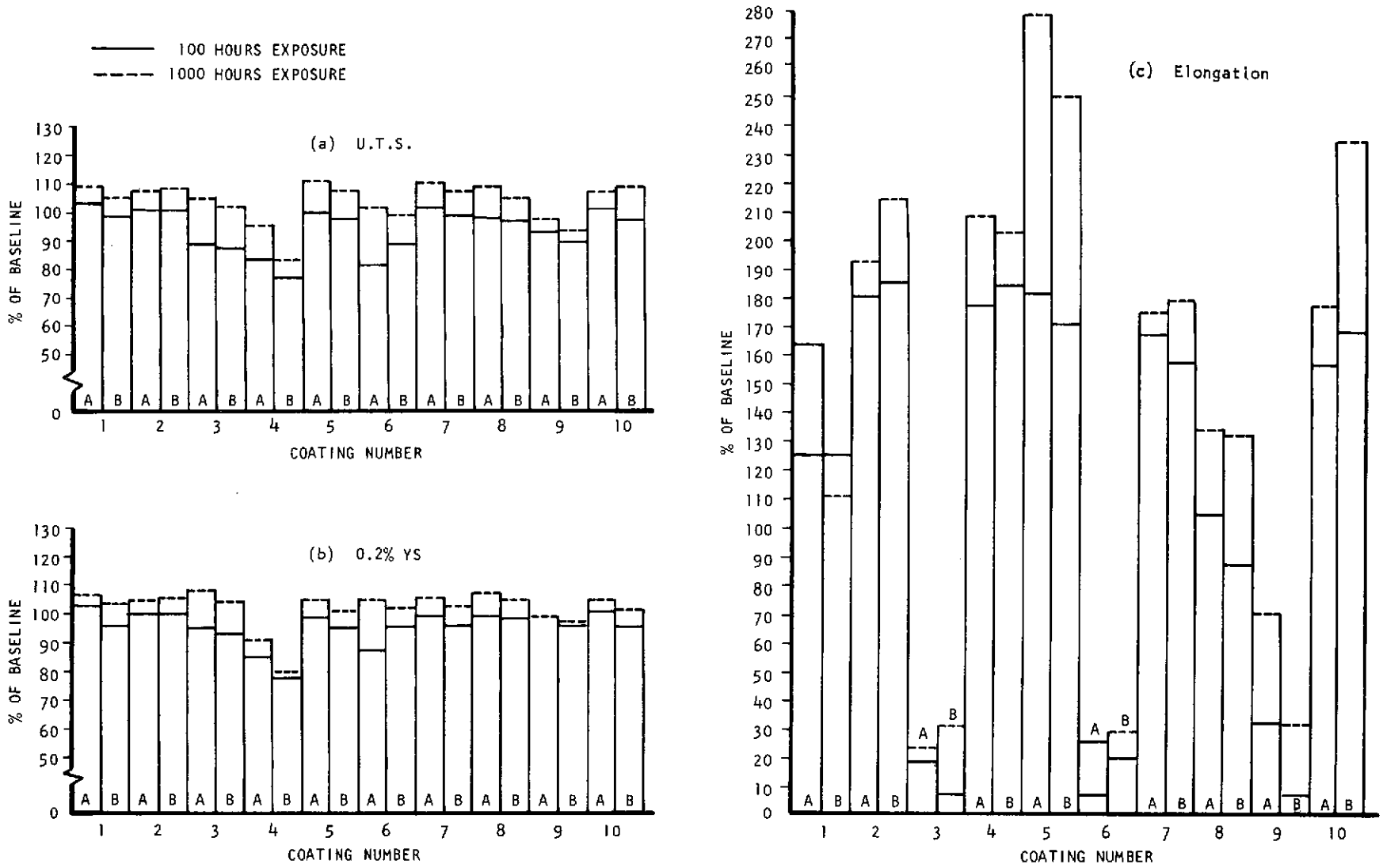

Figure 20. Tensile Properties of Coated Ti-6-2-4-2 After Exposure at 977°K(1200°F) Compared to Uncoated, Exposed, Heat Treated Ti-6-2-4-2

Tensile properties of the exposed coated specimens are compared to those of uncoated, exposed mill annealed specimens in Figure 19. After 100 hours of exposure, only a few coatings had strengths equivalent to uncoated, 100 hour exposed mill annealed material. Comparison of 1000 hour exposed specimens, however, indicates that about half of the coatings (1A, 1B, 2A, 2B, 3A, 3B, 5A, 6A, 7A, 8A, 8B and 9A) had strengths equivalent or somewhat higher than uncoated material. About half of the coatings provided increased ductility over the uncoated specimens for both 100 hour and 1000 hour exposures. Coatings 2, 4, 5, 7 and 10 were particularly outstanding. After 1000 hours of exposure, tensile elongation values of these coated specimens ranged from 177 to 278.7% of the baseline.

Tensile properties of the exposed, coated specimens are compared with the tensile properties of uncoated, 15 hr/1228°K (1750°F) heat treated, and exposed material in Figure 20. The relative performance of individual coatings is similar to the exposed mill annealed comparison. All values are increased, however, reflecting the lower tensile properties of the 15 hr/1228°K (1750°F) heat treated material.

To obtain a quantitative measure of the relative performances of the coatings under oxidation exposure conditions, the strength and elongation values for each coating relative to each baseline were averaged into a single value. No distinction was made between coating thickness or length of exposure. These data are presented in Table IX. All of the strength data (U.T.S. and 0.2% Y.S.) are consolidated in baseline A and all of the elongation data are consolidated in baseline B. Coatings are listed in descending order of achievement relative to each baseline and graded according to the rank achieved for each baseline. On the basis of these rankings, coating No. 2 outperformed the remainder of the coatings in respect to oxidation exposed tensile properties. Coating No. 5 ranked second, followed by coatings 1 and 7, 10, 8 and 4. The duplex coatings (3, 6 and 9) had large adverse effects on substrate tensile properties as reflected by their low ranking.

Coatings that degraded tensile properties to the greatest extent (Nos. 3, 6 and 9) contained β stabilized substrate/coating interface layers. Coatings containing α stabilized substrate/coating interface layers (Nos. 1 and 5) ranked relatively high in respect to tensile properties. Tensile properties of the exposed coatings were not directly related to weight gain as illustrated by the ranking given in Table VI.

3.2.4 Hot-Salt Stress-Corrosion Tests

All ten experimental coatings were evaluated for hot-salt stress-corrosion resistance using self-stressed Ti-6-2-4-2 specimens. Coated specimens at each thickness level were evaluated together with uncoated specimens (mill annealed and 15 hr/1228°K (1750°F) heat treatments) under the following conditions:

a) Unexposed, no salt.

b) 100 hr/755°K (900°F) static air exposure, salted.

c) 1000 hr/755°K (900°F) static air exposure, salted.

TABLE IX

RANKING OF COATINGS ACCORDING TO BASELINE ACHIEVEMENT[a]

A Strength[b]		B Ductility[b]		Grade per Rank	Summary Grade (20 Max) and Rank		
Coating	% Achievement	Coating	% Achievement		Coating	Grade	Rank
2	110.0	5	157.9	10	2	19	1
1	99.7	2	139.8	9	5	17	2
7,8	99.0	4	139.0	8	1,7	14	3
5	98.2	10	131.9	7	10	13	4
10	98.1	7	122.0	6	8	12	5
3	94.1	1	94.9	5	4	10	6
6	91.6	8	82.0	4	3,6,9	6	7
9	89.1	9	25.1	3			
4	81.2	6	14.7	2			
		3	14.4	1			

(a) $\%\ \text{Achievement} = \frac{\text{Property Value, Coated}}{\text{Property Value, Uncoated}} \times 100$

(b) Property Data from Figures 17, 18, 19, and 20.

To provide baseline data for evaluation of the salt exposure results, uncoated and coated (A thickness level) specimens were exposed for 100 and 1000 hours at 755°K (900°F) without salt.

Specimen salting was accomplished by applying two drops of a solution consisting of 10 w/o NaCl in deionized water on the center of the outside surface of each leg of the fabricated specimens. Drying for two hours at 366°K (200°F) produced a salt concentration of approximately 6 mg/cm^2. The specimens were designed to produce 0.2% creep in the outer fiber of an uncoated specimen during the scheduled exposure periods (100 or 1000 hours). Stress levels were based on the results of creep tests conducted on uncoated mill annealed Ti-6-2-4-2 (Appendix C) and were determined to be 275.6 MN/m^2 (40 ksi) for the 100 hour exposure and 144.7 MN/m^2 (21 ksi) for the 1000 hour exposure. The stress level induced in self-stressed specimens was determined by the bend angle of the tab prior to assembly. Details of the determination of the proper bend angle as well as experimental verification of the stress level in uncoated specimens are presented in Appendix C.

Following exposure the self-stressed specimens were slow strain rate compression tested to failure using a cross-head speed of 1.27 mm/min. (0.05 in/min). Three types of data were recorded: 1) compression to failure, 2) specimen bow and 3) maximum load (Figure 21). Fracture surfaces were examined at 30X magnification for the presence of pre-compression cracks to assess the extent of hot-salt stress-corrosion cracking.

Results of the compression tests and examinations of the fracture surfaces are presented in Table X. Compression to failure as a function of exposure time is summarized in Figures 22 and 23 for uncoated specimens and the A thickness level of the coated specimens. Lower compression values were obtained for nearly all coated specimens compared to comparable uncoated specimens. Salt application reduced the compression values obtained from coated specimens. Oxidized cracks of the type shown in Figure 24 were present in the fracture surfaces of nearly all coated specimens. These pre-compression cracks were generally about an order of magnitude greater in depth for salted specimens compared to unsalted specimens. Presence of the cracks in unsalted specimens indicated that the cracks were formed in the coatings during bending and fabrication of the specimens. The greater pre-compression crack depth associated with the salted specimens indicated that the presence of the salt intensified the cracking. Since coating cracks apparently existed prior to salting, the self-stressed tests did not provide a definitive ranking of the coatings in respect to hot-salt stress-corrosion cracking. It was concluded that more definitive hot-salt stress-corrosion data could be obtained if coating cracks during specimen fabrication were eliminated or minimized. Post-coat glass bead peening offered a means of increasing the ductility of the coatings by placing the outer surface in compression. All of the coatings were, therefore, evaluated for response to peening.

3.2.5 Effect of Glass Bead Peening

Each of the ten coatings at the A thickness level on Ti-6-2-4-2 were evaluated for response to post-coat glass bead peening. As-coated coupons (1.91 cm x 3.81 cm; 0.75 x 1.5 inch) were bent around a 2.54 cm (1 inch) diameter mandrel until cracking was visible at a magnification of 30X.

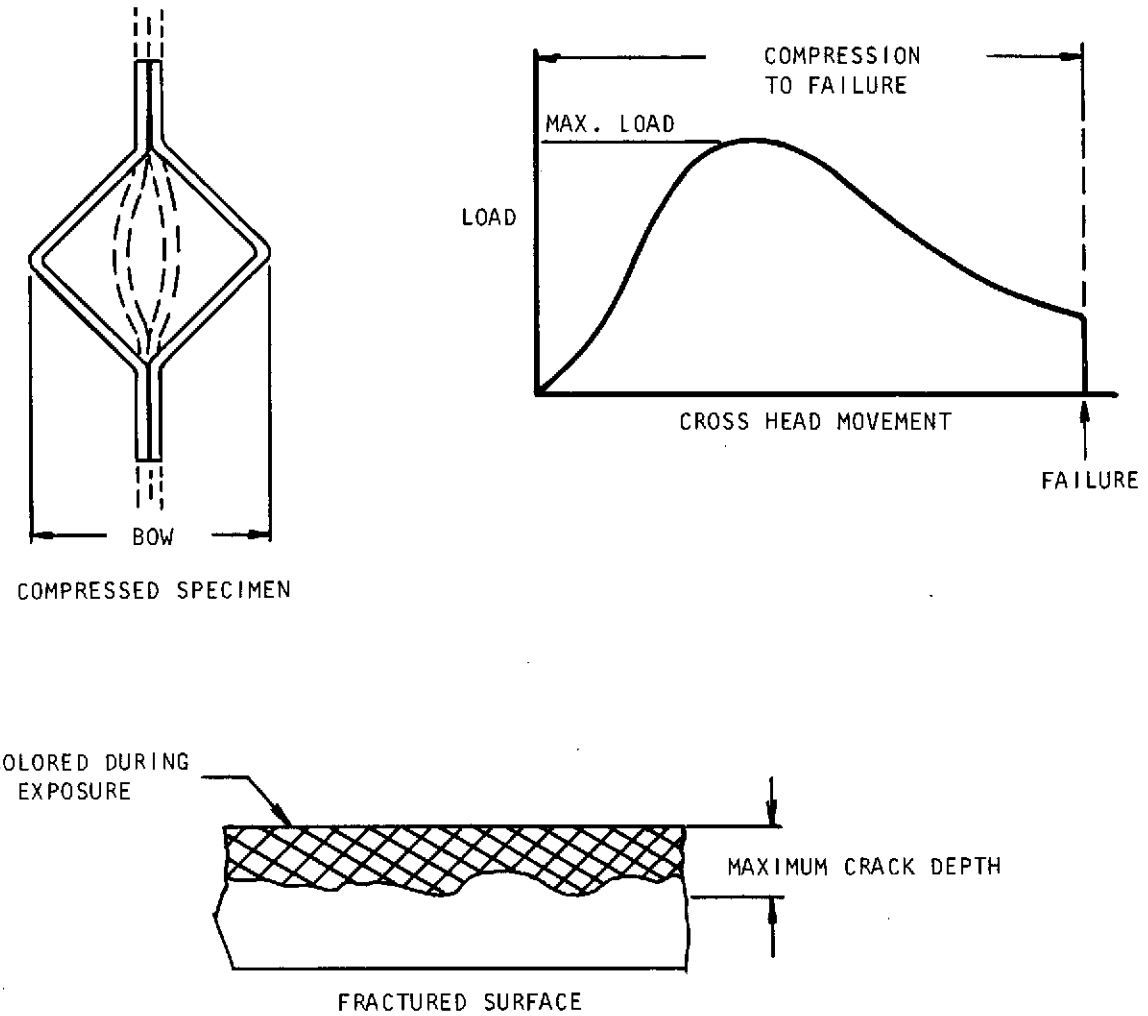

Figure 21. Self-Stressed Hot-Salt Stress-Corrosion Coating Performance Criteria

TABLE X

HOT-SALT STRESS-CORROSION TEST RESULTS FOR UNCOATED AND COATED Ti-6-2-4-2

Coating No.	Exposure[a] (hrs)	Post Exposure Compression to Failure[b] Compression (cm)	Compression (in)	Bow (cm)	Maximum Load (N)	Maximum Load (lb)	Pre-Compression Crack Depth[c] (mm)	Pre-Compression Crack Depth[c] (in)
Mill Annealed[d]	None	3.678	1.448	5.60	1872	421	0	0
	100(NS)	3.352	1.588	4.60	2126	478		
	100(S)	2.568	1.011	4.00	2233	502		
	1000(NS)	2.880	1.134	4.60	2896	651		
	1000(S)	2.380	0.937	4.00	2807	631		
1228°K (1750°F)/ 15 hrs[d]	None	2.804	1.104	5.80	2237	503	0	0
	100(NS)	2.840	1.118	3.20	2082	468	0	0
	100(S)	1.905	0.750	4.30	2135	480	.076	0.0030
	1000(NS)	2.306	0.908	4.30	2736	615	0	0
	1000(S)	1.554	0.612	3.30	2691	605	0	0
1A	None	3.480	1.370	4.70	2135	480	0	0
	100(NS)	3.345	1.317	4.50	1686	379	.089	0.0035
	100(S)	1.019	0.401	1.80	1521	342	.72	0.0285
	1000(NS)	2.256	0.888	3.60	2482	558	.089	0.0035
	1000(S)	0.584	0.230	1.30	2384	536	.3810	0.0150
1B	None	2.784	1.096	4.70	2135	480	0	0
	100(S)	0.653	0.257	1.55	1232	277	0.787	0.0310
	1000(S)	0.493	0.194	1.13	1913	430	0.559	0.0220
2A	None	3.009	1.184	4.60	2268	510	0	0
	100(NS)	3.393	1.336	4.80	1806	406	0	0
	100(S)	0.843	0.332	1.50	1583	356	0.470	0.0185
	1000(NS)	3.421	1.345	4.87	1939	436	0.216	0.0085
	1000(S)	0.673	0.265	1.67	2220	499	0.356	0.0140

TABLE X (continued)

Coating No.	Exposure[a] (hrs)	Post Exposure Compression to Failure[b] Compression (cm)	Compression (in)	Bow (cm)	Maximum Load (N)	Maximum Load (lb)	Pre-Compression Crack Depth[c] (mm)	Pre-Compression Crack Depth[c] (in)
2B	None	4.013	1.580	5.20	1935	435	0	0
	100(S)	0.881	0.347	1.70	1423	320	0.673	0.0265
	1000(S)	1.204	0.474	2.43	2420	544	0.203	0.0080
3A	None	1.010	0.398	2.00	2277	512	0	0
	100(NS)	1.156	0.455	1.85	1828	411	0.127	0.0050
	100(S)	0.508	0.200	1.40	1170	263	0.889	0.0350
	1000(NS)	0.907	0.357	2.02	2184	491	0.127	0.0050
	1000(S)	0.384	0.151	0.93	1668	375	0.775	0.0305
3B	None	0.630	0.248	1.30	1313	520	0	0
	100(S)	0.554	0.218	1.15	1374	309	0.635	0.0250
	1000(S)	0.411	0.162	1.05	1993	448	0.686	0.0270
4A	None	3.635	1.431	5.10	2188	492	0	0
	100(NS)	2.910	1.146	4.50	1868	420	0.076	0.0030
	100(S)	2.631	1.036	1.80	1521	342	0.991	0.0390
	1000(NS)	3.277	1.290	5.95	2633	592	0.152	0.0060
	1000(S)	0.305	0.120	1.25	2451	551	0.610	0.0240
4B	None	3.289	1.295	4.50	2260	508	0	0
	100(S)	0.439	0.173	1.45	1321	297	1.270	0.0500
	1000(S)	0.424	0.167	1.65	2713	610	0.635	0.0250
5A	None	3.223	1.269	5.10	2237	503	0	0
	100(NS)	3.564	1.403	4.55	1699	382	0.152	0.0060
	100(S)	0.765	0.301	1.55	1348	303	0.826	0.0325
	1000(NS)	2.223	0.875	4.23	2415	543	0.216	0.0085
	1000(S)	0.462	0.182	1.08	2019	454	0.597	0.0235
5B	None	3.068	1.208	4.60	1962	441	0	0
	100(S)	0.597	0.235	1.60	845	190	0.787	0.0310
	1000(S)	0.399	0.157	1.05	1499	337	0.749	0.0295

TABLE X (continued)

Coating No.	Exposure[a] (hrs)	Post Exposure Compression to Failure[b] Compression (cm)	Compression (in)	Bow (cm)	Maximum Load (N)	Maximum Load (lb)	Pre-Compression Crack Depth[c] (mm)	Pre-Compression Crack Depth[c] (in)
6A	None	0.884	0.348	1.80	2411	542	0	0
	100(S)	0.947	0.373	1.70	1797	404	0.140	0.0055
	100(NS)	0.546	0.215	1.90	752	169	1.016	0.0400
	1000(S)	0.693	0.273	2.10	2357	530	0.191	0.0075
	1000(NS)	0.734	0.121	0.90	1072	241	1.041	0.0410
6B	None	0.864	0.340	2.40	2268	510	0	0
	100(S)	0.386	0.152	1.40	503	113	0.889	0.0350
7A	None	3.937	1.550	4.50	1913	430	0	0
	100(NS)	3.772	1.485	4.45	1690	380	0.038	0.0015
	100(S)	1.209	0.476	1.90	1450	326	0.889	0.0350
	1000(NS)	1.755	0.691	3.40	2335	525	0.051	0.0020
	1000(S)	0.719	0.283	1.33	2010	452	0.406	0.0160
7B	None	3.315	1.305	4.80	2002	450	0	0
	100(S)	1.727	0.680	2.65	1530	344	0.445	0.0175
	1000(S)	0.277	0.109	1.00	1472	331	0.914	0.0360
8A	None	3.264	1.285	5.10	1913	430	0	0
	100(NS)	3.310	1.303	4.35	1890	425	0.064	0.0025
	100(S)	1.791	0.705	2.90	1668	375	0.318	0.0125
	1000(NS)	2.619	1.031	4.03	2380	535	0.064	0.0025
	1000(S)	0.627	0.247	1.20	1753	394	0.622	0.0245
8B	None	3.683	1.450	4.40	2389	537	0	0
	100(S)	0.330	0.130	1.00	1134	255	1.092	0.0430
	1000(S)	1.204	0.474	2.40	1588	357	0.635	0.0250
9A	None	0.914	0.360	1.80	2357	530	0	0
	100(NS)	1.207	0.475	1.95	2082	468	0	0
	100(S)	1.090	0.429	1.85	2015	453	0.279	0.0110
	1000(NS)	0.683	0.269	1.55	2424	545	0.038	0.0015
	1000(S)	0.572	0.225	1.35	2478	557	0.051	0.0020

TABLE X (continued)

Coating No.	Exposure[a] (hrs)	Post Exposure Compression to Failure[b] Compression (cm)	Compression (in)	Bow (cm)	Maximum Load (N)	Load (lb)	Pre-Compression Crack Depth[c] (mm)	Crack Depth (in)
9B	None	0.533	0.210	1.20	2366	532	0	0
↓	100(S)	0.630	0.248	1.45	1984	446	0.279	0.0110
	1000(S)	0.414	0.163	1.05	2446	550	0.038	0.0015
10A	None	2.858	1.125	4.50	2291	515	0	0
↓	100(NS)	2.939	1.157	4.55	1930	434	0.102	0.0040
	100(S)	0.935	0.368	1.10	1570	353	0.470	0.0185
	1000(NS)	2.258	0.889	3.65	2375	534	0.025	0.0010
	1000(S)	1.041	0.410	2.35	2486	559	0.038	0.0015
10B	None	3.937	1.550	5.35	2117	476	0	0
↓	100(S)	1.321	0.520	2.40	1446	325	0.432	0.0170
	1000(S)	0.810	0.319	1.90	2077	467	0.178	0.0070

NOTES: (a) Exposure to air at 755°K (900°F). (NS) - No Salt; (S) - Salted.

(b) Comp. - Compression measured by Instron Cross-head Movement. See Figure 20.

(c) Maximum crack depth in 1.27 mm (0.050 inch) sheet. Measured on fractured specimen surfaces.

(d) Uncoated Ti-6-2-4-2.

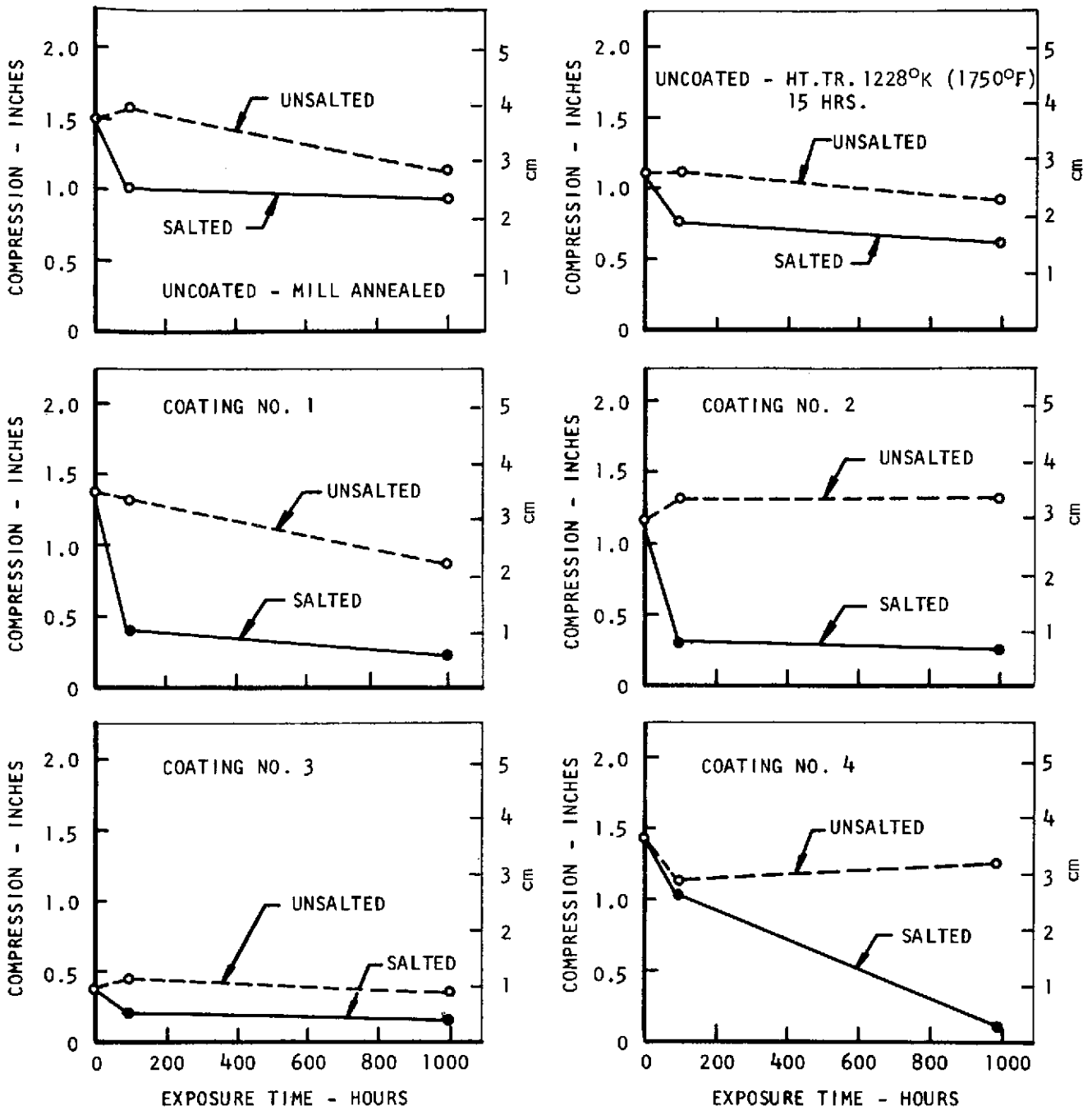

Figure 22. Effect of Exposure on the Ductility of Salted and Unsalted, Coated and Uncoated Ti-6-2-4-2

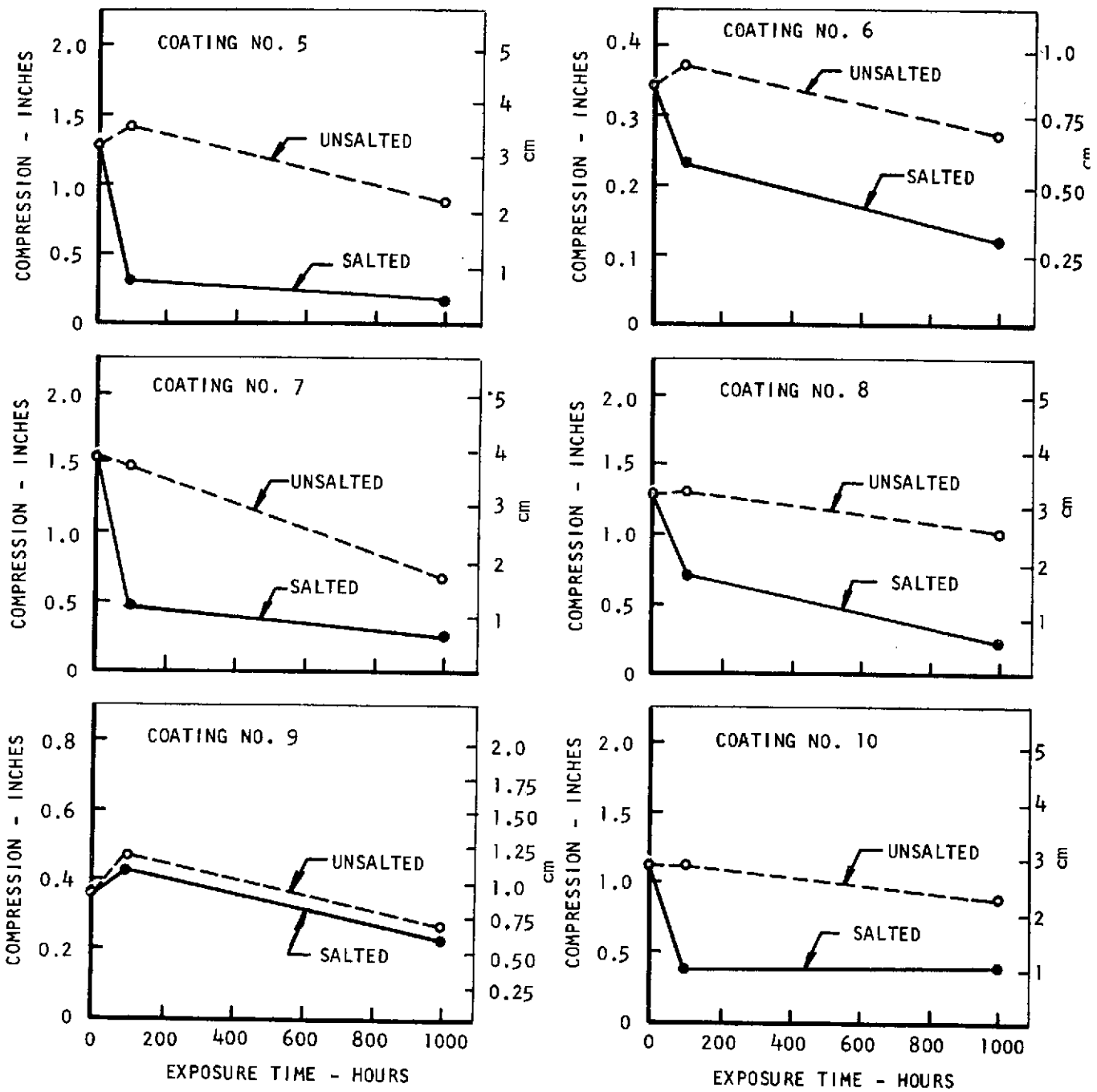

Figure 23. Effect of Exposure on the Ductility of Salted and Unsalted, Coated Ti-6-2-4-2

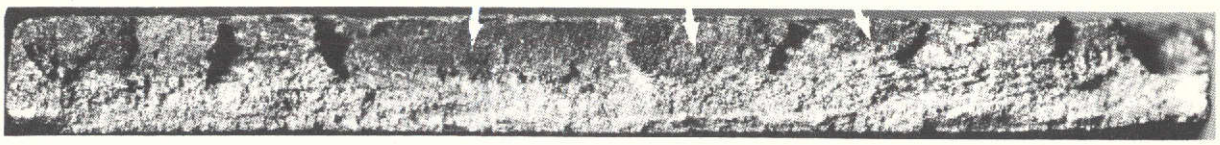

Fracture in Salted Specimen

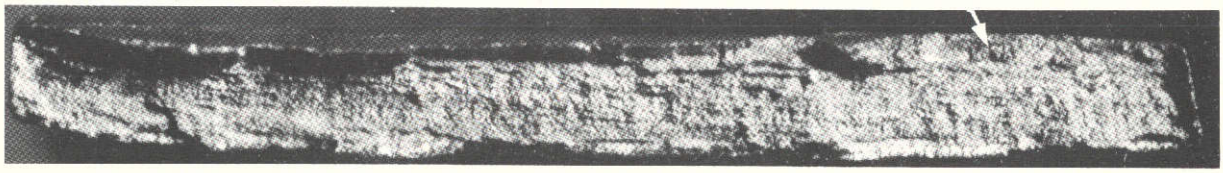

Fracture in Unsalted Specimen

Figure 24. Typical Fractures of Failed Stress Corrosion Specimens. Arrows Indicate Pre-Compression Test Fractures.

A duplicate set of specimens was glass bead peened under production conditions and similarly tested. The results are presented in Table XI. All coatings responded to varied extents. Coatings 1, 2, 4, 5, 7, 8 and 10 were capable of post-peen bending of at least 80 degrees without observable failure compared to bend angles ranging from 5 to 16 degrees before peening. Coatings 3, 6 and 9 responded slightly; however, severe cracking was encountered at bend angles of only 13-14 degrees. Metallographic examination of peend coatings indicated that coatings 2, 7, 8 and 10 were partially removed.

The results of the bend tests indicated that coating ductility could be improved by post-coat glass bead peening, therefore permitting more definitive evaluation of the relative susceptibility of the coatings to hot-salt stress-corrosion cracking.

3.2.6 Dust Erosion Tests

All ten coating systems at the greater coating thickness (B series) were evaluated for dust erosion erosion resistance using coated and uncoated (mill annealed) Ti-6-2-4-2 coupons. Erosion tests were conducted using a S.S. White Mini-Blast unit, Figure 25, at impingement angles of 20 and 90 degrees. The eroding abrasive used was 27 micron alumina carried through a 0.051 mm (0.019 inch) diameter nozzle at a 5.08 cm (2.0 inch) standoff in an argon gas stream under a pressure of 344.5 KN/m^2 (50 psig). Abrasion times of 30 to 60 seconds were electronically controlled.

Several means of determining or characterizing erosion resistance were considered. The most direct was weight loss; however, when coatings are not of the same density or do not possess a constant density across their effective thickness, weight loss can be misleading. Volume loss by direct measurement was not possible experimentally, nor was calculated volume loss which depends on an accurate determination of coating density. The following method was therefore developed for evaluation of erosion resistance:

a) Erosion test coated and uncoated specimens by exposing a constant surface area to the eroding media for a specific time period and determine weight losses. Constant surface areas were obtained by masking.

b) Calculate unit area weight losses for uncoated and coated specimens.

c) Calculate the fraction of the coating removed at each erosion time for each erosion angle using the following relation:

$$E_C = \frac{D-C}{D}$$ where: D = coating deposited (mg/cm^2)
C = material eroded (mg/cm^2)

E_C has the following significance:

1) For $E_C > 0$, no substrate was eroded. The larger the number, the larger the fraction of coating remaining on the specimen.

TABLE XI

EFFECT OF GLASS BEAD PEENING

Coating	Condition	Bend Angle No Cracking(*)	Bend Angle(*) To Produce Cracking
1A	As Coated	-	7.2
	Peened	82.5	108.7
2A	As Coated	-	13.0
	Peened	85.7	128.7
3A	As Coated	-	9.7
	Peened	-	14.5
4A	As Coated	-	13.5
	Peened	76.0	107.7
5A	As Coated	-	5.2
	Peened	84.0	98.5
6A	As Coated	-	4.7
	Peened	-	13.0
7A	As Coated	-	15.0
	Peened	90.7	102.5
8A	As Coated	-	15.0
	Peened	83.5	99.0
9A	As Coated	-	5.2
	Peended	-	14.5
10A	As Coated	-	16.0
	Peened	84.0	102.0
Uncoated	-	-	141.0

* Cracking observed at 30X magnification.

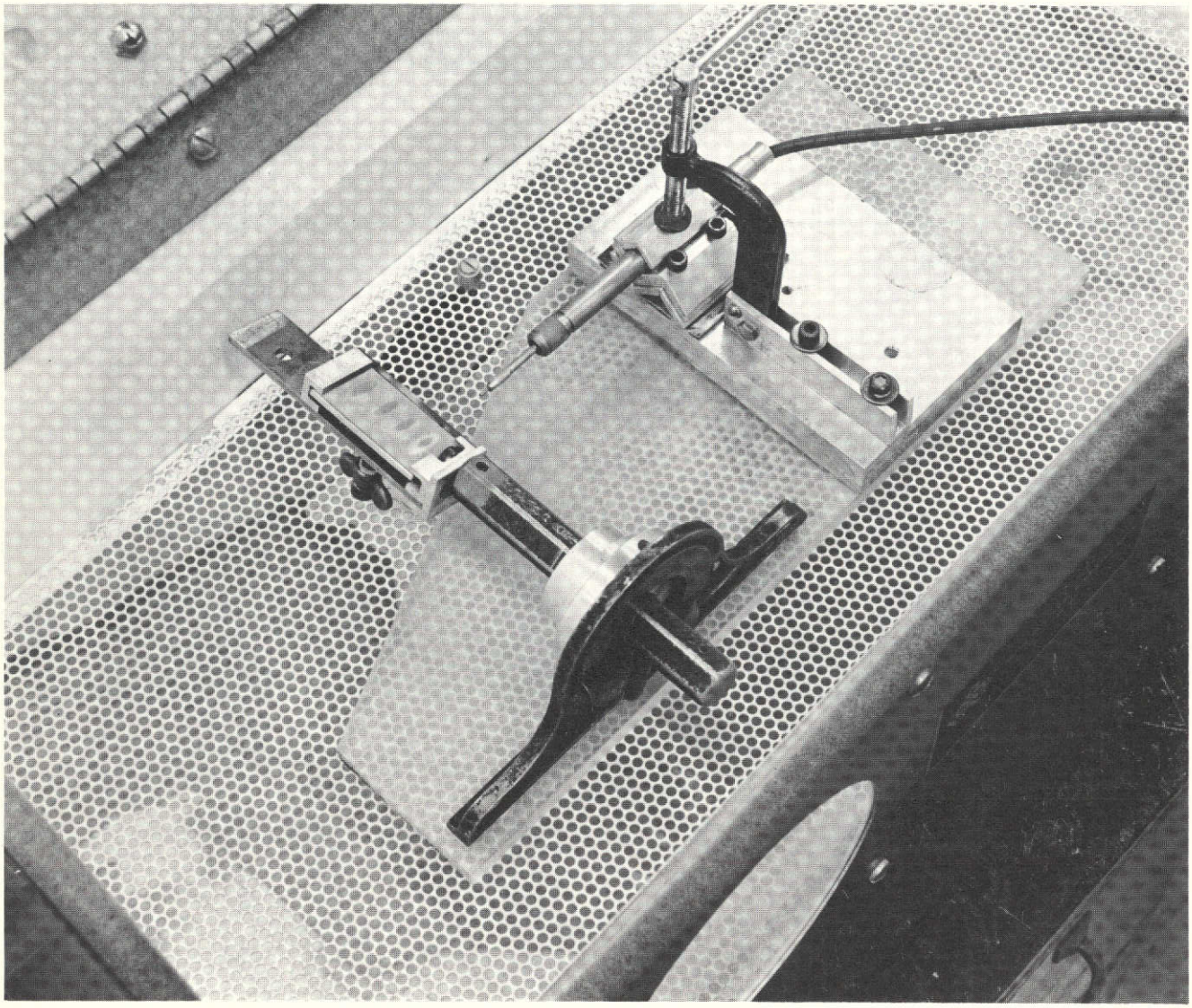

Figure 25. S. S. White Mini-Blast Unit

2) For $E_C = 0$, all coating was removed but substrate was not eroded.

3) For $E_C < 0$, all coating was removed and substrate was eroded. The numerical value has no special significance since weight gains from coating deposition were not the same for all coatings.

d) For coated specimens which exhibited substrate removal ($E_C < 0$), the fraction of substrate material eroded was compared to the amount removed from uncoated material using the following relation:

$$E_S = \left|\frac{D-C}{S}\right|$$ where: D = coating deposited (mg/cm^2).
C = material eroded (mg/cm^2) from coated specimens.
S = material eroded (mg/cm^2) from uncoated specimens.

E_S has the following significance:

1) For $E_S < 1$, less substrate was eroded when coated than when uncoated. The lower the numerical value of E_S, the more protective the coating.

2) For $E_S = 1$, no difference between the amount of substrate eroded in the coated and uncoated conditions.

3) For $E_S > 1$, more substrate was eroded in the coated condition than when uncoated.

The results of the erosion tests are summarized in Table XII along with calculated values of E_C and E_S. At the 20° impingement angle, E_C values indicate coatings 1, 3 and 5 protected the substrate from erosion for 30 seconds and coatings 3 and 5 protected the substrate from erosion after 60 seconds. The remainder of the coatings were completely removed and substrate was eroded*. E_S values calculated for the remainder of the coatings indicate that for the 30 second erosion time, all coated specimens had less substrate removed than uncoated specimens. At the 60 second erosion time, E_S values for coatings 4 and 8 indicate that more substrate material was eroded from these specimens than from uncoated material.

At the 90° impingement angle, E_C values indicate that coatings 1, 3, 5, 9 and 10 protected the substrate from erosion for 30 seconds, but none of the coatings protected the substrate from erosion for 60 seconds. Calculated E_S values indicate that at the 30 second erosion time only coating 2 intensified erosion of the substrate, while at the 60 second erosion time, coatings 2, 7 and 8 intensified erosion of the substrate.

Based on calculated values of E_C and E_S (where appropriate) for the 60 second erosion time, the coatings ranked in order of decreasing erosion resistance are as follows:

* Except coating 9 after 30 seconds, where all coating was removed but no substrate was eroded ($E_C = 0$).

TABLE XII

EROSION RESISTANCE OF COATED AND UNCOATED Ti-6-2-4-2

Coating No.	Impingement Angle (Deg)	Material Eroded (mg/cm^2)		$E_C = \frac{D-C}{D}$		$E_S = \left\|\frac{D-C}{S}\right\|$	
		t = 30 sec	t = 60 sec	t = 30 sec	t = 60 sec	t = 30 sec	t = 60 sec
Uncoated	20	1.33	2.55	-	-		
1	"	0.97	2.06	+0.52	-0.03		.03
2	"	1.18	2.06	-0.97	-3.33	0.44	0.76
3	"	1.47	2.35	+0.54	+0.27		
4	"	2.35	4.70	-0.57	-2.13	0.64	1.68
5	"	1.76	2.35	+0.32	+0.10		
6	"	2.05	2.64	-0.37	-0.76	0.41	0.60
7	"	1.76	2.94	-0.47	-1.45	0.12	0.91
8	"	2.05	3.23	-0.86	-1.94	0.71	1.12
9	"	2.10	3.82	0	-0.82	0	0.90
10	"	2.00	2.35	-0.25	-0.47	0.30	0.39
Uncoated	90	1.18	1.91	-	-		
1	"	1.06	2.65	+0.47	-0.33		0.25
2	"	2.55	4.41	-3.25	-6.35	1.65	1.49
3	"	1.56	4.71	+0.51	-0.47		0.59
4	"	4.00	7.06	-1.67	-3.7	0.21	0.22
5	"	1.35	2.65	+0.48	-0.02		0.02
6	"	2.06	2.94	-0.37	-0.96	0.47	0.56
7	"	2.23	4.10	-0.86	-2.42	0.87	1.14
8	"	1.35	4.12	-0.23	-2.75	0.21	1.18
9	"	1.76	4.41	+0.16	-1.1		0.91
10	"	1.06	3.23	+0.34	-1.02		0.64

Rank	Coating Number	
	20° Impingement Angle	90° Impingement Angle
1	3	5
2	5	4
3	1	1
4	10	6
5	6	3
6	2	10
7	9	9
8	7	7
9	8	8
10	4	2

3.2.7 Selection of Coatings for Further Evaluation in Task I

Coatings were selected for further evaluation in Task I on the basis of oxidation resistance (weight gain and electron microprobe analysis), tensile properties, peening response and erosion resistance. The hot-salt stress-corrosion tests results were not definitive and were not included in the evaluation. Relative performance of the coatings in various testing categories are summarized in Table XIII. Coatings selected for further evaluation were Nos. 1, 2, 5, 8 and 10. The duplex coatings (3, 6 and 9) were not considered for further evaluation because of poor ductility and peening response. Coatings 1 and 5 were selected on the basis of consistently superior performance in all three categories. Coatings 2 and 10 were selected on the basis of tensile properties. Of the remaining coatings (4, 7 and 8), coating 8 was selected over 4 because it had somewhat better tensile properties and over 7 because its smaller decrease in ductility due to extended exposure indicated better thermal stability.

3.2.8 Ballistic Impact Tests

Coatings selected for further evaluation in Task I (Nos. 1, 2, 5, 8 and 10) were evaluated for ballistic impact resistance at the B thickness level. All coatings were glass bead peened prior to impacting to an Almen intensity of 11N using an air pressure of 144.7 kN/m^2 (21 psi) and 0.254 mm (0.010 inch) diameter Type D.C. glass beads. Uncoated mill annealed specimens and the coated specimens were impact damaged at room temperature using a 0.656 gm steel ball fired from a gas operated pellet gun at a standoff distance of 38.1 cm (15 inches). Velocities up to 232 m/sec (760 ft/sec) were employed and specimens were examined at 30X magnification to detect cracking.

Uncoated specimens were tested at successively increasing velocities to provide baseline data for comparison with coating performance. Similar procedures were then used on coated specimens to determine the minimum velocity at which coating cracks occurred without rupture of the substrate material. This minimum velocity was defined as the threshold level for a particular coating. The influence of impact damage on the protectiveness of the coatings was then determined by damaging tensile and self-stressed hot corrosion specimens at velocities which were 10% above the threshold level. Damaged tensile specimens were exposed at 922°K (1200°F) for 100 hours and subsequently tested at room temperature using slow strain rates. Self-stressed hot-salt stress-corrosion

TABLE XIII

SUMMARY OF TASK I - COATING PERFORMANCE RATINGS

Coating No.	Oxidation Resistance	Tensile Properties	Response to Peening	Erosion Resistance	Selected for Continued Evaluation
1	Adequate	G	G	G	X
2	"	E	F	P	X
3	"	P	P	G	
4	"	F	G	P	
5	"	E	G	G	X
6	"	P	P	F	
7	"	G	F	P	
8	"	F	F	P	X
9	"	P	P	F-P	
10	"	G	F	F	X

NOTES: E - Excellent
G - Good
F - Fair
P - Poor

specimens were assembled such that the impact damage was in tension. These specimens were salted (6 mg/cm^2 concentration), exposed at 755°K (900°F) for 100 hours and tested at room temperature using evaluation procedures described in Section 3.2.4.

Tests on uncoated specimens indicated gross rupture at velocities above 198 m/sec (650 ft/sec). Threshold velocities determined for the coated specimens are listed in Table XIV in order of decreasing impact resistance. Coating No. 2 had the best resistance to impact damage. Cracks were not observed in the coating; however, gross rupture of the substrate consistently occurred above an impact velocity of 145 m/sec (475 ft/sec). This value was taken as the threshold velocity for coating No. 2. All cracking observed on the coatings occurred on the backside of the coupons; i.e., cracking was not observed on the side of the coupon that was struck by the steel ball.

Results of tensile tests conducted on damaged and undamaged specimens are presented in Table XV. Coatings 1 and 5 failed in undamaged areas with decreases in ductility of 5 and 11%, respectively, and strengths comparable to undamaged coatings. Coatings 2, 8 and 10 failed in damaged areas with losses in ductility of 54, 26 and 27%, respectively, compared to undamaged specimens. Impact damage reduced the yield strength of coating No. 2 approximately 11-12% and coating No. 8 by 4-8% but did not affect the yield strength of coating No. 10.

Results of the self-stressed hot-salt stress-corrosion tests are presented in Table XVI. Coating No. 1 showed no obvious degradation after impact damage; however, a pre-compression crack was found in the undamaged specimen. All of the remaining coatings suffered some degradation after impact damage. On the basis of compression values, Coating No. 10 with a 7% decrease in compression was the best performer followed by 8 (11% decrease), 2 (25% decrease) and 5 (46% decrease). Bow and maximum load values followed the same trend. All coatings, with the exception of coating No. 10, contained pre-compression cracks in at least one specimen.

The rankings of the coatings in order of decreasing resistance to impact damage, oxidation exposure after damage, and hot-salt stress-corrosion after damage are summarized below:

Rank	Impact Damage	Tensile	HSSC
1	2	5	10
2	8	1	8
3	5	8 & 10	2
4	1 & 10	2	5
5	-	-	1

None of the coatings were consistent performers in all three categories. For example, coatings 2 and 8 displayed good resistance to impact damage but poor resistance to oxidation after damage. Coating No. 10 was one of the two coatings that had the poorest resistance to impact damage but, nevertheless, had the best resistance to hot salt corrosion.

TABLE XIV

THRESHOLD IMPACT VELOCITIES AND SPECIMEN DAMAGE VELOCITIES FOR COATINGS ON Ti-6-2-4-2

Coating No.	Threshold Velocity (m/sec)	(ft/sec)	Specimen Damage Velocity (m/sec)	(ft/sec)
2B	145	475*	145	475*
8B	114	375	127	417
5B	81	264	88	290
1B	76	248	84	275
10B	76	248	84	275

* Highest velocity that would not produce rupture of the substrate.

TABLE XV

RESULTS OF TENSILE TESTS CONDUCTED ON IMPACT DAMAGED AND UNDAMAGED SPECIMENS AT SLOW STRAIN RATES AFTER EXPOSURE AT 922°K (1200°F) FOR 100 HOURS

Coating No.	Test Condition[a]	Weight Gain (Mg)	U.T.S.[b]		0.2% Y.S.[b]		Elongation[c]			Comments[d]
			(MN/m^2)	(ksi)	(MN/m^2)	(ksi)	%	Avg.	% Decrease	
1B	Damaged	1	879.2	127.6	830.2	120.5	6.3			U
1B	Damaged	0	894.3	129.8	829.6	120.4	8.7	7.5	11	U
1B	Undamaged	0	902.6	131.0	837.8	121.6	9.7			
1B	Undamaged	1	892.3	129.5	838.5	121.7	7.2	8.4		
2B	Damaged	14	864.7	125.5	743.4	107.9	4.7			D
2B	Damaged	14	855.7	124.2	735.9	106.8	4.0	4.3	54	D, C
2B	Undamaged	14	884.0	128.3	824.0	119.6	8.4			
2B	Undamaged	14	903.3	131.1	839.2	121.8	10.6	9.5		
5B	Damaged	0	914.3	132.7	781.3	113.4	12.2			U
5B	Damaged	1	920.5	133.6	834.4	121.1	10.6	11.4	5	U
5B	Undamaged	0	905.3	131.4	809.6	117.5	12.0			
5B	Undamaged	0	908.8	131.9	830.9	120.6	12.1	12.0		
8B	Damaged	5	896.4	130.1	784.8	113.9	7.8			D
8B	Damaged	4	886.7	128.7	817.8	118.7	5.5	6.7	26	D
8B	Undamaged	5	904.7	131.3	835.8	121.3	9.0	9.0		
10B	Damaged	1	904.0	131.2	822.7	119.4	9.0			D
10B	Damaged	1	909.5	132.0	834.4	121.1	9.5	9.3	27	D
10B	Undamaged	1	899.1	130.5	834.4	119.3	11.9			
10B	Undamaged	1	898.5	130.4	832.3	120.8	12.7	12.3		

NOTES:
(a) Damaged - Ballistic impact damaged per schedule listed in Table XIV. All coated specimens were glass bead peened prior to exposure or impact damage.
(b) Values for impact damaged specimens calculated on the basis of undamaged cross-section dimensions.
(c) 2.54 cm (1 inch) gage length.
(d) U - fractured in undamaged area; D - fractured in damaged area; C - crack existing prior to testing.

TABLE XVI

RESULTS OF IMPACT DAMAGED AND UNDAMAGED SELF-STRESSED CORROSION SPECIMENS AFTER EXPOSURE AT 755°K (900°F) FOR 100 HOURS

Coating No.	Test Condition[a]	Post Exposure Compression to Failure[b]					Substrate Pre-Compression Crack Depth[c]		Comments
		Compression (cm)	(in)	Bow (cm)	Max. Load (N)	(lb)	(mm)	(in)	
1B	Damaged, Salted	1.19	.469	3.50	1846	415	-	0	
1B	Damaged, Salted	0.75	.295	2.60	1846	415	0.508	.020	
1B	Salted	0.88	.345	3.10	1846	415	0.254	.010	
2B	Damaged, Salted	0.95	.373	2.90	1579	355	0.381	.015[d]	
2B	Damaged, Salted	0.71	.281	2.85	1592	358	0.254	.010[d]	
2B	Salted	1.10	.433	3.30	1935	435	0	0	
5B	Damaged, Salted	0.51	.200	2.55	1668	375	0.625	.025	
5B	Damaged, Salted	0.50	.195	2.10	1726	388	0	0	
5B	Salted	0.95	.375	3.20	1753	394	0	0	
8B	Damaged, Salted	0.41	.163	2.30	1957	440	0.508	.020	
8B	Damaged, Salted	0.45	.178	2.10	1979	445	0.508	.020	
8B	Salted	0.52	.203	2.60	2123	475	0	0	
8B	Salted	0.45	.178	1.90	2237	503	0	0	
10B	Damaged, Salted	0.85	.334	3.30	2055	462	0	0	e
10B	Damaged, Salted	0.77	.303	2.90	1846	415	0	0	
10B	Salted	0.85	.333	3.05	2015	453	0	0	

NOTES: (a) Salted - 2 drops of 10 w/o NaCl solution placed on specimen and dried at 366°K (200°F) approximately 0.006 grams NaCl deposited.

Damaged - Ballistic impact damaged per schedule in Table XIV.

(b) Compression, bow and maximum load defined in Figure 21.

(c) Maximum crack depth in substrate existing prior to compression.

(d) Cracks in impact damaged area.

(e) Neither leg of the specimen fractured in the damaged area.

3.2.9 Fatigue Tests

Coatings 1, 2, 5, 8 and 10 were evaluated for fatigue resistance on Ti-6-2-4-2 at the B coating thickness levels. Prior to testing the specimens were glass bead peened to an Almen intensity of 11N using an air pressure of 144.7 kN/m^2 (21 psi) and 0.254 mm (0.010 inch) diameter type DC glass beads. Uncoated specimens were also tested in three different heat treated conditions: mill annealed, duplex annealed, and the 15 hr/1228°K (1750°F) simulated coating thermal cycle. Tests were performed at room temperature on a Baldwin-Universal fatigue machine operating at a frequency of 30 Hz. The endurance limit at a maximum of 10^7 cycles was determined in tension-tension utilizing an A ratio* of 0.67.

Results of the fatigue tests are summarized in Figure 26. An endurance limit of 723.4 MN/m^2 (105 ksi) was obtained for the uncoated duplex annealed material and an endurance limit of 654.6 MN/m^2 (95 ksi) was obtained for both the uncoated mill annealed and uncoated 15 hr/1228°K (1750°F) heat treated materials. Fatigue Achievement Ratios (F.A.R.)** for the five coatings varied from 0.57 to 0.74 with coating No. 8 displaying the highest FAR as shown below.

Rank	Coating	F.A.R. Based on Mill Annealed and on 15 hr/(1228°K)1750°F Heat Treated Material	F.A.R. Based on Duplex Annealed Material
1	8	0.74	0.67
2	2	0.71	0.64
3	5 & 10	0.68	0.62
4	1	0.63	0.57

3.2.10 Beta Alloy

Coatings No. 1, 2, 5, 8 and 10 were evaluated for oxidation resistance and hot-salt stress-corrosion resistance on the β alloy, Ti-13V-11Cr-3Al. These coatings were deposited on tensile and self-stressed hot-salt stress-corrosion specimens using deposition parameters listed in the Appendix (Table A-3) for the heavier coating thicknesses (B series). Following coating, the specimens were glass bead peened to an Almen intensity of 11N using an air pressure of 144.7 kN/m^2 (21 psi) and 0.254 mm (0.010 inch) diameter type D.C. glass beads. Tensile specimens were exposed at 922°K (1200°F) in static air for 1000 hours together with uncoated Ti-13-11-3 in the solution treated and aged (STA)*** condition. Exposed specimens were tensile tested at room temperature at 0.127 mm/min. (0.005 inch/min.). Self-stressed hot-salt stress-corrosion specimens were salted (6 mg/cm^2 salt concentration), exposed at 755°K (900°F) in static air for 1000 hours, compression tested and evaluated using procedures described in Section 3.2.4. The self-stressed specimens were fabricated to produce a 48 MN/m^2 (7.0 ksi) stress in the outer fibers. Preliminary tests (Appendix C) on uncoated material indicated that this stress would cause 0.2% creep strain in 1000 hours.

---

* Ratio of alternating to mean stress.

** Fatigue Achievement Ratio = endurance limit of coated substrate/endurance limit of uncoated substrate.

*** 1033°K (1400°F), 1/2 hour, AC + 755°K (900°F) 48 hours, AC.

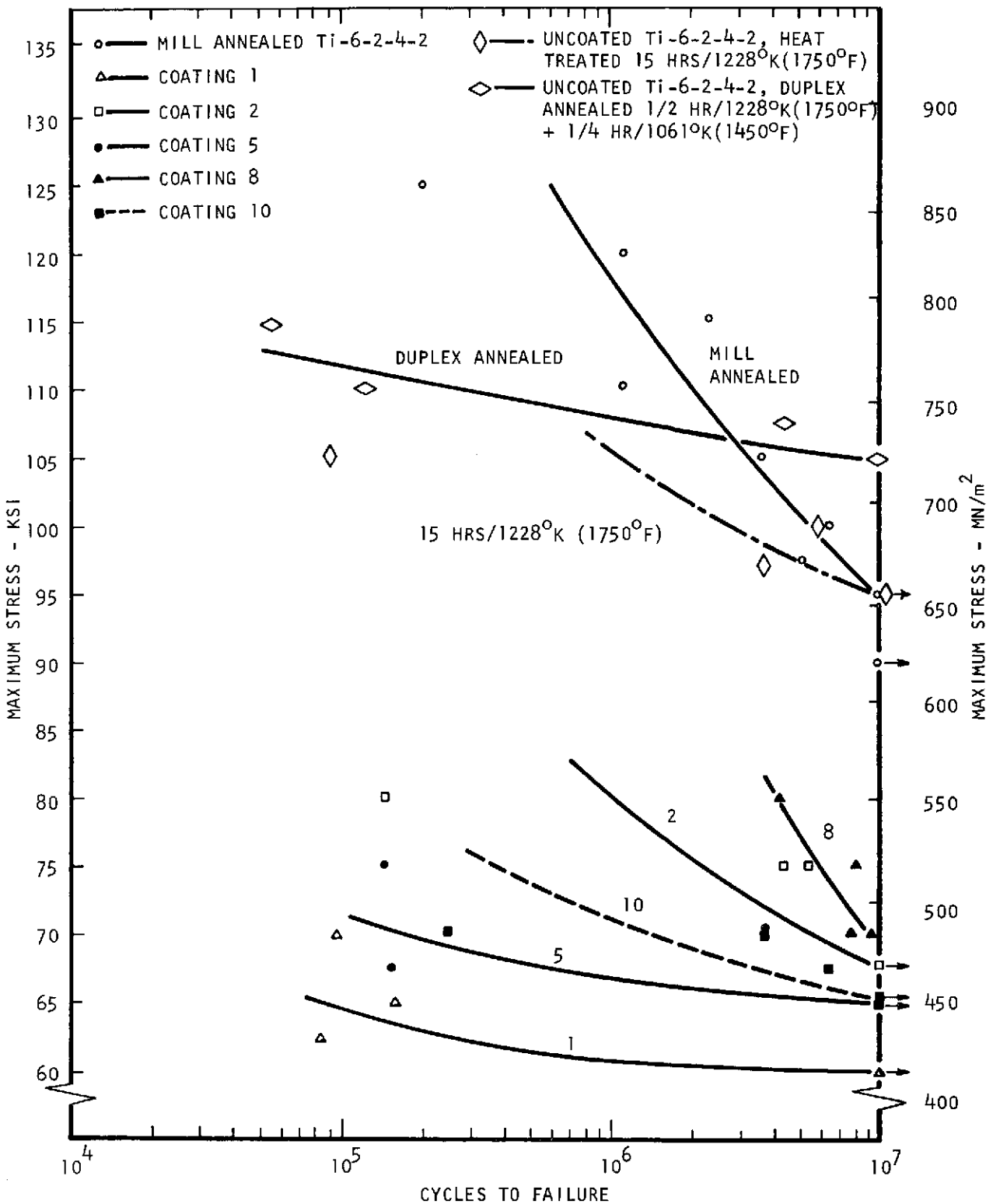

Figure 26. Fatigue Properties of Coated and Uncoated Ti-6-2-4-2

Tensile test results and total weight gained for each specimen over the 1000 hours of exposure are presented in Table XVII along with room temperature tensile properties of unexposed STA Ti-13-11-3. All coatings were protective with respect to oxidation of the β titanium alloy as evidenced by significantly lower weight gains on the coated specimens. The poorest of the coated specimens (Coating 2B) exhibited an average weight gain of 22 mg, as compared to a 41 mg average for bare substrate. The balance of coated specimens exhibited weight gains between 1 and 7 mg. Tensile properties of both the uncoated and coated specimens after exposure were characterized by drastic reductions in both strength and ductility. Ultimate strength was reduced to 22-48% of the strength of uncoated, unexposed substrate while elongation was reduced to approximately 3% of the elongation of unexposed material. Using the exposed uncoated results as a baseline, the coatings offered some degree of protectiveness as reflected by the fact that UTS values for coated and exposed specimens were slightly higher than for the exposed uncoated condition. Post-exposure ductility of the coated specimens was somewhat poorer than the exposed uncoated material; however, this result was attributed to grain growth during the coating cycle rather than oxidation.

The reduction in tensile properties of the uncoated material after exposure was attributed to oxygen contamination during exposure. Fractures of the coated specimens were characterized by various amounts of intergranular fracture which indicated a large grain size in the substrate. The reduction in tensile properties of the coated material was attributed to excessive grain growth occurring in the substrate material during the coating cycle. Typical scanning electron micrographs of the fractures observed for the uncoated and coated material are presented in Figure 27. Fractures from coating No. 2 (Figure 27a) failed primarily by an intergranular mode. The coating cycle for this coating (15 hours at 1228°K (1750°F)) was the most severe in regards to grain growth. Figure 27b shows a typical fracture encountered in coated specimens processed under the least severe coating cycle from the standpoint of grain growth (12 hours) at 1200°K (1700°F)). Approximately equal amounts of intergranular and transgranular failure and an indication of a somewhat finer grain size were observed in substrates coated with the less severe thermal cycle. Figure 27c shows the transgranular mode of failure exhibited by the uncoated-exposed Ti-13-11-3 tensile specimens.

Results of compression tests on the self-stressed specimens are presented in Table XVIII. All specimens failed in the vicinity of the weld area, either in the weld itself or adjacent to the weld. In addition, with the exception of one specimen, all specimens exhibited multiple fractures. Failure in the various areas in a given specimen occurred nearly simultaneously, and it was impossible to determine whether the maximum load corresponded to the initiation of fracture in the salted area or one of the other areas. Similarly, the compression and bow for each specimen could not be interpreted in relation to the relative performance of each coating. Compression on the test record could not be interpreted relative to the specimen area where the failure occurred, and the specimens could not be reconstructed to determine bow. Fractures in the coated self-stressed specimens were similar to fractures observed in the tensile specimens. In addition, fractures in salted areas contained pre-compression cracks as indicated in Table XVIII. These cracks were attributed to either the extremely low ductility of the substrate material after coating and/or low coating ductility.

TABLE XVII

TOTAL WEIGHT GAINS AND TENSILE TEST RESULTS FOR UNCOATED AND COATED Ti-13-11-3 ALLOY EXPOSED AT 922°K (1200°F) FOR 1000 HOURS

Coating	Total Weight Gain (Mg)	U.T.S.		.2% Y.S.		% Elongation[a]
		(MN/m^2)	(ksi)	(MN/m^2)	(ksi)	
Uncoated	35	509.1	73.9	-	-	0.5
Uncoated	46	550.5	79.9	-	-	0.5
1B	2	554.6	80.5	-	-	0.3
1B	1	638.7	92.7	-	-	0.4
2B	22	642.8	93.3	-	-	0.4
2B	21	598.7	86.9	-	-	0.2
5B	1	652.5	94.7	-	-	0.3
5B	1	736.5	106.9	-	-	- [b]
8B	7	598.1	86.8	-	-	0
8B	5	564.3	81.9	-	-	0.8
10B	3	663.5	96.3	-	-	0.5
10B	3	575.3	83.5	-	-	0.1
Uncoated[c]	-	1332.5	193.4	1223.0	177.5	2.9

NOTES: (a) 2.54 cm (1 inch) gage length.

(b) Pin hole failure.

(c) Average data for unexposed solution treated and aged Ti-13V-11Cr-3Al (Appendix C)

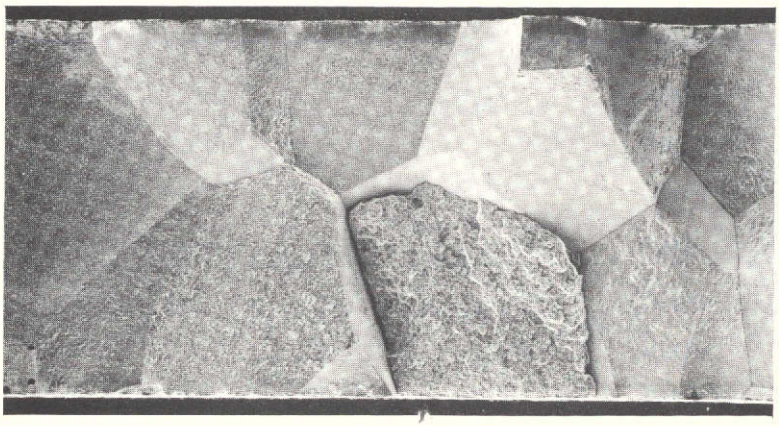

(a) Specimen 2B - Coating Cycle 15 Hr/1228°K (1750°F)

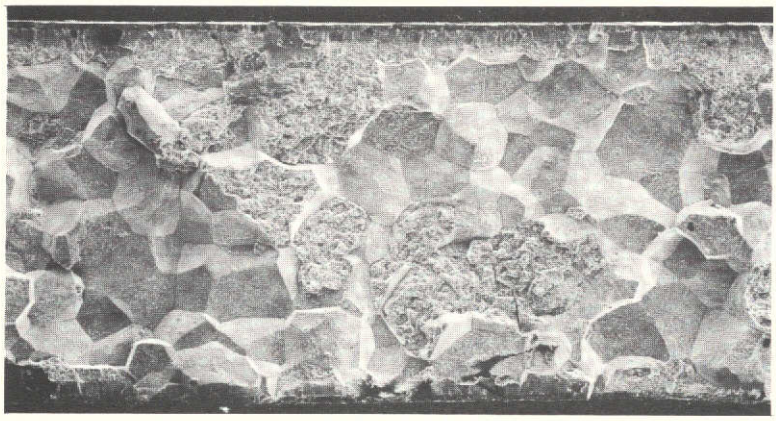

(b) Specimen 1B - Coating Cycle 12 Hr/1200°K (1700°F)

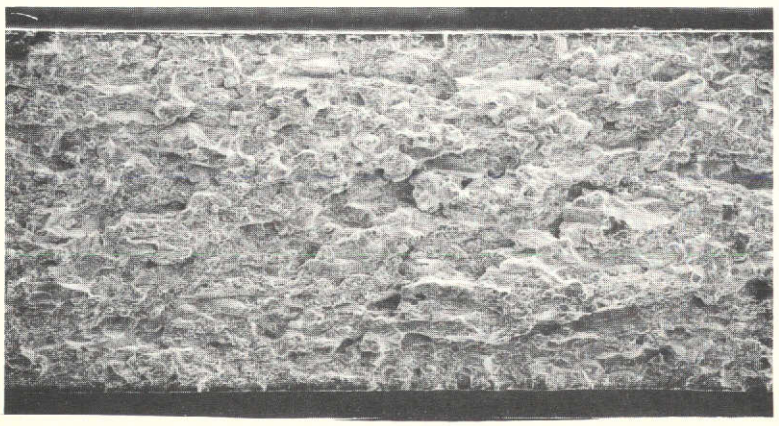

(c) Uncoated Tensile Specimen

Figure 27. Scanning Electron Microscope Fractographs of Failures in Exposed (1000 Hr/922°K (1200°F)) Tensile Specimens

TABLE XVIII

RESULTS OF UNCOATED AND COATED Ti-13-11-3 SELF-STRESSED SPECIMENS AFTER SALTING AND EXPOSURE AT 755°K (900°F) FOR 1000 HOURS

Coating No.	Maximum Load to Failure (N)	(lb)	Failure Areas[a]	Pre-Compression Crack in Salted Areas Observed at 30X (mm)	(in.)
Uncoated	2313	520	W, S	-	-
Uncoated	2135	480	W, S	-	-
1B	1334	300	W, S	0.254	0.010
1B	1624	365	W, S	1.016	0.040
2B	1913	430	W, L	-	-
2B	1557	350	W, S	0.254	0.010
5B	2068	465	W, S	0.508	0.020
5B	1979	445	W, S	0.508	0.020
8B	1535	345	W, L	-	-
8B	1801	405	W, L	-	-
10B	1668	375	W, S	0.889	0.035
10B	1913	430	W	-	-

NOTES: (a) W - Weld Area
S - Salted Area
L - Leg Area Outside of Salted Area

To summarize the results obtained on the β alloy, weight gain data indicated that the coatings protected the Ti-13-11-3 substrate from oxidation. It is apparent, however, that the coating thermal cycles seriously degrade the mechanical properties of this alloy.

3.2.11 Summary of Task I Results

Ten experimental diffusion coatings based on aluminum and silicon were deposited on Ti-6-2-4-2. All ten coatings protected the substrate from oxidation. Tensile properties of about half of the coatings compared favorably with comparably exposed uncoated Ti-6-2-4-2. Particularly outstanding was the increase in tensile ductility exhibited by some of the coated specimens. Tensile properties of the exposed coated specimens, particularly tensile elongation, were degraded in respect to uncoated, unexposed Ti-6-2-4-2. Several of the coatings protected the substrate from erosion when tested at a particle impingement angle of 20°. However, under a particle impingement angle of 90°, none of the coatings were protective. The five most promising coatings were further evaluated in fatigue. All five coatings reduced the fatigue properties of Ti-6-2-4-2. The five most promising coatings were also deposited on Ti-13-11-3. The coating thermal cycles used in depositing these coatings seriously degraded the mechanical properties of this alloy.

The most serious problem was the occurrence of coating cracks during the fabrication of self-stressed hot-salt stress-corrosion specimens. Presence of the cracks prior to exposure masked the relative performances of the coatings. Therefore, it was not possible to make a definitive interpretation of the hot-salt stress-corrosion tests.

The excellent oxidation protection and minimal tensile property degradation demonstrated in Task I warranted further investigation of the hot-salt stress-corrosion resistance of the coatings in Task II.

3.3 Task II - Hot-Salt Stress-Corrosion Resistance

Task II was directed towards determining a hot-salt stress-corrosion threshold stress for each of the coatings selected for further evaluation in Task 1.0 (Coatings 1, 2, 5, 8 and 10). To avoid pre-cracking problems associated with the self-stressed bend test and to provide more control over applied exposure stress levels, the creep exposure test described by Gray[12] was used to evaluate HSSC embrittlement in Task 2. Gray's test uses post-exposure tensile ductility of salted creep exposed tensile specimens as a measure of embrittlement from HSSC. Material form (sheet vs. bar stock) and applied salt concentration were varied in these tests in an effort to improve the sensitivity of the test so that the relative protectiveness of the coatings could be measured. Initial work was performed with the Ti-6-2-4-2 program sheet material at a salt concentration of 6 mg/cm^2. Additional testing was performed on separate heat of Ti-6-2-4-2 sheet material and Ti-6-2-4-2 bar stock at both 6 and 0.2 mg/cm^2 salt concentration levels.

3.3.1 HSSC Threshold Stress Evaluation of Coated and Uncoated Ti-6-2-4-2 Sheet

3.3.1.1 Baseline Data on Program Sheet Material

The five selected coatings were deposited on program sheet tensile specimens (Figure 1a) at the B thickness level and glass bead peened to an Almen intensity

of 11N prior to salting. Salting consisted of a 6 mg/cm^2 salt concentration placed on both sides of the reduced section of the tensile specimens. The threshold stress that caused hot-salt stress-corrosion cracking or embrittlement at 755°K (900°F) within 100 hours of exposure was selected as the evaluation criteria. The initial creep stress was 275.6 MN/m^2 (40 ksi) and stress was progressively lowered with each succeeding series of tests. Specimens that survived the creep-exposure were tensile tested at room temperature using slow strain rates. Uncoated Ti-6-2-4-2 specimens in two heat treated conditions, simulated coating thermal cycle and duplex annealed, were salted and tested under the same conditions as the coated specimens.

The results of the creep-exposure tests are presented in Table XIX. None of the coated specimens survived 100 hours of exposure at 755°K (900°F) under a 275.6 Mil/m^2 (40 ksi) stress. The stress level was therefore progressively decreased to as low as 34.5 MN/m^2 (5.0 ksi) for coating No. 2 and 17.2 MN/m^2 (2.5 ksi) on the remainder of the coated specimens. At these reduced stress levels, the coated specimens did not fail in stress rupture but were embrittled by the presence of salt as evidenced by the low residual elongation values (0.8 to 3.2%) after exposure. The uncoated specimens also exhibited evidence of embrittlement at very low creep-stress levels. The initial creep exposure stress for the uncoated specimen was 68.9 MN/m^2 (10 ksi) and was progressively lowered to 17.2 MN/m^2 (2.5 ksi) on specimens heat treated with the simulated coating thermal cycle and to 6.89 MN/m^2 (1.0 ksi) for specimens in the duplex annealed condition. At these low stress levels, residual elongation was only 1.2 and 1.3% for the uncoated specimens.

3.3.1.2 Effect of Deposition Parameter Variations on HSSC

The effect of deposition parameter variations on the hot-salt stress-corrosion resistance of coating No. 5 on Ti-6-2-4-2 creep exposure specimens was investigated using the parameter variations listed in Table XX. Magnesium content of the pack was varied from 10 to 40 weight percent. Deposition temperature was varied from 1089°K (1500°F) to 1200°K (1700°F) and deposition time was varied from 8 to 20 hours. The resulting weight gains (Table XX and Figure 28) indicate that the parameter variations resulted in considerable differences in deposition characteristics. At a constant deposition temperature of 1200°K (1700°F) and constant pack composition (10 weight percent Mg), the weight gain increased parabolically with time (Figure 28a). The maximum deposition time resulted in a weight gain of 3.4 mg/cm^2. The weight gain obtained from the pack containing 20 w/o Mg and deposited at 1200°K (1700°F) for 11 hours lies on the curve indicated from the 10 weight percent Mg pack while the pack containing 40 weight percent Mg and deposited under the same conditions resulted in substantially less weight gain, as shown in Figure 28a. Using a constant pack composition (10 weight percent Mg) and constant deposition time (12 hours), the weight gain increased with temperature as indicated in Figure 28b.

The specimens coated using the parameter variations were glass bead peened, salted and the creep exposed under a 275.6 MN/m^2 (40 ksi) stress for 100 hours at 755°K (900°F) together with uncoated mill annealed specimens. The results of this series of creep exposure tests are presented in Table XXI. Only the two uncoated specimens and one of the coated specimens survived the creep exposure and were subsequently tensile tested. Although these three specimens did not fracture during the exposure, low residual tensile elongation and the presence of oxidized areas in the fracture indicated the occurrence of hot-salt stress-corrosion cracking.

TABLE XIX

RESULTS OF CREEP-EXPOSURE TESTS AT 755°K (900°F)

(6 mg/cm^2 SALT CONCENTRATION)

Coating No.	Exposure Stress		Rupture Time	U.T.S.		0.2% Y.S.		% Elongation	Heat Tint Cracks
	(MN/m^2)	(ksi)	(hr)	(MN/m^2)	(ksi)	(MN/m^2)	(ksi)		
1	275.6	40.0	17.08	-	-	-	-	~0	Yes
	137.8	20.0	-	252.9	36.7	-	-	1.3	
	103.4	15.0	-	562.9	81.7	474.7	76.7	1.8	
	68.9	10.0	-	846.1	122.8	844.0	122.5	1.7	
	34.5	5.0	-	808.9	117.4	805.4	116.9	2.5	
	17.2	2.5	-	841.3	122.1	836.4	121.4	2.8	-
2	275.6	40.0	47.66	-	-	-	-	-	Yes
	137.8	20.0	-	347.3	50.4	345.2	50.1	1.6	
	103.4	15.0	70.8	-	-	-	-	-	
	86.1	12.5	-	474.7	119.0	-	-	2.2	
	68.9	10.0	-	890.2	129.2	842.0	122.2	7.8	No
	79.2	11.5	-	880.5	127.8	859.2	124.7	3.3	No
	62.0	9.0	-	881.9	128.0	851.6	123.6	3.6	Yes
	34.5	5.0	-	871.6	126.5	850.9	123.5	3.2	No
5	275.6	40.0	19.2	-	-	-	-	-	Yes
	275.6	40.0	7.5	-	-	-	-	-	
	137.8	20.0	70.1	-	-	-	-	-	
	103.4	15.0	-	206.7	30.0	-	-	1.3	
	68.9	10.0	18.1	-	-	-	-	-	
	34.5	5.0	-	780.6	113.3	767.5	111.4	1.0	
	17.2	2.5	-	799.2	116.0	767.5	111.4	2.6	No
8	275.6	40.0	13.1	-	-	-	-	-	Yes
	137.8	20.0	22.2	-	-	-	-	-	
	68.9	10.0	-	744.1	108.0	-	-	1.4	
	20.7	3.0	-	654.6	95.0	-	-	0.6	No
10	275.6	40.0	4.3	-	-	-	-	-	Yes
	137.8	20.0	-	309.4	44.9	288.0	41.8	1.3	
	103.4	15.0	-	370.7	53.8	365.2	53.0	1.6	
	68.9	10.0	-	881.9	128.0	881.9	128.0	1.5	
	34.5	5.0	-	854.4	124.0	-	-	0.8	No
	17.2	2.5	-	906.0	131.5	-	-	1.1	No
Uncoated[a]	68.9	10.0	-	888.1	128.9	802.7	116.5	2.2	Yes
	51.7	7.5	-	908.8	131.9	-	-	6.6	
	34.5	5.0	-	906.7	131.6	-	-	1.3	
	17.2	2.5	-	855.0	124.1	-	-	1.3	

TABLE XIX (continued)

Coating No.	Exposure Stress (MN/m^2)	Exposure Stress (ksi)	Rupture Time (hr)	U.T.S. (MN/m^2)	U.T.S. (ksi)	0.2% Y.S. (MN/m^2)	0.2% Y.S. (ksi)	% Elongation	Heat Tint Cracks
Uncoated[b]	68.9	10.0	-	755.1	109.6	-	-	0.8	Yes
↓	51.7	7.5	-	837.1	121.5	-	-	1.0	↓
	17.2	2.5	-	791.7	114.9	-	-	0.8	
	6.9	1.0	-	810.3	117.6	-	-	1.2	

NOTES: (a) Heat Treated 15 hr/1228°K (1750°F)

(b) Heat Treated 1/2 hr/1228°K (1750°F) + 1/4 hr/1061°K (1450°F) (duplex annealed)

TABLE XX

DEPOSITION PARAMETERS USED IN OPTIMIZATION OF COATING 5 ON Ti-6-2-4-2 AND RESULTING WEIGHT GAINS

Pack Composition	Deposition Temp. (°K)	Deposition Temp. (°F)	Deposition Time (hrs)	Weight Gain (Mg/Cm^2)
90 w/o (Cr/Al) + 10 w/o Mg	1200	1700	8	2.2
	↓	↓	12	2.9
			20	3.4
	1089	1500	12	1.0
	1144	1600	12	1.8
80 w/o (Cr/Al) + 20 w/o Mg	1200	1700	11	2.8
60 w/o (Cr/Al) + 40 w/o Mg	1200	1700	11	2.2

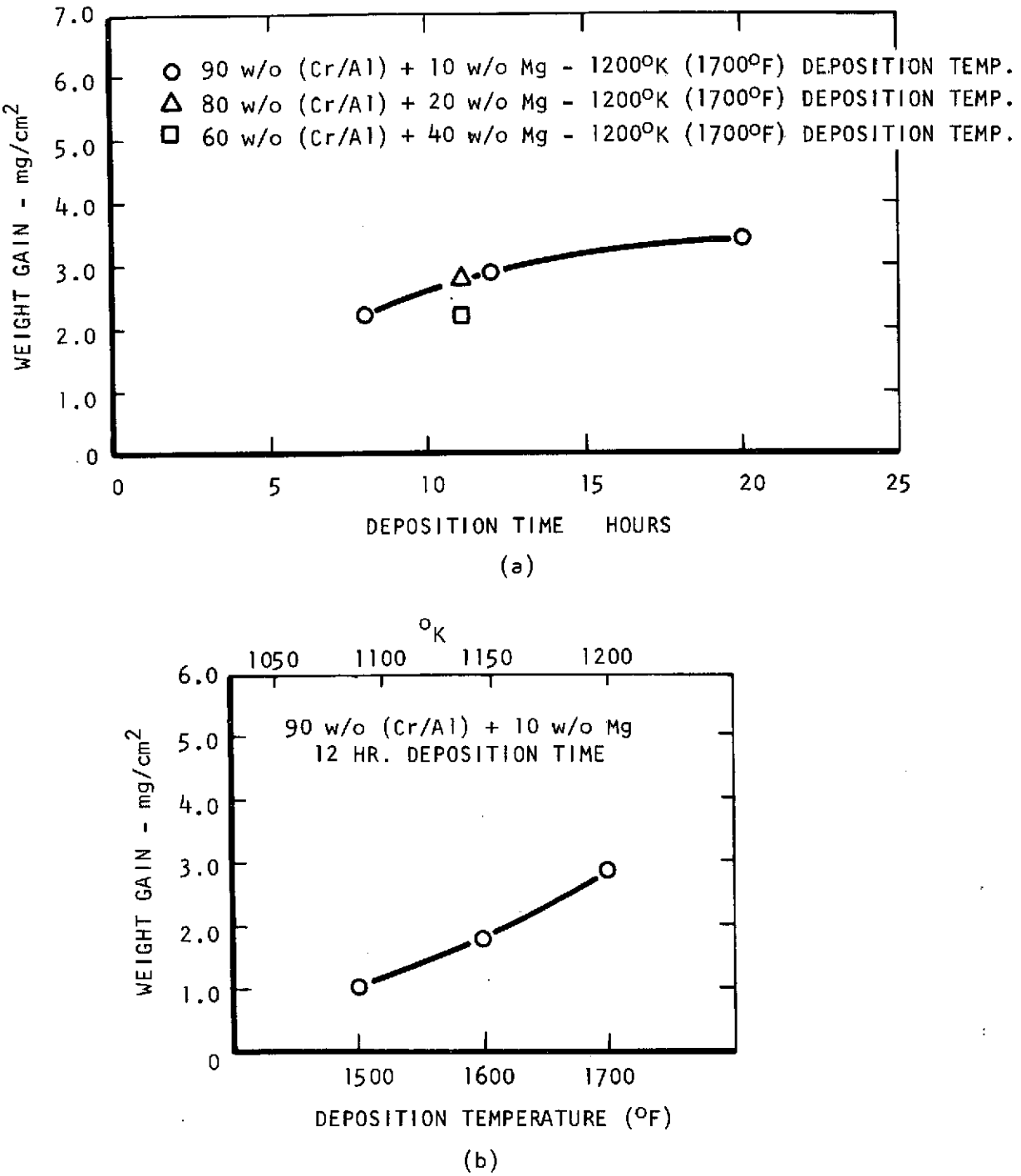

Figure 28. Weight Gains Obtained by Varying Deposition Parameters for Coating No. 5 on Ti-6-2-4-2

TABLE XXI

RESULTS OF CREEP EXPOSURE ON SALTED SPECIMENS

COATED WITH COATING NO. 5 VARIATIONS

Specimen No.	Pack Composition	Deposition Temp. (°K)	Deposition Temp. (°F)	Deposition Time (hrs)	Rupture Time[a] (hrs)	Post Exposure Tensile Properties U.T.S. (MN/m^2)	U.T.S. (ksi)	.2% Y.S. (MN/m^2)	.2% Y.S. (ksi)	% Elongation	HSSC Cracks
A	Uncoated				>100	946.0	137.3	940.5	136.5	2.3	Yes
B	"				>100	785.5	114.0	709.0	102.9	1.5	
5B-1	90w/o(Cr/Al)+10w/o Mg	1200	1700	12	19.2						
5B-2		1200	1700	12	7.5						
5C-1		1200	1700	8	2.0						
5C-2		1200	1700	8	62.4						
5D-1		1200	1700	20	8.0						
5D-2		1200	1700	20	47.2						
5E-1		1089	1500	12	54.3						
5E-2		1089	1500	12	>100	849.5	123.3	828.9	120.3	2.2	
5F-1		1144	1600	12	21.2						
5F-2		1144	1600	12	8.8						
5G-1	80w/o(Cr/Al)+20w/o Mg	1200	1700	12	31.8						
5G-2	" " " "	1200	1700	12	16.3						
5H-1	60w/o(Cr/Al)+40w/o Mg	1200	1700	12	16.4						
5H-2	" " " "	1200	1700	12	20.2						

NOTE: (a) 755°K (900°F)/275.6 MN/m^2 (40 ksi) exposure.

3.3.1.3 Unstressed HSSC Exposure Tests on Program Sheet

From the results of the preceding creep-exposure tests, it was apparent that the coatings did not protect the substrate from hot-salt stress-corrosion. In addition, the Ti-6-2-4-2 program sheet material appeared to have abnormally high sensitivity to hot-salt stress-corrosion compared to the hot-salt stress-corrosion resistance of Ti-6-2-4-2 bar stock. A threshold embrittlement stress of 447.9 MN/m^2 (65 ksi) has been reported[12] for uncoated Ti-6-2-4-2 bar stock exposed at 755°K (900°F) for 96 hours with a salt concentration of 0.12 mg/cm^2. In view of this comparison, the hot-salt stress-corrosion resistance of the program sheet was further investigated in a series of unstressed exposure tests.

Mill annealed tensile specimens were exposed at 755°K (900°F) for 100 hours in still air under no load. Specimens were exposed in both the salted and unsalted conditions and tensile tested at slow strain rates together with unexposed, unsalted specimens. Tensile tests results for the program sheet material (Heat No. V3467) are presented in Table XXII. Unexposed, unsalted specimens had an average elongation of 15.3%. Exposure at 755°K (900°F) reduced the ductility of unsalted specimens to an average of 13.5% while the exposed salted specimens had an average elongation of only 8.1%. Apparently, the presence of salt at 755°K (900°F) was sufficient to embrittle the Ti-6-2-4-2 program material even in the absence of applied stress.

3.3.1.4 HSSC Exposure Tests on a Second Heat of Sheet Material

Because the HSSC sensitivity of the program sheet material seemed abnormally high when compared to Gray's results, a second heat of Ti-6-2-4-2 sheet material was procured and evaluated under the same conditions as the program material. Tensile tests results for the second heat (RMI 302824) of Ti-6-2-4-2 sheet are presented in Table XXII. The test results were similar to those obtained on the program material. Unexposed specimens had an average elongation of 14.8%. Exposure at 755°K (900°F) in the unsalted condition reduced reduced the elongation to an average of 14.2%. Exposure at 755°K (900°F) after salting reduced the elongation to an average of 6.8%. In addition to the exposure under no load, two specimens from the second heat were salted and creep-exposed for 100 hours at 755°K (900°F) under a 137.8 MN/m^2 (20 ksi) load. These specimens had an average residual elongation of 4.6% after the creep exposure.

3.3.2 Influence of Material Form and Salt Concentration on HSSC Sensitivity

The extremely high sensitivity of the sheet materials to HSSC embrittlement precluded a judgment as to the effect of the coatings on HSSC. In an effort to improve the discriminating power of the HSSC tests, variations of material form and salt concentration were studied. The alternate material investigated was a heat of Ti-6-2-4-2 bar stock that had exhibited good HSSC resistance in a previous study[12] at NASA. Salt concentrations of 6 and 0.2 mg/cm^2 were applied to this material and to the previously studied sheet specimens.

Coatings selected for further evaluation in Task I (Nos. 1, 2, 5, 8 and 10) were evaluated for hot-salt stress-corrosion resistance on mill annealed Ti-6-2-4-2 bar stock. The substrate material was machined into tubular tensile specimens having a 1.27 mm (0.050 inch) thick wall in the reduced area as previously shown in Figure 2. Coatings were deposited on both the I.D. and O.D. of the specimens

TABLE XXII

TENSILE PROPERTIES OF MILL ANNEALED Ti-6-2-4-2 SHEET MATERIAL

Heat No.	Specimen No.	Test Condition	U.T.S. (MN/m^2)	U.T.S. (ksi)	0.2% Y.S. (MN/m^2)	0.2% Y.S. (ksi)	% Elongation
V-3467	TU-1	Chem Mill[a]	964.6	140.0	870.2	126.3	15.7
	TU-2	" "	954.3	138.5	856.4	124.3	14.8
	TE-1	Chem Mill[a], Expose[b]	1062.4	154.2	1005.3	145.9	13.7
	TE-2	" " "	1043.8	151.5	980.4	142.3	13.2
	TSE-1	Chem Mill[a], Salt[c], Expose[b]	1023.9	148.6	973.6	141.3	8.2
	TSE-2	" " " "	1025.2	148.8	974.9	141.5	8.0
302824	UU-1	Chem Mill[a]	996.3	144.6	908.1	131.8	13.9
	UU-2	" "	1001.1	145.3	915.7	132.9	15.6
	UE-1	Chem Mill[a], Expose[b]	1039.0	150.8	970.8	140.9	15.5
	UE-2	" " "	1032.8	149.9	960.5	139.4	12.9
	SE-1	Chem Mill[a], Salt[c], Expose[b]	997.0	144.7	949.4	137.8	6.3
	SE-2	" " " "	968.0	140.5	934.3	135.6	7.2
	CE-1	Chem Mill[a], Salt[c], Creep Expose[d]	983.9	142.8	927.4	134.6	5.1
	CE-2	" " " "	1060.3	153.9	939.1	136.3	4.1

NOTES: (a) 1-2 mils per side removed using a solution of 3 v/o HF + 30 v/o HNO_3 + 67 v/o H_2O.

(b) Expose - 100 hours at 755°K (900°F).

(c) Salt - approximately 6 mg/cm^2 concentration.

(d) Creep Expose - 100 hours of exposure at 755°K (900°F) under 275.6 MN/m^2 (40 ksi) stress.

using deposition parameters previously established for producing the B coating thickness level on Ti-6-2-4-2 sheet specimens. The I.D. of the specimens was packed with coating material to obtain a deposit in this area of the specimens. For the pack coatings, the material in the I.D. was identical to the pack composition. For the slurry coatings, the material in the I.D. was the same except no cellulose nitrate binder was used. Some variation in coating pickup between the sheet specimens and tubular specimens was noted for the individual coating systems as shown in Table XXIII. In particular, coatings 2 and 8 had much larger weight gains on the tubular specimens. Coating No. 2 had a weight gain of 4.93 mg/cm^2 and 11.55 mg/cm^2 in two separate coating runs with tubular specimens compared to a weight gain of 0.6 mg/cm^2 on the sheet specimens. Coating No. 8 had a weight gain of 1.25 mg/cm^2 on the tubular specimens compared to 0.4 mg/cm^2 on the sheet specimens. There is no obvious explanation for the variations in weight gains between the tubular specimens and the sheet specimen.

Coated and uncoated specimens were salted and creep exposed at 755°K (900°F) for 100 hours under dead weight loading. The tensile specimens were salted by spraying a 10 weight percent NaCl solution in deionized water on the OD of the reduced section as the specimen was rotated about its longitudinal axis. The specimens were then air dried at 366°K (200°F) for two hours. Initially, a salt concentration of 6 mg/cm^2 was deposited (uncoated specimens only). The salt concentration was then reduced to 0.2 mg/cm^2 to increase the discrimination of the tests and allow ranking of the HSSC resistance of the coatings. Following creep-exposure, the specimens were tensile tested at room temperature using slow strain rates.

Results of the HSSC tests on coated and uncoated tubular specimens are presented in Table XXIV. Initially, uncoated specimens were exposed under a 344.5 MN/m^2 (50 ksi) creep stress using salt concentrations of 6 mg/cm^2 and 0.2 mg/cm^2 (specimens N-1 and N-2). Both specimens exhibited HSSC as evidenced from the low elongation values and presence of oxidized cracks in the fracture surfaces. HSSC occurred to a lesser extent with the lower salt concentration (Specimen N-2) as indicated by the higher residual strength and elongation of the specimen. Subsequent specimens were therefore tested with the 0.2 mg/cm^2 salt concentration. An embrittlement threshold stress of 103.4 MN/m^2 (15.0 ksi) was determined for the uncoated Ti-6-2-4-2 bar stock based on Gray's[12] criteria for embrittlement by hot-salt stress-corrosion. Gray considered a specimen embrittled by salt/stress exposure if the subsequent tensile test indicated less than 15.5% residual elongation and less than 25% residual apparent reduction in area.

The embrittlement threshold stress determined in the present program (103.4 MN/m^2, 15.0 ksi) is far less than the threshold embrittlement stress (447.9 MN/m^2, 65 ksi) reported by Gray[12]. Gray exposed the material under substantially the same conditions (96 hr/755°K (900°F) with a salt concentration in the range of 0.07 to 0.12 mg/cm^2. It is unlikely that small differences in salt concentration (0.2 mg/cm^2 in the present program) and the exposure air would result in the widely different values of threshold stress. It is more probable that less moisture was present in the salt deposits on the NASA program and may account for the difference in HSSC resistance. In the NASA study, salt was applied by exposing the I.D. of the specimen for 1 hour to a salt-in-air concentration of 40 parts per billion at an air velocity of 300 m/sec (1000 ft/sec) with an air temperature of 478°K (400°F).

TABLE XXIII

COATING WEIGHT GAINS ON SHEET TENSILE SPECIMENS AND TUBULAR TENSILE SPECIMENS

Coating No.	Sheet Specimens, Weight Gain, (mg/cm^2)	Tubular Specimen, Weight Gain, (mg/cm^2)
1	2.00	2.49
2	0.60	4.93
2	-	11.55
5	2.60	1.96
8	0.40	1.25
10	1.60	1.60

TABLE XXIV

TENSILE PROPERTIES OF COATED AND UNCOATED Ti-6-2-4-2

AFTER 100 HR/755°K (900°F) CREEP EXPOSURE

Coating	Specimen Type[a]	Specimen No.	Salt Concentration mg/cm²	Exposure Stress (MN/m²)	Exposure Stress (ksi)	U.T.S. (MN/m²)	U.T.S. (ksi)	0.2% Y.S. (MN/m²)	0.2% Y.S. (ksi)	El. (%)	Apparent R.A. (%)[c]	Heat Tint Cracks	Failure Areas[d]
Uncoated	Tubular	(b)	-	-	-	1120.0	162.0	-	-	18.0	33.0	-	-
		N-1	6	344.5	50.0	380.3	55.2	-	-	~0	~0	Yes	S
		N-2	0.2	344.5	50.0	833.7	121.0	624.9	90.7	0.6	~0	Yes	
		N-3		68.9	10.0	1101.7	159.9	1064.5	154.5	15.5	36.0	No	
		N-4		137.8	20.0	1103.8	160.2	1057.0	153.4	11.4	16.0		
		N-20		103.4	15.0	1044.5	151.6	1014.2	147.2	15.7	33.8		
Uncoated	Flat	TSE-3	0.2	344.5	50.0	577.0	83.7	566.4	82.2	0.8	-	Yes	S
Uncoated	Flat	TSE-4	0.2	68.9	10.0	1042.5	151.3	988.0	143.4	5.8	-	No	S
1	Tubular	N-5	0.2	68.9	10.0	880.5	127.8	-	-	1.4	~0	Yes	S
		N-6		34.5	5.0	910.9	132.2	905.3	131.4	4.2	~0	No	S
		N-19		17.2	2.5	858.5	124.6	-	-	1.1	~0	No	Su
2	Tubular	N-9	0.2	68.9	10.0	684.2	99.3	-	-	1.3	~0	Yes	S
		N-7		34.5	5.0	906.0	131.5	863.3	125.3	16.7	7.9[e]	No	
		N-8		51.7	7.5	888.1	128.9	849.5	123.3	2.0	~0		
		N-21		34.5	5.0	784.8	113.9	746.9	108.4	3.8	~0		
		N-22		None	None	780.6	113.3	748.3	108.6	7.6	14.2		-
5	Tubular	N-16	0.2	68.9	10.0	334.2	48.5	277.0	40.2	2.3	~0	Yes	Su
		N-17		34.5	5.0	885.0	124.1	850.9	123.5	2.9	~0	No	Su
		N-18		17.2	2.5	848.2	123.1	-	-	2.2	~0	No	S
8	Tubular	N-13	0.2	68.9	10.0	881.9	128.0	-	-	2.6	3.4	Yes	Su
		N-14		34.5	5.0	893.6	129.7	-	-	2.7	5.9	No	S
		N-15		17.2	2.5	888.1	128.9	-	-	2.5	3.6	No	S

TABLE XXIV (continued)

Coating	Specimen Type[a]	Specimen No.	Salt Concentration mg/cm^2	Exposure Stress (MN/m^2)	Exposure Stress (ksi)	U.T.S. (MN/m^2)	U.T.S. (ksi)	0.2% Y.S. (MN/m^2)	0.2% Y.S. (ksi)	El. (%)	Apparent R.A.[b] (%)	Heat Tint Cracks	Failure Areas[c]
10	Tubular	N-10	0.2	68.9	10.0	885.4	128.5	-	-	1.0	~0	Yes	S
↓	↓	N-11	↓	34.5	5.0	900.5	130.7	898.5	130.4	2.9	~0	No	S
		N-12		17.2	2.5	873.0	126.7	-	-	2.5	~0	No	S

NOTES: (a) Tubular - Machined from barstock.
Flat - Machined from program sheet.
(b) Data from NASA TND-6498 (Reference 12).
(c) Based on changes in outside diameter only.

(d) S - beneath salt coating.
Su - at salt coating/no-salt interface.

(e) Slant Fracture - Accurate Determination of R.A. was not possible.

In order to determine the effect of salt concentration on the program sheet material, a few specimens from Heat No. V3467 were creep exposed with the lower salt concentration. Post-exposure tensile test results on these specimens (TSE-3 and TSE-4) are presented in Table XXIV. Both specimens were embrittled by the exposure. Specimen TSE-3, exposed under a 344.5 MN/m^2 (50 ksi) stress had a residual elongation of 0.8% while specimen TSE4, exposed under a 68.9 MN/m^2 (10.0 ksi) stress, had a residual elongation of 5.8%. By comparison, unsalted, uncoated mill annealed Ti-6-2-4-2 exposed at 922°K (1200°F) for 100 hours had an average residual elongation of 11.7% (see Appendix B, Table B-1).

All of the coated tubular specimens were creep-exposed using the lower salt concentration (0.2 mg/cm^2). The creep-exposure stress on coatings 1, 5, 8 and 10 was progressively lowered to 17.2 MN/m^2 (2.5 ksi), but subsequent tensile tests still disclosed evidence of embrittlement. At the 17.2 MN/m^2 (2.5 ksi) exposure stress level, residual elongation values for these coatings ranged from 1.1 to 2.5%. Residual apparent reduction in area at the 17.2 MN/m^2 (2.5 ksi) exposure stress level was 3.6% for coating 8 and not measurable on coatings 1, 5 and 10. Coating No. 2 had an apparent crack threshold stress of 34.5 MN/m^2 (5.0 ksi) as indicated by specimens N-7, N-8 and N-9. When it was attempted to verify the 34.5 MN/m^2 (5.0 ksi) threshold stress level (Specimen N-21), embrittlement was again evidenced in a post-exposure tensile test. This discrepancy may be due to differences in coating thicknesses. Specimens N-7, N-8 and N-9 had an average weight gain of 4.93 mg/cm^2. Specimen N-21 was coated in a separate run and specimens coated in this run had an average weight gain of 11.55 mg/cm^2. An additional specimen, N-22, coated together with N-21 was exposed for 100 hours at 482°C (900°F) without an applied stress or salt, had a residual elongation of only 7.6% as shown in Table XXII. Previously, 100 hr/922°K (1200°F) exposed sheet specimens of coating No. 2 had average residual elongations of 14.0% compared to 14.2% residual elongation obtained for uncoated, unexposed mill annealed Ti-6-2-4-2 (see Appendix B, Table B-1). Thus, the heavier coating thickness on specimen N-21 and N-22 results in reduced ductility and may have increased the susceptibility to hot-salt stress-corrosion.

3.3.3 Metallography and EMP Analyses of Coating No. 2

Metallographic examination and electron microprobe spot analyses were performed on coating No. 2 deposited on coupons of the Ti-6-2-4-2 bar stock in the as-deposited condition and after 1000 hr/922°K (1200°F) oxidation exposure. The coupons were coated in the same run as the tubular specimens N-7, N-8 and N-9. Microstructures of the as-deposited and 1000 hr/922°K (1200°F) oxidation exposed condition are shown in Figure 29. The as-deposited microstructure consists of a light etching outer coating matrix with a fine dispersion of second phase particles concentrated near the outer surface. A second layer, virtually free of the second phase particles, appears adjacent to the unaffected substrate. Except for a small amount of oxide penetration, the 1000 hour exposure made no discernible change in the microstructure.

Spot microprobe analyses of the major elements in the substrate and Si are presented in Figures 30 and 31. In the as-deposited condition (Figure 30), the coating consisted primarily of Si and Ti. Zirconium was the only other substrate element that was present in the coating to any appreciable extent. At a maximum of 14 weight percent, zirconium was present at a distance of 25.4 μm (0.001 inch) from the surface. This corresponded to the beginning of the second layer of the

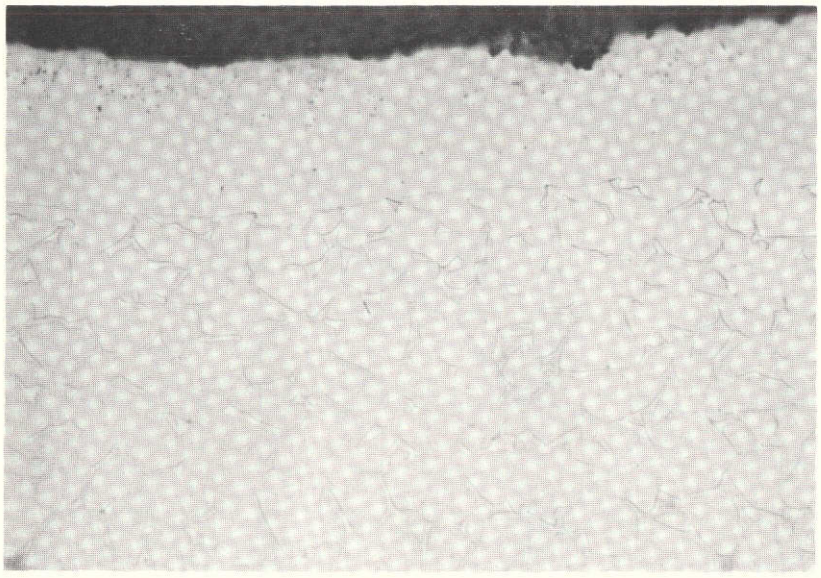

(a) As-Deposited

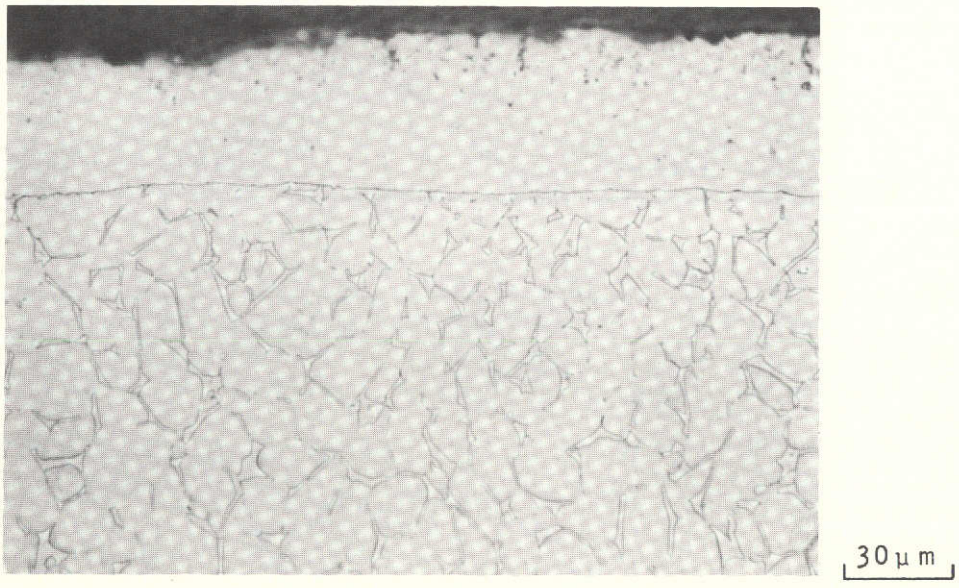

(b) 1000 Hr/922°K (1200°F) Exposed

Figure 29. Microstructure of Coating 2 (Si) Deposited on Ti-6-2-4-2 Bar Stock in the As-Deposited Condition (a) and After 1000 Hr/922°K (1200°F) Oxidation Exposure

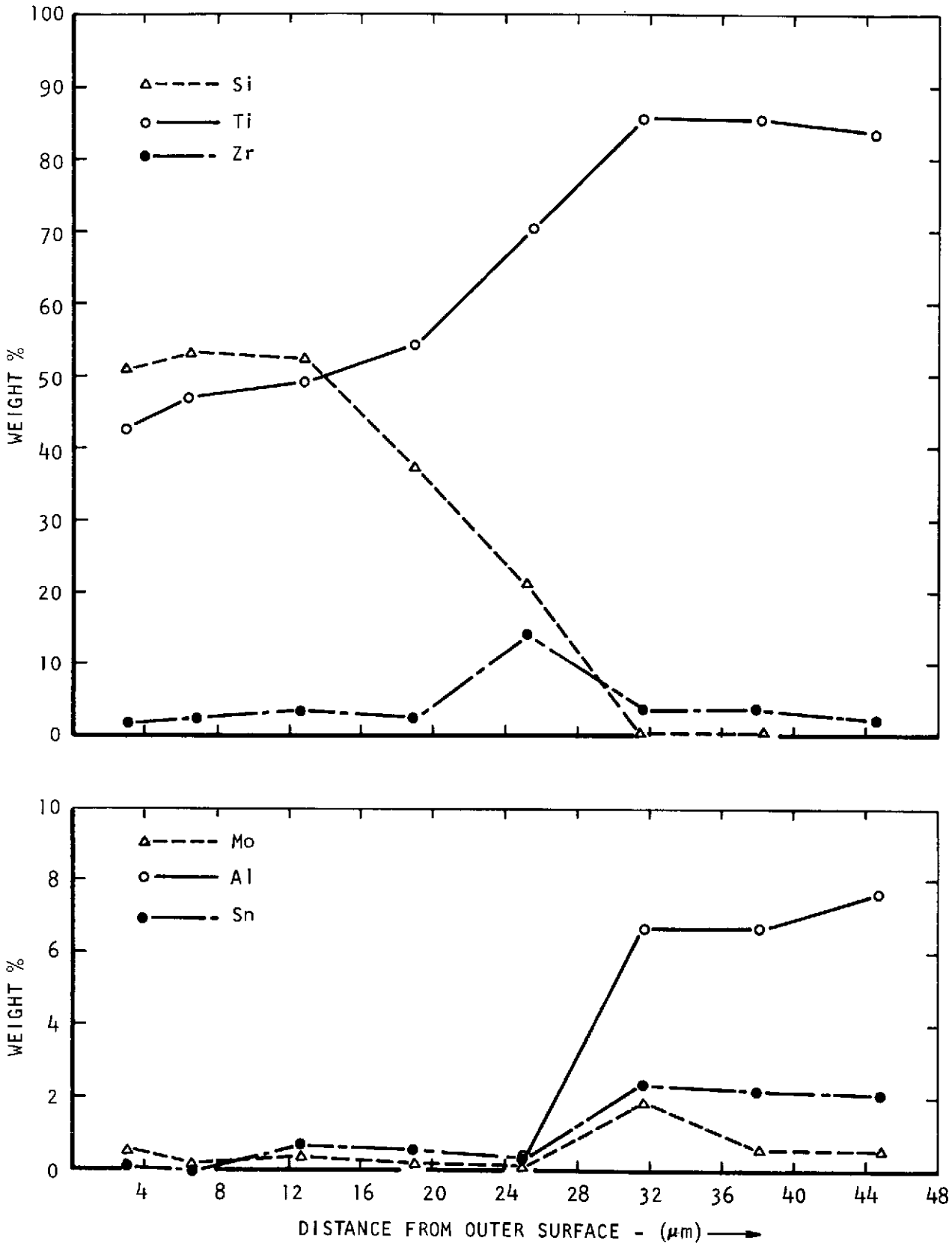

Figure 30. Chemical Composition Profiles of Coating No. 2 on Ti-6-2-4-2 in the As-Deposited Condition

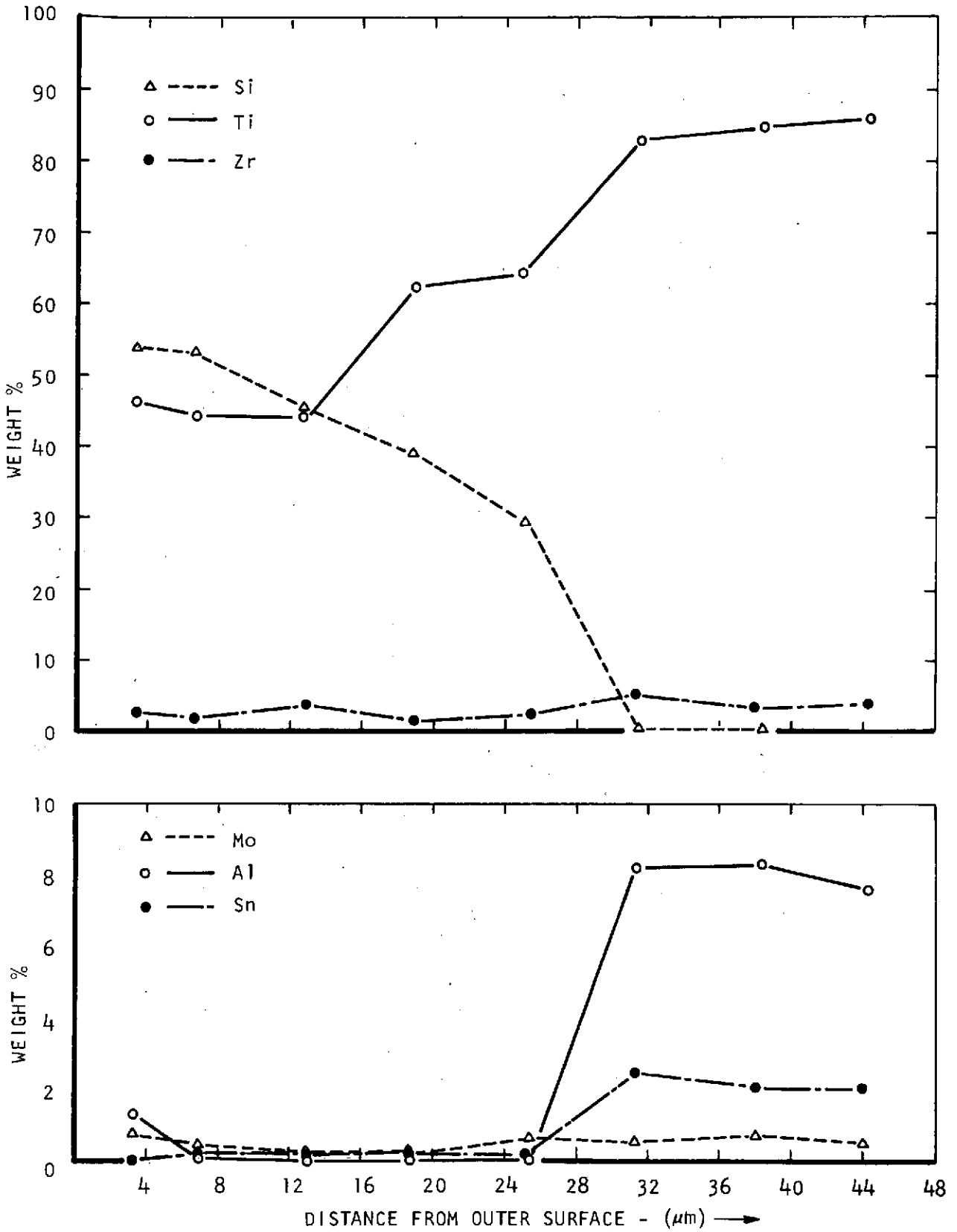

Figure 31 Chemical Composition Profiles of Coating No. 2 on Ti-6-2-4-2 After 1000 Hr/922°K (1200°F) Exposure.

coating adjacent to the unaffected substrate. Only a trace amount of aluminum was found in the layer adjacent to the unaffected substrate. Aluminum was not detected in the remainder of the coating. Small amounts of Sn and Mo were detected throughout the coating.

Compositional profiles of the exposed specimen (Figure 31) are substantially similar to those of the as-deposited condition. The only major changes were the migration of trace amounts of aluminum to the outer surface of the coating and the disappearance of the Zr peak.

3.3.4 Discussion of Results

The present study has shown that hot-salt stress-corrosion cracking at 755°K (900°F) is the most serious problem associated with diffusion coatings. While good oxidation protection and tensile properties could be obtained with the coatings, the presence of the coatings intensified HSSC. The reason that the coatings intensified HSSC may be related to inherently poor coating ductility or a combination of poor coating ductility and an electrochemical cell type of reaction similar to that proposed by Garfinkle[13]. While there is disagreement as to the exact mechanism involved in stress corrosion cracking of titanium alloys, it is generally accepted that hydrogen embrittles the substrate and is followed by crack initiation and propagation. The combination of an inherently brittle coating and a low modulus substrate could lead to fine coating cracks formed at very low stresses. HSSC in the coatings would only require the propagation of an existing crack. In addition, crack tips represent local stress concentrations and the elastic stresses in these areas would be higher than the nominal stress levels. The coating elements may also be involved in an electrochemical cell reaction. Garfinkle[13] has proposed a model for HSSC in titanium alloys which assumes that an oxygen concentration gradient exists between the exposed surface and shielded areas such as under salt crystals and at crack tips. Oxygen is reduced at the exposed cathodic areas while substrate dissolution and formation of halides occurs at the shielded cathodic areas. Subsequent hydrolysis of the halides produces hydrogen. Whether an element promotes HSSC is dependent upon its electronegativity with respect to the substrate and whether it forms halides susceptible to hydrolysis. In particular, Garfinkle[13] has demonstrated that a partial coating of vapor deposited aluminum on Ti-8Al-1Mo-1V intensifies HSSC.

The diffusion coatings used in the program, containing Al, Si, Cr as major coating elements, are similar to coatings that have been used successfully to protect superalloy components from the hostile gas turbine environment. From the results of the HSSC tests, it is apparent that a different approach is required to develop coatings that will protect titanium from HSSC.

4.0 SUMMARY OF RESULTS

The following summation can be made from the experimental work performed on this program.

1. All coatings protected the substrate from oxidation under 1000 hr/922°K (1200°F) exposure conditions.

2. Tensile tests of coated Ti-6-2-4-2 specimens oxidation exposed at 922°K (1200°F) indicated that tensile properties, particularly elongation, were degraded with respect to uncoated, unexposed Ti-6-2-4-2.

3. Tensile properties of coated Ti-6-2-4-2 specimens oxidation exposed at 922°K (1200°F) compared more favorably to uncoated Ti-6-2-4-2 that was comparably exposed. After 1000 hours of exposure, about half of the coated specimens had strength equivalent or somewhat higher than uncoated materials and increased ductility over the uncoated specimens.

4. Erosion test results indicate that only two coatings (3 and 5) protected the substrate from erosion at an impingement angle of 20°, while none of the coatings protected the substrate from erosion at an impingement angle of 90°.

5. All of the coatings selected for fatigue testing (coatings 1, 2, 5, 8 and 10) reduced the fatigue properties of Ti-6-2-4-2 compared to uncoated material. Coating No. 8 displayed the best fatigue properties.

6. Ballistic impact damage, followed by oxidation exposure, reduced the tensile properties of coatings 1, 2, 5, 8 and 10 on Ti-6-2-4-2. Coating No. 2 had the highest impact resistance, but coating No. 5 had the best residual tensile properties.

7. Deposition of the selected coatings (1, 2, 5, 8 and 10) on Ti-13V-11Cr-3Al drastically reduced the tensile properties of this alloy.

8. All of the coatings displayed poor resistance to hot-salt stress-corrosion cracking. The presence of the coatings intensified the attack on the substrate.

5.0 CONCLUSIONS AND RECOMMENDATIONS FOR FUTURE WORK

The present study has shown that the most serious problem associated with the diffusion coatings tested on the program is their poor resistance to hot-salt stress-corrosion at 755°K (900°F). While good oxidation protection and minimal reduction in tensile properties could be obtained with some of the coatings, the fact that the coatings intensified hot-salt stress-corrosion would preclude their use in turbine engine environments. The problem may lie with the inherently poor ductility of the diffusion coatings or a combination of poor coating ductility and unfavorable electrochemical reactions. In either case, the program results indicate that the diffusion coating approach, utilizing elements such as Si, Al and Cr, that has been used successfully for protecting superalloy components, will probably not be useful for protecting titanium alloys from HSSC. Further work should involve the investigation of other types of coatings, such as overlays, that would be mechanically or chemically compatible with the substrate.

APPENDIX A

COATING DEPOSITION DATA

TABLE A-1

COATING DATA FOR Ti-6-2-4-2

Run	Coating	Temperature (°K)	Temperature (°F)	Time (Hr)	Weight Gain, mg/cm^2	Metallographic Thickness ($In. \times 10^{-3}$)	Metallographic Thickness (μm)	Remarks
N1	No. 5 - Al-Mg	1200	1700	4	1.3	1.0	25.4	
N2	No. 5 - Al-Mg	↓	1700	8	1.7	1.5	38.1	
N3	No. 1 - Al	↓	1700	8	2.3	1.5	38.1	
N4	No. 2 - Si	1228	1750	6	0.95	0.5	12.7	
N5	No. 7 - Si-Cr-Al	↓	1750	6	0.95	0.2-0.5	0.51-12.7	
N6	No. 2 - Si	↓	1750	12	1.1	0.5-0.75	12.7-19.1	
N7	No. 7 - Si-Cr-Al	↓	1750	12	1.1	0.75	19.1	
N8	No. 4 - Al-Si	1200	1700	2	88.2[c]	1.5	38.1	
N9	↓	1033	1400	2	68.7[c]	0.38-0.5	9.7-12.7	
N10	↓	922	1200	2	15.1[c]	0.5	12.7	
N11	↓	922	1200	4	17.7[c]	1.0	25.4	Dusted with Fe/50Al
N12	Cr-Cr Precoat	1228	1750	4	5.0	2.25	57.2	Light sanding to remove bisque
	Cr-Cr Precoat	↓	↓	↓	-0.57	-	-	
	Fe/Cr-Fe/Cr Precoat	↓	↓	↓	-5.6	1.5	38.1	
N13	Cr-Cr Precoat	↓	↓	8	3.8	3.0	76.2	Light sanding to remove bisque
	Cr-Cr Precoat	↓	↓	↓	6.6	-	-	
	Fe/Cr-Fe/Cr Precoat	↓	↓	↓	-3.0	1.75	44.5	
N14	No. 4 - Al-Si	922	1200	2	23.9[c]	0.38	9.7	Dusted with Fe/50Al
N15	No. 3 - Cr + (Al-Mg)	1200	1700	6	5.3	0.75; 3.0[d]	19.1;76.2[d]	Cr Precoat, N12
	No. 6 - (Cr-Fe) + (Al-Mg)	↓	↓	↓	2.4	1.0; 2.5[d]	25.4;63.5[d]	Fe-75Cr Precoat - Run N12
	No. 3 - Cr + (Al-Mg)	↓	↓	↓	2.9	1.0; 4.0[d]	25.4;101.6[d]	Cr Precoat, N13
	No. 6 - (Cr-Fe) + (Al-Mg)	↓	↓	↓	2.5	0.75; 2.5[d]	19.1;63.5[d]	Fe-75Cr Precoat - Run N13
	(Al-Mg on Cr and Fe/Cr Precoats)	↓	↓					

TABLE A-1 (continued)

Run	Coating	Temperature (^{o}K)	Temperature (^{o}F)	Time (Hr)	Weight Gain (mg/cm^2)	Metallographic Thickness (In. x 10^{-3})	Metallographic Thickness (μm)	Remarks
N16	No. 9 - Cr + (Al-Si)	922	1200	2	22.5[c]	0.25; 2.5[d]	6.4; 63.5[d]	Cr Precoat N12
	(Al-Si on Cr Precoat)	922	1200	2	19.4	0.25; 3.25[d]	6.4; 82.6[d]	Cr Precoat N13
N17	No. 8 - Ni-Cr-Al	1200	1700	3	0.57[a]	0.25	6.4	
					0.50[b]	0.25	6.4	
N18	↓	↓	↓	6	0.37[a]	0.35	8.9	
					0.57[b]	0.35	8.9	
N19	No. 10 - Ni-Fe-Al-Si	1228	1750	3	1.0	0.5	12.7	
N20	No. 10 - Ni-Fe-Al-Si	1228	1750	6	1.5	0.75	19.1	

NOTES: (a) Elemental Cr and Ni Powders

(b) Pre-alloyed Cr-Ni Powder

(c) Includes Bisque

(d) Total Coating Thickness

TABLE A-2

COATING DATA FOR Ti-6-2-4-2 EVALUATION SPECIMENS

Coating No.	Coating Source Material		Run No.	Temperature (°K)	Temperature (°F)	Time (hrs)	Weight Gain (mg/cm²)	Coating Thickness (μm)	Coating Thickness In.x10⁻³
1A	56Cr/44Al		N-30	1200	1700	4	1.3	9.7	0.38
1B	56Cr/44Al		N-31	1200	1700	12	2.0	19.1	0.75
2A	Si		N-34	1228	1750	6	0.6	6.4	0.25
2B	Si		N-35	1228	1750	15	0.6	6.4	0.25
3A	Cr + (Al-Mg)	Cr	N-40	1228	1750	2	0.8	25.4	1.0
		Al-10Mg	N-46	1200	1700	6	2.2	12.7-25.4	0.5-1.0
3B	Cr + (Al-Mg)	Cr	N-41	1228	1750	5	1.8	45.7	1.80
		Al-10Mg	N-46	1200	1700	6	3.2	50.8	2.00
4A	Al/13Si		N-28	922	1200	2	0.89	6.4	0.25
4B	Al/13Si		N-29	922	1200	4	1.50	20.8	0.82
5A	56Cr/44Al + 10Mg		N-32	1200	1700	4	1.3	12.7	0.50
5B	56Cr/44Al + 10Mg		N-33	1200	1700	12	2.6	19.1	0.75
6A	(Fe-Cr) + (Al-Mg)	Fe/75Cr	N-38	1228	1750	4	0.44	9.7	0.38
		Al-10Mg	N-46	1200	1700	6	1.60	9.7	0.38
6B	(Fe-Cr) + (Al-Mg)	Fe/75Cr	N-39	1228	1750	10	0.74	12.7	0.50
		Al-10Mg	N-46	1200	1700	6	1.50	12.7	0.50
7A	Si-25Cr-4(Al/13Si)		N-26	1228	1750	4	0.70	5.1	0.20
7B	Si-25Cr-4(Al/13Si)		N-27	1228	1750	15	1.20	12.7	0.50
8A	50Ni-20Cr-30(Al/13Si)		N-24	1200	1700	3	1.10	12.7	0.50
8B	50Ni-20Cr-30(Al/13Si)		N-25	1200	1700	12	0.40	19.1	0.75
9A	Cr + (Al-Si)	Cr	N-42	1228	1750	2	1.20	12.7	0.50
		Al/13Si	N-44	922	1200	2	0.06	19.1	0.75
9B	Cr + (Al-Si)	Cr	N-43	1228	1750	5	2.10	31.8	1.25
		Al/13Si	N-45	922	1200	2	0.00	33.0	1.30
10A	40Ni-40(Fe/50Al)-20(Al/13Si)		N-36	1228	1750	3	0.80	6.4	0.25
10B	40Ni-40(Fe/50Al)-20(Al/13Si)		N-37	1228	1750	10	1.60	19.1	0.75

TABLE A-3

COATING DATA FOR Ti-13-11-3 EVALUATION COUPONS

Coating No.	Coating Source Material		Run No.	Temperature (°K)	Temperature (°F)	Time (hr)	Weight Gain (mg/cm^2)	Coating Thickness (μm)	Coating Thickness (In. x 10^{-3})
1A	56Cr/44Al		N-30	1200	1700	4	1.6	11.2	0.44
1B	56Cr/44Al		N-31	1200	1700	12	2.7	19.1	0.75
2A	Si		N-34	1228	1750	6	1.4	4.8	0.19
2B	Si		N-35	1228	1750	12	0.56	6.4	0.25
3A	Cr + (Al-Mg)	Cr	N-40	1228	1750	2	0.09	12.7	0.50
		Al-10Mg	N-46	1200	1700	6	2.70	16.0	0.63
3B	Cr + (Al-Mg)	Cr	N-41	1228	1750	5	0.18	15.2	0.60
		Al-10Mg	N-46	1200	1700	6	2.70	15.2	0.60
4A	Al/13Si		N-28	922	1200	2	2.40	3.8	0.15
4B	Al/13Si		N-29	922	1200	4	2.50	6.4	0.25
5A	56Cr/44Al + 10Mg		N-32	1200	1700	4	1.60	12.7	0.50
5B	56Cr/44Al + 10Mg		N-33	1200	1700	12	3.50	19.1	0.75
6A	(Fe-Cr) + (Al-Mg)	Fe/25Cr	N-38	1228	1750	4	0.00	12.7	0.50
		Al-10Mg	N-46	1200	1700	6	2.60	16.0	0.63
6B	(Fe-Cr) + (Al-Mg)	Fe/25Cr	N-39	1228	1750	10	0.28	15.2	0.60
		Al-10Mg	N-46	1200	1700	6	2.50	15.2	0.60
7A	Si-25Cr-4(Al/13Si)		N-26	1228	1750	4	1.10	3.3	0.13
7B	Si-25Cr-4(Al/13Si)		N-27	1228	1750	15	1.40	12.7	0.50
8A	50Ni-20Cr-30(Al/13Si)		N-24	1200	1700	3	1.20	6.4	0.25
8B	50Ni-20Cr-30(Al/13Si)		N-25	1200	1700	12	1.10	12.7	0.50
9A	Cr + (Al-Si)	Cr	N-42	1228	1750	2	0.90	15.2	0.60
		Al/13Si	N-44	922	1200	2	-	15.2	0.60
9B	Cr + (Al-Si)	Cr	N-43	1228	1750	5	0.74	31.8	1.25
		Al/13Si	N-45	922	1200	2	0.00	31.8	1.25
10A	40Ni-40(Fe/50Al)-20(Al/13Si)		N-36	1228	1750	3	1.10	6.4	0.25
10B	40Ni-40(Fe/50Al)-20(Al/13Si)		N-37	1228	1750	10	2.60	15.2	0.60

APPENDIX B

TENSILE TEST DATA

TABLE B-1

SLOW STRAIN RATE ROOM TEMPERATURE TENSILE PROPERTIES OF UNCOATED AND COATED Ti-6-2-4-2 EXPOSED TO 922°K (1200°F) IN AIR

Coating No.	Coating Thickness (μm)	Coating Thickness In.x10^{-3}	Exposure Time (hr)	U.T.S. (MN/m^2)	U.T.S. (ksi)	0.2% Y.S. (MN/m^2)	0.2% Y.S. (ksi)	Elongation %
Mill Annealed			None	952.2	138.2	851.6	123.6	14.3
↓			None	939.1	136.3	833.7	121.0	14.1
			100	952.2	138.2	881.2	127.9	11.4
			100	952.2	138.2	883.3	128.2	12.0
			1000	878.5	127.5	837.8	121.6	4.8
			1000	877.1	127.3	841.3	122.1	4.7
Ti-6-2-4-2[a]			None	920.5	133.6	797.9	115.8	9.2
↓			None	924.6	134.2	850.2	123.4	9.9
			100	913.6	132.6	851.6	123.6	7.5
			1000	817.8	118.7	792.4	115.0	4.7
1A	9.7	0.38	100	961.8	139.6	884.7	128.4	12.7
1A	↓	↓	100	926.0	134.4	860.6	124.9	11.8
1A			1000	882.6	128.1	850.2	123.4	5.2
1A			1000	908.1	131.8	853.0	123.8	6.6
1B	19.1	0.75	100	897.1	130.2	811.0	117.7	8.5
1B	↓	↓	100	906.7	131.6	818.5	118.8	10.2
1B			1000	866.8	125.8	822.0	119.3	6.0
1B			1000	857.8	124.5	824.0	119.6	4.5
2A	6.4	0.25	100	932.2	135.3	850.9	123.5	13.7
2A	↓	↓	100	928.8	134.8	859.2	124.7	13.5
2A			1000	917.7	133.2	819.2	118.9	9.6
2A			1000	844.0	122.5	840.6	122.0	8.6
2B	6.4	0.25	100	928.8	134.8	852.3	123.7	12.9
2B	↓	↓	100	927.4	134.6	850.2	123.4	15.0
2B			1000	906.7	131.6	820.6	119.1	11.2
2B			1000	861.9	125.1	848.8	123.2	9.0
3A	25.4	1.0	100	817.8	118.7	817.8	118.7	1.4
3A	↓	↓	100	802.0	116.4	798.6	115.9	1.4
3A			1000	855.7	124.2	855.7	124.2	0.5
3A			1000	859.9	124.8	858.5	124.6	1.7
3B	50.8	2.0	100	766.9	111.3	766.9	111.3	0.6
3B	↓	↓	100	819.9	119.0	819.9	119.0	0.4
3B			1000	832.3	120.8	832.3	120.8	1.9
3B			1000	817.8	118.7	817.8	118.7	1.1

TABLE B-1 (continued)

Coating No.	Coating Thickness (μm)	Coating Thickness In.x10^{-3}	Exposure Time (hr)	U.T.S. (MN/m^2)	U.T.S. (ksi)	0.2% Y.S. (MN/m^2)	0.2% Y.S. (ksi)	Elongation %
4A	6.4	0.25	100	700.0	101.6	664.2	96.4	13.3
4A	↓	↓	100	829.6	120.4	775.1	112.5	13.2
4A	↓	↓	1000	790.3	114.7	734.5	106.6	9.0
4A	↓	↓	1000	757.2	109.9	701.4	101.8	10.7
4B	20.8	0.82	100	647.0	93.9	607.7	88.2	14.4
4B	↓	↓	100	771.7	112.0	715.9	103.9	13.3
4B	↓	↓	1000	709.0	102.9	658.0	95.5	10.9
4B	↓	↓	1000	648.3	94.1	609.8	88.5	8.2
5A	12.7	0.50	100	913.6	132.6	845.4	122.7	13.6
5A	↓	↓	100	911.5	132.3	828.9	120.3	13.6
5A	↓	↓	1000	902.6	131.0	827.5	120.1	12.3
5A	↓	↓	1000	904.7	131.3	832.3	120.8	13.9
5B	19.1	0.75	100	894.3	129.8	819.2	118.9	12.5
5B	↓	↓	100	884.7	128.4	805.4	116.9	13.2
5B	↓	↓	1000	879.9	127.7	808.2	117.3	11.5
5B	↓	↓	1000	875.0	127.0	791.0	114.8	11.9
6A	9.7	0.38	100	806.8	117.1	806.8	117.1	0.4
6A	↓	↓	100	687.6	99.8	687.6	99.8	0.6
6A	↓	↓	1000	832.3	120.8	832.3	120.8	1.1
6A	↓	↓	1000	819.9	119.0	819.9	119.0	1.2
6B	12.7	0.50	100	826.1	119.9	826.1	119.9	1.4
6B	↓	↓	100	796.5	115.6	796.5	115.6	1.5
6B	↓	↓	1000	831.6	120.7	831.6	120.7	1.2
6B	↓	↓	1000	790.3	114.7	790.3	114.7	1.5
7A	5.1	0.20	100	927.4	134.6	853.7	123.9	11.5
7A	↓	↓	100	927.4	134.6	848.2	123.1	13.4
7A	↓	↓	1000	907.4	131.7	844.0	122.5	8.2
7A	↓	↓	1000	897.8	130.3	830.2	120.5	8.2
7B	12.7	0.50	100	890.2	129.2	806.8	117.1	12.5
7B	↓	↓	100	904.7	131.3	825.4	119.8	11.2
7B	↓	↓	1000	869.5	126.2	811.6	117.8	8.4
7B	↓	↓	1000	884.7	128.4	812.3	117.9	8.3
8A	12.7	0.50	100	900.5	130.7	850.9	123.5	7.7
8A	↓	↓	100	899.1	130.5	840.6	122.0	7.8
8A	↓	↓	1000	889.5	129.1	837.8	121.6	6.3
8A	↓	↓	1000	889.5	129.1	855.7	124.2	6.3

TABLE B-1 (continued)

Coating No.	Coating Thickness (μm)	Coating Thickness In.x10^{-3}	Exposure Time (hr)	U.T.S. (MN/m^2)	U.T.S. (ksi)	0.2% Y.S. (MN/m^2)	0.2% Y.S. (ksi)	Elongation %
8B	19.1	0.75	100	912.2	132.4	847.5	123.0	8.2
8B	↓	↓	100	857.8	124.5	837.8	121.6	4.7
8B			1000	823.4	119.5	819.9	119.0	3.3
8B			1000	886.7	128.7	832.3	120.8	9.1
9A	19.1	0.75	100	846.8	122.9	839.2	121.8	2.8
9A	↓	↓	100	850.2	123.4	835.8	121.3	2.0
9A			1000	795.1	115.4	789.6	114.6	2.8
9A			1000	795.1	115.4	788.2	114.4	3.9
9B	33.0	1.30	100	819.9	119.0	819.9	119.0	0.2
9B	↓	↓	100	813.0	118.0	813.0	118.0	0.7
9B			1000	761.3	110.5	758.6	110.1	1.5
9B			1000	863.3	125.3	823.4	119.5	7.3
10A	6.4	0.25	100	921.2	133.7	858.5	124.6	10.8
10A	↓	↓	100	923.9	134.1	851.6	123.6	12.7
10A			1000	863.3	125.3	823.4	119.5	7.3
10A			1000	886.7	128.7	832.3	120.8	9.3
10B	19.1	0.75	100	886.1	128.6	799.9	116.1	12.6
10B	↓	↓	100	888.8	129.0	812.3	117.9	12.4
10B			1000	886.7	128.7	804.8	116.8	9.4
10B			1000	886.7	128.7	806.1	117.0	12.5

NOTE: (a) Heat Treated 15 hrs/1228°K (1750°F).

APPENDIX C

CREEP DATA AND CALCULATIONS

APPENDIX C

The purpose of the work described below was to determine the stresses necessary to produce 0.2% creep strain in the self-stressed hot corrosion specimens used in Task 1.0 and the creep-exposure specimens used in Task 2.0. The work involved the following tasks:

1. Design of the self-stressed specimen.
2. Determination of creep and tensile data for the Ti-6-2-4-2 and Ti-13-11-3 alloys.
3. Experimental verification of the stress levels in the self-stressed specimens.

Self-stressed Specimen Design

The configuration shown in Figure C-1(a) may be used to derive an equation relating the bend angle of the specimen tabs to the maximum outer fiber stress.

Maximum Outer Fiber Stress Between Sections B and C

$\sigma = \frac{Mc}{I}$ where σ = maximum outer fiber stress.
M = bending moment from applied load, W, at a distance a (tab length).
c = distance from neutral axis.
I = section modulus.

$$\sigma = \frac{Wac}{I} = \frac{Wah/2}{\frac{bh^3}{12}} = \frac{6Wa}{bh^2} \qquad (1)$$

Maximum Deflection at Sections A and D

$$Y_A = Y_D = Y = \frac{Wa^2}{EI}(2a + 3L) \qquad (2)$$

where E = Modulus of Elasticity.
L = Length of mid-section.

or

$$W = \frac{6EIY}{a^2(2a+3L)} = \frac{6E\frac{bh^3}{12}Y}{a^2(2a+3L)} = \frac{E\,b\,h^3\,Y}{2a^2(2a+3L)} \qquad (3)$$

The relationship between σ, the maximum outer fiber stress and Y, the deflection of the tabs can be found by substituting the expression for W (Equation 3) into Equation 1.

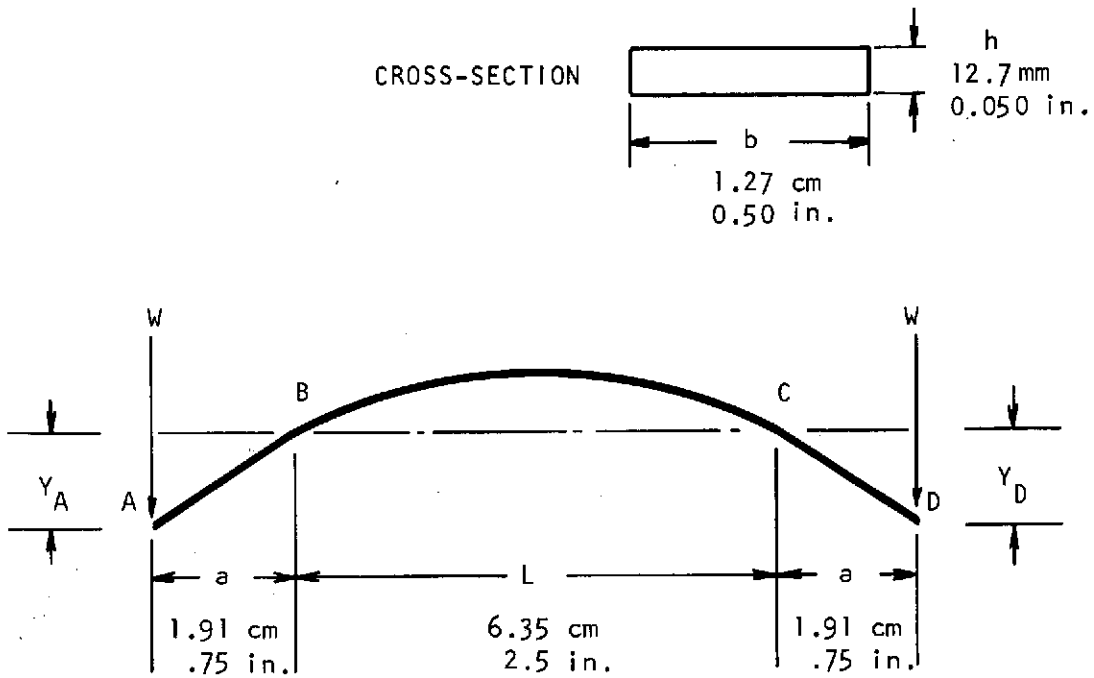

(a)

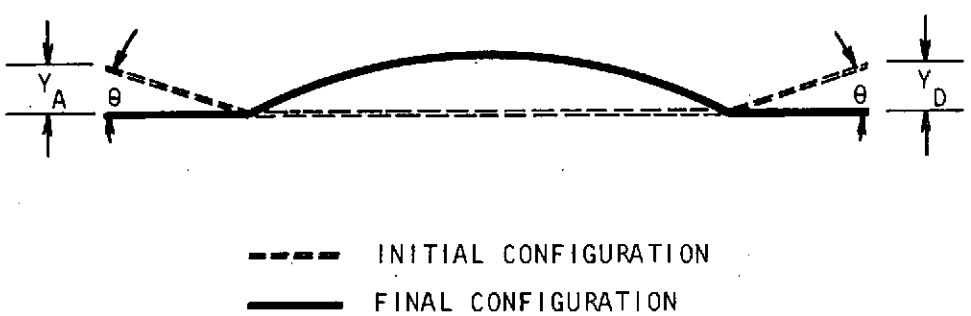

(b)

Figure C-1. Self-Stressed Specimen Configuration (One Leg)

$$\sigma = \frac{6(E\ b\ h^3\ Y)\ a}{bh^2\ [2a^2(2a+3L)]} = \frac{3\ E\ h\ Y}{a(2a+3L)} \tag{4}$$

$$Y = \frac{a(2a+3L)}{3\ E\ h} \tag{5}$$

Equation 5 also applies to each leg of the self-stressed specimen shown in Figure C-1(b)..

Mechanical Property Data for Ti-6-2-4-2 and Ti-13-11-3 Alloys

Longitudinal tensile properties were determined for Ti-6-2-4-2 and Ti-13-11-3 sheet using the specimen configuration shown in Figure C-1(a). The Ti-6-2-4-2 alloy was tested in the duplex heat treated condition (1/2 hr/1228°K (1750°F), A.C. + 1/4 hr/1061°K (1450°F), A.C.) and the Ti-13-11-3 alloy was tested in the solution treated and aged condition (1/2 hr/1033°K (1400°F) A.C. + 48 hr/755°K (900°F)). Testing was performed on an Instron test machine using a strain rate of 0.02 min^{-1}. Duplicate specimens were tested in air at room temperature and 755°K (900°F). Results of the tensile tests are presented in Table C-1, along with an estimated modulus of elasticity for each test temperature.

Creep testing was performed on Ti-6-2-4-2 and Ti-13-11-3 to determine stress levels that would produce 0.2% creep during exposure periods of 100 and 1000 hours at 755°K (900°F). Testing was performed in argon using the modified tensile specimen shown in Figure 2.. Minimum creep extension rates were determined at various stress levels from slopes of the second stage creep portion of the creep curves. Creep rates determined at various stress levels for the two alloys are summarized in Table C-2. Log-log plots of stress-level versus creep rate at 755°K (950°F) are presented in Figure C-2. From these plots, the applied stress levels for obtaining 0.2% creep strain in Ti-6-2-4-2 at 755°K (900°F) were determined as 275.6 MN/m^2 (40 ksi) for 100 hours of exposure and 144.7 MN/m^2 (21 ksi) for 1000 hours of exposure. Stress levels that produce 0.2% creep strain in Ti-13-11-3 at 755°K (900°F) were determined to be 117.1 MN/m^2 (17.0 ksi) for 100 hours of exposure and 48.2 MN/m^2 (7.0 ksi) for 1000 hours of exposure.

Determination of Bend Angle for Self-stressed Specimens

Since the self-stressed specimens were to be fabricated at room temperature and tested at 755°K (900°F), the bend angle must be calculated on the basis of a corrected stress. The following relation can be used to find σ_R, the stress at room temperature, required to obtain σ_T, the desired stress at 755°K (900°F).

$$\sigma_R = \frac{E_R}{E_T}\sigma_T \tag{6}$$

where E_R = modulus of elasticity at room temperature,

E_T = modulus of elasticity at 755°K (900°F).

Using Equation 5 and 6, the bend angle for the Ti-6-2-4-2 self-stressed specimens were calculated as follows:

TABLE C-1

TENSILE PROPERTIES OF Ti-6-2-4-2 AND Ti-13-11-3
AT 295°K (72°F) AND 755°K (900°F)

Substrate	Test Temperature		U.T.S.		0.2% Y.S.		% Elongation	E Ex 10^{-6}	
	(°K)	(°F	(MN/m^2	(ksi)	(MN/m^2)	(ksi)		(GN/m^2)	(psi)
Ti-6-2-4-2[a]	295	72	967.4	140.4	813.0	118.0	13.1	101.0	14.66
	295	72	939.8	136.4	795.8	115.5	13.5	94.9	13.77
	755	900	717.9	104.2	532.6	77.3	13.0	83.4	12.11
	755	900	688.3	99.9	498.8	72.4	13.7	76.4	11.09
Ti-13-11-3[b]	295	72	1345.6	195.3	1228.5	178.3	32.0	96.5	14.0
	295	72	1319.4	191.5	1217.5	176.7	26.9	109.6	15.9
	755	900	994.9	144.4	896.4	130.1	16.5	73.0	10.6
	755	900	1066.6	154.8	897.1	130.2	16.8	94.4	13.7

NOTES: (a) Heat Treatment - 1/2 hr/1228°K (1750°F), A.C. + 1/4 hr/1061°K (1450°F) A.C.

(b) Heat Treatment - 1/2 hr/1033°K (1400°F), A.C. + 48 hr/755°K (900°F).

TABLE C-2

CREEP RATES OF Ti-6-2-4-2 AND Ti-13-11-3
AT 755°K (900°F) IN AN ARGON ATMOSPHERE

Substrate	Applied Stress (MN/m^2)	Applied Stress (ksi)	Creep Rate %/Hr
Ti-6-2-4-2[a]	379.0	55	5.8×10^{-3}
↓	310.1	45	2.25×10^{-3}
↓	241.2	35	1.25×10^{-3}
↓	206.7	30	6.95×10^{-4}
Ti-13-11-3[b]	172.3	25	6.18×10^{-3}
↓	137.8	20	2.94×10^{-3}
↓	68.9	10	5.26×10^{-4}

NOTES: (a) Heat Treatment - 1/2 hr/1228°K (1750°F), A.C. + 1/4 hr/1061°K (1450°F) A.C.

(b) Heat Treatment - 1/2 hr/1033°K (1400°F), A.C. + 48 hrs/755°K (900°F).

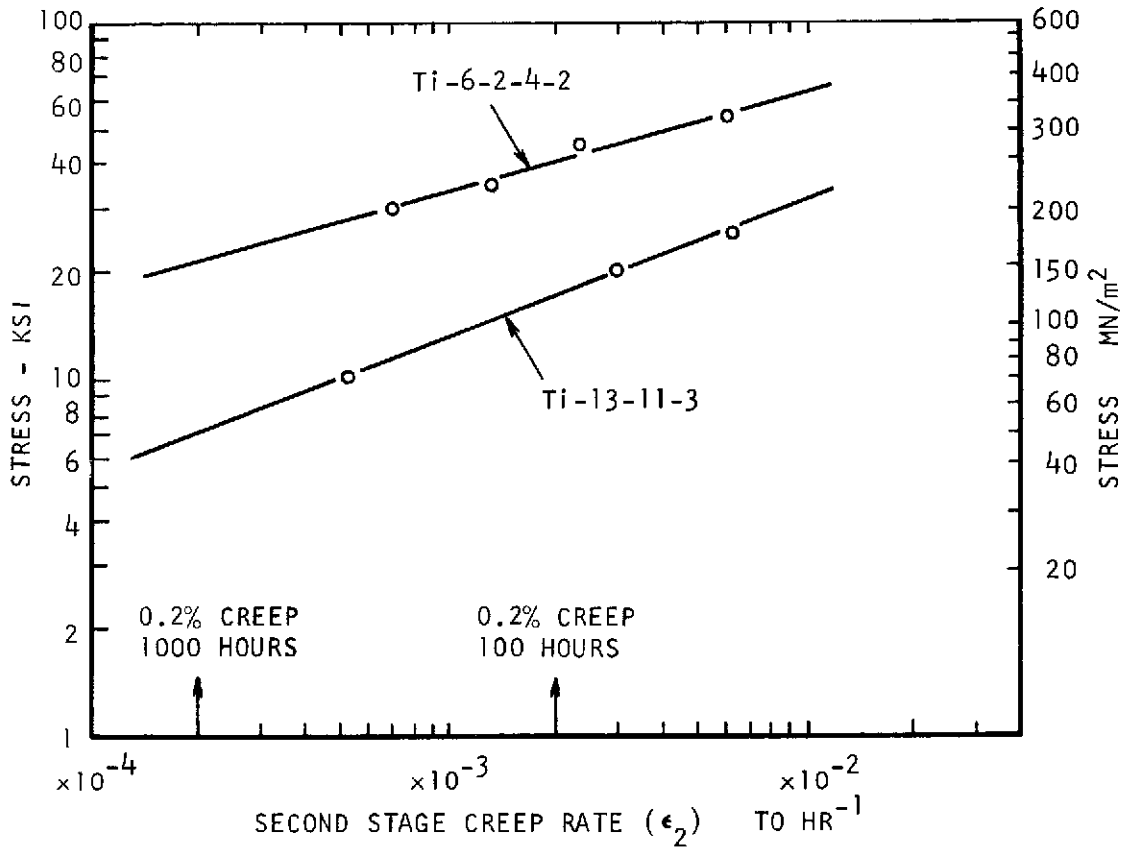

Figure C-2. Second Stage Creep Rate for Ti-6-2-4-2 and Ti-13-11-3 at Various Stress Levels in an Argon Atmosphere

For 100 Hours of Exposure:

$$\sigma_R = \frac{E_R}{E_T}\ \sigma_T = \frac{97,200}{79,980}\ (275.6) = 334.9\ MN/m^2\ (48.6\ ksi)$$

$$Y = \frac{a(2a+3L)}{3\ E\ h}\ \sigma = \frac{1.91\ [2\ (1.91) + 3\ (6.35)]\ (334.9)}{3\ (97,200)\ (0.127)} = 0.395\ cm\ (0.155\ In)$$

$$\theta = \tan^{-1}\ \frac{0.395}{1.910} \approx 12^o$$

Note: Literature value of E = 97.2 GN/m^2 used for the room temperature modulus of elasticity.

For 1000 Hour Exposure:

$$\sigma_R = \frac{E_R}{E_T}\ \sigma_T = \frac{97,200}{79,980}\ (144.7) = 175.9\ MN/m^2\ (25.5\ ksi)$$

$$Y = \frac{a(2a+3L)}{3\ E\ h}\ \sigma = \frac{1.91\ [2\ (1.91) + 3\ (6.35)]\ (175.9)}{3\ (97,200)\ (0.127)} = 0.207\ cm\ (0.082\ In)$$

$$\theta = \tan^{-1}\ \frac{0.207}{1.910} \approx 6.5^o$$

Note: Literature value of E = 97.2 GN/m^2 used for the room temperature modulus of elasticity.

Similar calculations for Ti-13-11-3 result in the following bend angles:

$\theta = 5^o$, for 100 hour exposure.
$\theta = 2^o$, for 1000 hour exposure.

Experimental Verification of Stresses in Self-stressed Specimens

To verify the stress levels in the specimens, strain gages were placed on two Ti-6-2-4-2 self-stressed bend specimens. One specimen had bend angles of $6\text{-}1/2^o$ and the other specimen had bend angles of 12^o. After assembly strain readings at room temperature were used to determine the maximum outer fiber stress. Figure C-3 shows the excellent agreement obtained between the experimentally determined stresses and stresses calculated from Equation 4.

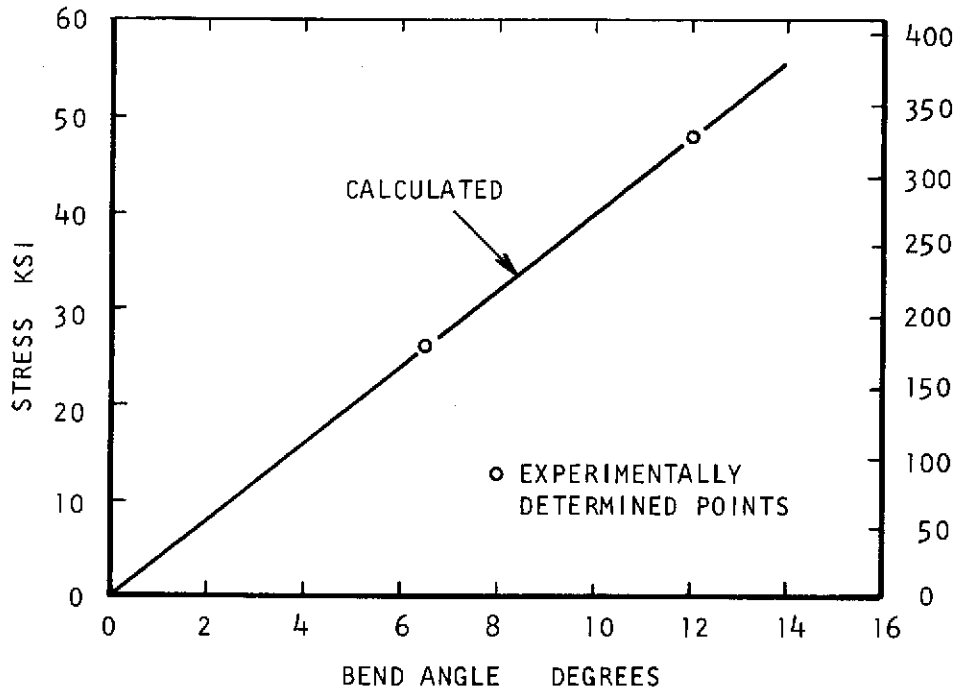

Figure C-3. Comparison between Calculated and Experimental Values of Maximum Outer Fiber Stress in Ti-6-2-4-2 Self-Stressed Specimens

REFERENCES

1. Wood, R. A., "Current and Future Usage of Materials in Aircraft Gas Turbine Engines," DMIC Memo 245, February 1970.

2. Anon, "The Characteristics and Uses of Aluminum Coatings on Titanium and Titanium Alloys," TML Memo No. 79, October 1956.

3. Kluz, S., Kolinowski, C. and Wehrman, R., "Development of Protective Coatings for Titanium Alloys," Watertown Arsenal Report WAL-401-51-22, October 1953.

4. Nejedlik, J. F., Protective Coatings for Titanium Alloy Compressor Blades," TRW Report TM-4580, December 1970.

5. Coatings of High Temperature Materials, H. H. Hauser, Editor, Plenum Press (1966).

6. Latva, J. D., "Selection and Fabrication of Ceramics and Intermetallics," Metal Progress, October 1962.

7. "Structures and Properties of Heat Resistant Metals and Alloys," M. V. Pridantseu, Editor, NASA TTF-557, 1970.

8. Stein, B. A. and Dexter, H. G., "Coatings and Surface Treatments for Longtime Protection of Ti-8Al-1Mo-1V Alloy Sheet from Hot-Salt Stress-Corrosion," NASA TND-4319, March 1968.

9. Schwartz, R., "Development of Improved Corrosion Protection for Long Time Exposure of S-11 Stage and/or Hardware," Final Report to Contract NAS7-200, Supplemental Agreement 2049, North American Rockwell Space Division, December 1971.

10. Rapp, G. C. and Rosenthal, S. H., "Problems and Solutions for Sand Environment Operation of Helicopter Gear Turbines," ASME Paper 65-WA/Prod-7, 1965.

11. Gulbransen, E. A. and Andrew, K. F., "Kinetics of the Reactions of Titanium with O_2, N_2 and H_2," Transactions AIME, October 1949.

12. Gray, H. R., "Relative Susceptibility of Titanium Alloys to Hot-Salt Stress-Corrosion," NASA TND-6498.

13. Garfinkle, M. F., "An Electrochemical Model for Hot-Salt Stress-Corrosion of Titanium Alloys," NASA TND-6779, April 1972.

DISTRIBUTION LIST FOR REPORT NASA CR-134537

CONTRACT NAS3-14339

(THE NUMBER IN PARENTHESES SHOWS HOW MANY COPIES
IF MORE THAN ONE ARE TO BE SENT TO AN ADDRESS.)

DR. R.L. ASHBROOK
MS 49-3
NASA LEWIS RESEARCH CTR.
21000 BROOKPARK ROAD
CLEVELAND, OHIO 44135

MR. G.M. AULT
MS 3-13
NASA LEWIS RESEARCH CTR
21000 BROOKPARK ROAD
CLEVELAND, OHIO 44135

MR. J.C. FRECHE
MS 49-1
NASA LEWIS RESEARCH CTR
21000 BROOKPARK ROAD
CLEVELAND, OHIO 44135

DR. H.R. GRAY
MS 49-1
NASA LEWIS RESEARCH CTR.
21000 BROOKPARK ROAD
CLEVELAND, OHIO 44135

MR. S.J. GRISAFFE
MS 49-3
NASA LEWIS RESEARCH CTR
21000 BROOKPARK ROAD
CLEVELAND, OHIO 44135

MISS T.D. GULKO
MS 49-3
NASA LEWIS RESEARCH CTR.
21000 BROOKPARK ROAD
CLEVELAND, OHIO 44135

MR. R.W. HALL
MS 105-1
NASA LEWIS RESEARCH CTR
21000 BROOKPARK ROAD
CLEVELAND, OHIO 44135

MR. F.H. HARF (25)
MS 49-3
NASA LEWIS RESEARCH CTR
21000 BROOKPARK ROAD
CLEVELAND, OHIO 44135

MR. J.P. MERUTKA
MS 49-3
NASA LEWIS RESEARCH CTR.
21000 BROOKPARK ROAD
CLEVELAND, OHIO 44135

DR. H.B. PROBST
MS 49-3
NASA LEWIS RESEARCH CTR.
21000 BROOKPARK ROAD
CLEVELAND, OHIO 44135

DR. I. ZAPLATYNSKY
MS 49-3
NASA LEWIS RESEARCH CTR.
21000 BROOKPARK ROAD
CLEVELAND, OHIO 44135

CONTRACTS SECTION B
MS 500-313
NASA LEWIS RESEARCH CTR
21000 BROOKPARK ROAD
CLEVELAND, OH 44135

LIBRARY (2)
MS 60-3
NASA LEWIS RESEARCH CTR
21000 BROOKPARK ROAD
CLEVELAND, OHIO 44135

PATENT COUNSEL
MS 500-311
NASA LEWIS RESEARCH CTR
21000 BROOKPARK ROAD
CLEVELAND, OHIO 44135

REPORT CONTROL OFFICE
MS 5-5
NASA LEWIS RESEARCH CTR
21000 BROOKPARK ROAD
CLEVELAND, OHIO 44135

TECHNOLOGY UTILIZATION
MS 3-19
NASA LEWIS RESEARCH CTR
21000 BROOKPARK ROAD
CLEVELAND, OHIO 44135

MR G. C. DEUTSCH / RW
NASA HEADQUARTERS
WASHINGTON, DC
20546

MR. N. REKOS / RL
NASA HEADQUARTERS
WASHINGTON, DC
20546

LIBRARY - REPORTS
MS 202-3
NASA AMES RESEARCH CENTER
MOFFETT FIELD,CA 94035

LIBRARY
NASA FLIGHT RESEARCH CTR
P.O. BOX 273
EDWARDS, CALIFORNIA 93523

LIBRARY
NASA
GODDARD SPACE FLIGHT CTR
GREENBELT, MARYLAND 20771

LIBRARY - ACQUISITIONS
JET PROPULSION LAB.
4800 OAK GROVE DRIVE
PASADENA,CA 91102

LIBRARY MS 185
NASA
LANGLEY RESEARCH CENTER
LANGLEY FIELD,VA 23365

TECHNICAL LIBRARY / JM6
NASA
MANNED SPACECRAFT CENTER
HOUSTON, TX 77058

NASA REPRESENTATIVE (10)
SCIENTIFIC AND TECHNICAL
INFORMATION FACILITY
BOX 33
COLLEGE PARK, MD 20740

DEFENCE DOCUMENTATION CTR
CAMERON STATION
5010 DUKE STREET
ALEXANDRIA, VIRGINIA
22314

MR. J.J. CROSBY
AFML/LLP
HEADQUARTERS
WRIGHT PATTERSON AFB,
OH 45433

MR. J.K. ELBAUM
AFML/LLP
HEADQUARTERS
WRIGHT PATTERSON AFB,
OH 45433

MR. N. GEYER
AFML/LLP
HEADQUARTERS
WRIGHT PATTERSON AFB,
OH 45433

MR. J.R. WILLIAMSON
AFML/LT
HEADQUARTERS
WRIGHT PATTERSON AFB,
OH 45433

MR. M. LEVY AMXMR-RM
ARMY MATERIALS AND
MECHANICS RESEARCH CTR.
WATERTOWN, MA 02172

MR. I. MACHLIN AIR-52031B
NAVAL AIR SYSTEMS COMMAND
NAVY DEPARTMENT
WASHINGTON, DC 20360

DR. T. LYMAN
AM. SOCIETY FOR METALS
METALS PARK
NOVELTY, OHIO 44073

MR. E. BARTLETT
BATTELLE MEMORIAL INST.
505 KING AVENUE
COLUMBUS, OH 43201

DR. R.I. JAFFEE
BATTELLE MEMORIAL INST.
505 KING AVENUE
COLUMBUS OHIO 43201

MCIC
BATTELLE MEMORIAL INST.
505 KING AVENUE
COLUMBUS, OHIO 43201

DR. B. WILCOX
BATTELLE MEMORIAL INST.
505 KING AVENUE
COLUMBUS, OHIO 43201

DR. N.A. TINER
INSTIT. OF SURFACE TECHN.
CALIFORNIA STATE COLLEGE
LONG BEACH, CALIFORNIA
90801

LIBRARY
UNIVERSITY OF DAYTON
RESEARCH INSTITUTE
300 COLLEGE PARK AVE
DAYTON, OHIO 45409

MR. R.A. GRAFF
CITY COLLEGE OF NEW YORK
DEPT.CHEM.ENGR.
NEW YORK N.Y. 10031

MR. G.B. BARTHOLD
ALUMINUM CO. OF AMERICA
1200 RING BLDG
WASHINGTON, DC 20036

MR. W.E. BINZ
BOEING COMPANY
P.O. BOX 3733
SEATTLE, WA 98124

MR. J.B. GUERSEY
COLT INDUSTRIES
CRUCIBLE INC.
P.O. BOX 88
PITTSBURGH, PA. 15230

MR. R.K. MALIK
CONVAIR AEROSPACE DIV.
GENERAL DYNAMICS CORP.
P. O. BOX 80847
SAN DIEGO, CA 92138

LIBRARY
GENERAL ELECTRIC COMPANY
R. AND D. CENTER
P.O. BOX 8
SCHENECTADY, N.Y. 12301

DR. I.I. BESSEN MPTL
AETD
GENERAL ELECTRIC COMPANY
CINCINNATI, OHIO 45215

MR. L.P. JAHNKE MPTL
AETD
GENERAL ELECTRIC COMPANY
CINCINNATI, OHIO 45215

MR. T.K. REDDEN MPTL
AETD
GENERAL ELECTRIC COMPANY
CINCINNATI, OHIO 45215

MR.D. HANINK
ENGINEERING OPERATIONS
DETROIT DIESEL ALLISON
GENERAL MOTORS CORP.
INDIANAPULIS,IN 46206

MR. E.S. NICHOLS PT.8 T2B
DETROIT DIESEL ALLISON DV
P.O. BOX 894
INDIANAPOLIS, IN 46206

MR. L.C. MCCANDLESS
GENERAL TECHNOLOGIES CORP
1821 M.FARADAY DRIVE
RESTON, VIRGINIA 22070

MR. F. BOTT
INSULATION SYSTEMS INC.
11233 CONDOR AVENUE
FOUNTAIN VALLEY, CALIF.
92708

MR. A. STETSON
SOLAR DIVISION
INT.HARVESTER CORP.
2200 PACIFIC HIGHWAY
SAN DIEGO, CAL. 92112

MR.R. PERKINS
LOCKHEED PALO ALTO R.LAB.
3251 HANOVER STREET
PALO ALTO,CA 94304

DR. J.C. WILLIAMS
NORTH AMERICAN ROCKWELL
SCIENCE CENTER
THOUSAND OAKS, CALIFORNIA
91360

DR. J.W. BOND
DIRECTOR OF RESEARCH
PHYSICS TECHNOLOGY LABS.
7841 EL CAJON BOULEVARD
LA MESA, CALIFORNIA 92041

DR. H.B. BOMBERGER
DIRECTOR OF RESEARCH
REACTIVE METALS CORP
NILES, OHIO 44446

MR. H.D. KESSLER
REACTIVE METALS INC.
100 WARREN AVENUE
NILES,OHIO 44446

MR. E. WAKEFIELD MS144
TEXAS INSTRUMENTS INC.
P.O. BOX 5936
DALLAS TX 75222

MR. R. BROADWELL
TITANIUM METALS CORP.
WEST CALDWELL, NJ

MR. E.F. BRADLEY
PRATT + WHITNEY AIRCRAFT
UNITED AIRCRAFT CORP
400 MAIN STREET
EAST HARTFORD CONN 06108

DR. G.W. GOWARD
PRATT + WHITNEY AIRCRAFT
UNITED AIRCRAFT CORP
400 MAIN STREET
EAST HARTFORD CONN 06108

RESEARCH LIBRARY
UNITED AIRCRAFT CORP.
400 MAIN STREET
EAST HARTFORD, CONN. 06108

MR. D. GOLDBERG
WESTINGHOUSE ELECTRIC
P. O. BOX 10864
PITTSBURGH, PA. 15236

MR. R. SPRAGUE
PRATT & WHITNEY AIRCRAFT
UNITED AIRCRAFT CORP.
400 MAIN STREET
EAST HARTFORD, CONN. 06108

MR. R. G. SHERMAN
DIRECTOR OF ENGINEERING
VALLEY-TOLEDO, INC.
SYLMAR, CALIFORNIA 91342

MR. A. HAUSER
PRATT&WHITNEY AIRCRAFT
UNITED AIRCRAFT CORP.
400 MAIN STREET
EAST HARTFORD, CONN. 06108